Fall 2006

Remote detection of forest structure in the White Mountains of New Hampshire: An integration of waveform lidar and hyperspectral remote sensing data

Jeanne Elizabeth Anderson

University of New Hampshire, Durham

REMOTE DETECTION OF FOREST STRUCTURE
IN THE WHITE MOUNTAINS OF NEW HAMPSHIRE:
AN INTEGRATION OF
WAVEFORM LIDAR AND HYPERSPECTRAL REMOTE SENSING
DATA

BY

JEANNE ELIZABETH ANDERSON
B.A., Bucknell University, 1981
M.F.S., Yale University, 1984

DISSERTATION

Submitted to the University of New Hampshire
In Partial Fulfillment of
the Requirements for the Degree of

Doctor of Philosophy
in
Earth and Environmental Sciences

September, 2006

UMI Number: 3231346

Copyright 2006 by
Anderson, Jeanne Elizabeth

All rights reserved.

INFORMATION TO USERS

The quality of this reproduction is dependent upon the quality of the copy submitted. Broken or indistinct print, colored or poor quality illustrations and photographs, print bleed-through, substandard margins, and improper alignment can adversely affect reproduction.

In the unlikely event that the author did not send a complete manuscript and there are missing pages, these will be noted. Also, if unauthorized copyright material had to be removed, a note will indicate the deletion.
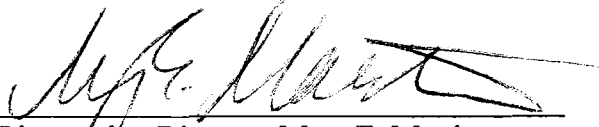
UMI®

UMI Microform 3231346
Copyright 2006 by ProQuest Information and Learning Company.
All rights reserved. This microform edition is protected against
unauthorized copying under Title 17, United States Code.
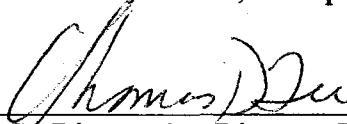
ProQuest Information and Learning Company
300 North Zeeb Road
P.O. Box 1346
Ann Arbor, MI 48106-1346
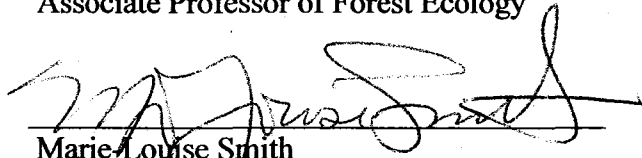
This dissertation has been examined and approved.
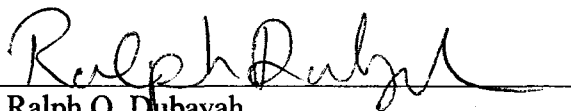
Dissertation Director, Mary E. Martin
Research Assistant Professor of Natural Resources
and Earth, Oceans, and Space

Co-Dissertation Director, Thomas D. Lee
Associate Professor of Forest Ecology

Marie-Louise Smith
Research Ecologist, USDA Forest Service,
Northeastern Research Station

Ralph O. Dubayah
Professor, Geography, University of Maryland

Bobby H. Braswell
Research Assistant Professor of Earth, Oceans, and Space

5/10/06
Date

DEDICATION

To my sons, Galen Thomas and Erik Anders

iv

ACKNOWLEDGEMENTS

I extend my deepest thanks to Mary Martin. Her selflessness in sharing so much of her knowledge and time to guide me through this process has been both inspiring and humbling. She is an unceasingly wonderful person, as advisor and friend. This work is much in her debt. Tom Lee, M.L. Smith, and Rob Braswell have also provided many needed hours of sage advice and gentle correction. I particularly want to thank Ralph Dubayah for so willingly taking a chance on a student from afar and granting me access to the realm of waveform lidar. I, likewise, thank M.L. Smith for providing open access to the substantial data and expertise of the Forest Service. I am truly grateful for all of the efforts and support of my committee.
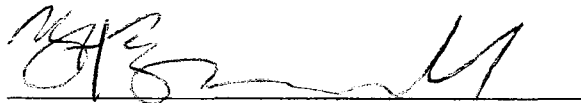
I have many, many people to thank from the University of New Hampshire, the University of Maryland, NASA, and the USDA Forest Service Northeastern Research Station. Lucie Plourde, Peter Hyde, Birgit Peterson, Michelle Hofton, Bryan Blair, Jason Drake, Chris Campbell, Jen Pontius, Andy Fast, Mark Ducey, Bill Frament, and Bill Leak are among many wonderful people who worked with me throughout this process. The permanent and seasonal staffs of the Complex Systems Research Center at UNH and Bartlett Experimental Forest have provided substantial support, often in the field, for my research. Much of this work was made possible by the fellowship support of the NASA Earth Systems Science Fellowship Program, the Switzer Foundation and the New Hampshire Space Grant Program.

Lacking the gift of prophecy, it was never entirely clear to me when I began this research whether my life at home as the mother of two young boys would allow me to complete this journey in a timely manner. My husband, sons, and parents, however, have made every effort to allow me to persevere in this quest over the past six years. This is a truly special gift and I thank them for their exceptional love and support.

TABLE OF CONTENTS

LIST OF TABLES

LIST OF FIGURES

ABSTRACT

REMOTE DETECTION OF FOREST STRUCTURE IN THE WHITE MOUNTAINS OF NEW HAMPSHIRE: AN INTEGRATION OF WAVEFORM LIDAR AND HYPERSPECTRAL REMOTE SENSING DATA.

by

Jeanne E. Anderson

University of New Hampshire, September, 2006

The capability of waveform lidar, used singly and through integration with high-resolution spectral data, to describe and predict various aspects of the structure of a northern temperate forest is explored. Waveform lidar imagery was acquired in 1999 and 2003 over Bartlett Experimental Forest in the White Mountains of central New Hampshire using NASA's airborne Laser Vegetation Imaging Sensor (LVIS). High-resolution spectral imagery from 1997 and 2003 was likewise acquired using NASA's Airborne Visible/Infrared Imaging Spectrometer (AVIRIS). USDA Forest Service Northeastern Research Station (USFS NERS) 2001-2003 inventory data was used to define basal area, above-ground biomass, quadratic mean stem diameter and proportional species abundances within each of over 400 plots. Field plots scaled to LVIS footprints were also established.

At the smallest scale, metrics derived from single LVIS footprints were strongly correlated with coincident forest measurements. At the larger scale of USFS NERS plots, strong correlations encompassing the full variability of the Forest Service data could not be established. Restrictions set by species composition and land-use, however, significantly improved both the descriptive and predictive power of the regression analyses.

Higher amplitude values of 1999 LVIS ground return metrics, obtained within two years of the January 1998 ice storm, were found to provide a spatial record of higher levels of canopy damage within older, unmanaged forest tracts. Subjected to repeated disturbance of intermediate severity over the time frame of decades, these particular tracts, predominately found on southeastern aspects, simultaneously support high levels of sugar maple abundance and low levels of sugar maple coarse woody debris. LVIS height metrics were used here to establish a statistical relationship with coarse woody debris data.

The integration of waveform lidar with hyperspectral data did enhance the ability to remotely describe a number of common measures of forest structure. Compositional abundance patterns, however, were not improved over use of AVIRIS data alone. Maps predicting species abundance patterns (primarily derived from AVIRIS data) with coincident patterns of stem size (derived from LVIS data) can be created for several of the dominant tree species of this region. The results are the near equivalent of a field-based forest inventory.

INTRODUCTION

The spatial patterning of forest structure throughout the world reflects complex climatic, environmental and historical controls (Foster et al. 2003, Franklin et al. 2002, Foster et al. 1998, Bormann and Likens 1979). Tremendous acreage of the northern woods of New England, New York and Canada exists in a stage of re-growth from one to two centuries or more of intensive cutting and altered land-use (Irland 1999, Northern Forest Lands Council 1994, Whitney 1994, Cronon 1983). Patterns of biological diversity and ecological complexity of much of this forest have been altered by this history and it is increasingly recognized that the legacies of such land-use will continue to influence ecosystem structure and function for decades or centuries into the future (Foster et al. 2003, Franklin et al. 2002, Pickett et al. 1997, Christensen 1989, Foster and Boose 1992). These temperate forests are recognized as important components of the global carbon cycle, but assessing landscape-level variation in forest biomass and carbon stocks has proved to be a challenging task. This stems, in part, from the effects of historical use and the scarcity of information regarding disturbance patterns across complex landscapes. High levels of structural complexity are recognized as an indicator of persisting biological legacies (Franklin et al. 2000, Anderson 1999, Christensen et al. 1997,

1

Christensen et al. 1996) particularly in late-successional temperate forests (Franklin et al. 2002, Hagen 2001, Hagen and Whitman 2001). The use of structure-based indices combining factors such as stand structural complexity, connectivity and landscape-level heterogeneity is now advocated as an adaptive approach to addressing the conservation of biological diversity as part of ecologically sustainable forest management (Keeton et al. 2001, Whitman and Hagen 2001, Lindenmayer et al. 2000, Zenner & Hibbs 2000, Pickett et al. 1997, Onal 1997, Christensen et al. 1996). Yet to date, the spatial variation of forest structure across large tracts of land has been rarely assessed (Parker 1995, Zimble 2003) and the knowledge base regarding the impacts of historical legacies on forest structure and biological diversity is also largely lacking.

Forest structure has been assessed in the guise of many different ecological terms and compilations of data (Parker 1995, Parker and Brown 2000, Pommerening 2002, Barker and Pinard 2001, Brokaw and Lent 1999, Latham et al. 1998, Campbell and Norman 1989). Most directly, it is explored and assessed through measures of height, canopy architecture, canopy cover, light transmittance, canopy profiles and biomass amongst other variables. The patterning and variance in structure between various forest stands is encompassed and described within concepts such as forest heterogeneity, landscape patch dynamics and structural complexity (Lindenmayer et al. 2000, Christensen et al. 1997, Spies 1997, McGarigal and Coombs 1995, Franklin and Forman 1987, Runkle 1985). These concepts have been defined and explored in the ecological literature of past decades. But, these data are particularly time-consuming and difficult to collect across large areas in the field. In recent decades, three-dimensional structural data, from either

field or remote methods, have been infrequently measured. But on the strength of recent advances in laser altimetry sensors (Blair et al. 1994, Blair et al. 1999, Lefsky et al. 2002), airborne lidar sensors now provide an option for the rapid collection of image data at a scale sufficient to describe structural metrics for thousands of acres at a time. Furthermore, there is evidence that historical legacies can be detected within the remotely sensed patterns of forest structure and composition provided by lidar sensors as well (Dubayah et al. 2000). Integration with optical sensor data will potentially increase the ability to discriminate compositional detail as well.

Waveform Lidar

Laser altimetry, or lidar (light detection and ranging) is an emerging active remote sensing technology with a wide variety of applications in the Earth and planetary sciences (Blair et al. 1999, Wehr and Lohr 1999, Dubayah et al. 2000, Dubayah and Drake 2000, Lefsky et al. 2001a, Lefsky et al. 2002, Lim et al. 2003a). Of particular appeal to terrestrial ecologists is the promise of lidar to increase the accuracy of biophysical measurements and measurement of vertical structure (Lefsky et al. 2002, Dubayah et al. 2000). The basic measurement made by a lidar device is the distance between the sensor and a target surface, obtained by determining the elapsed time between the emission of a short-duration laser pulse and the arrival of the reflection of that pulse (the return signal) to the sensor's receiver. Multiplying this time interval by the speed of light results in a

3

measurement of the round-trip distance traveled, and dividing that figure by two yields the distance between the sensor and target (Bachman 1979 in Lefsky et al. 2002). Lefsky et al. (2002) summarize the key differences among lidar sensors to include the laser's wavelength, power, pulse duration and repetition rate, beam size and divergence angle, the specifics of the scanning mechanism, and the information recorded for each reflected pulse. Lasers for terrestrial applications generally have wavelengths in the infrared range of 900-1064 nanometers, where vegetation reflectance is highest. One drawback of working in this range of wavelengths is absorption by clouds, which impedes the use of these devices during overcast conditions (Lefsky et al. 2002).

A new generation of instruments including most recently, the medium-altitude Laser Vegetation Imaging Sensor (LVIS) developed at NASA's Goddard Flight Space Center in the 1990's (Blair et al. 1994, Blair et al. 1999, Blair and Hofton 1999, Hofton et al. 2000a, Hofton et al. 2000b) has expanded the capability of traditional laser altimeters by recording the laser backscatter amplitude with very high temporal resolution (Harding et al. 2001). At any particular height, the amplitude of the return waveform measures the strength of the return. Thus, for surfaces with a similar set of reflectances and geometry within a footprint, larger amplitudes indicate more canopy material per se (Dubayah et al. 2000). The waveform provides only an apparent canopy profile because of attenuation of the beam through the canopy and must be adjusted to the true canopy profile. (Drake 2001, Lefsky et al.1999b). Harding et al. (2001) present methods of developing representative canopy height profiles of the relative vertical distribution of canopy surface areas from full waveform data. LVIS is a pulsed laser altimeter and measures

4

range by timing a short pulse of laser light between the instrument and the target surface. The entire time history of the outgoing and return laser pulses is digitized using a single detector, digitiser and timing clock and unambiguously describes the range to the surface as well as the vertical distribution of surfaces within each laser footprint (Blair et al. 1999). These sensors are used in combination with other instruments such as global positioning system (GPS) receivers to obtain the position of the platform and inertial navigation systems (INS) to measure the attitude (roll, pitch and yaw) of the lidar sensor in order to locate the source of the return signal in three dimensions (Lefsky et al. 2002). Additional specifications specific to LVIS are detailed in Blair et al. (1999).

As a waveform-recording device, LVIS is at an advantage over discrete return (small footprint) systems in its enhanced ability to characterize canopy (including sub-canopy) structure, the ability to concisely describe canopy information over increasingly large areas, and the ability to acquire global data sets (Lefsky et al. 2002) from space-borne satellites. Large-footprint lidar systems (Blair et al. 1994, Blair et al.1999), by increasing the footprint size to the approximate crown diameter of a canopy-forming tree (approximately 10-25 meters), allow laser energy to consistently reach the ground even in dense forests (Weishampel et al. 1996, Drake 2001) and therefore, avoid the biases of small-footprint systems that frequently miss the tops of trees (see Nelson 1997). Conversely, large footprint fully-digitising lidar data is hard to obtain; with most commercial systems still using largely small-footprint (5-30 cm diameter), high pulse rate systems (1000-10,000 Hz) that record the range to the highest (and sometimes lowest)

5

reflecting surface within the footprint (Dubayah et al. 2000). Small footprint, waveform-recording, lidar sensors are, however, emerging (Gutierrez et al. 2005).

Research over the past decade has demonstrated that large footprint, waveform sampling lidar altimetry (hereinafter referred to as lidar) can characterize the structural complexity and associated functional properties of natural landscapes relevant to ecological investigations by providing vertical and volumetric profiles of forest vegetation. The metrics have proven useful for predicting a range of ecological variables such as canopy height and structure, the density of forest cover, biomass, and light transmittance (Dubayah et al. 2000, Lefsky et al. 2002, Means et al. 1999, Harding et al. 2001, Parker et al. 2001, Ni-Meister et al. 2001). Lidar remote sensing can also generate data that can be used to provide three-dimensional, or volumetric characterizations of vegetation structure (Weishampel et al. 2000, Lefsky et al. 1999a, Harding et al. 2001). It can accurately capture spatial patterns of canopy heights (Drake and Weishampel 2000). The height data provided directly by laser altimetry sensors can serve as a surrogate estimator of stand age or successional state when coupled with species composition and site quality information (Dubayah et al. 2000). Lidar waveforms generated by medium-large footprint sensors such as LVIS, by themselves, can also be used to distinguish among important land-use types reflecting both historical and other environmental controls (Dubayah et al. 2000).

According to the overview published by Lefsky and his colleagues (2002), current ecological applications of lidar remote sensing tend to fall within three categories: remote

sensing of ground topography, measurement of three-dimensional structure and function of vegetation canopies, and prediction of forest stand structure attributes (such as aboveground biomass). The ability of lidar to predict these variables has been very good, as compared with non-lidar remotely sensed estimates, with coefficients of determination usually in excess of 75% of variance explained. (Lefsky et al. 1999d, Hyde et al. 2005). It is important, however, that the relationships between lidar metrics and directly measured forest structural characteristics be examined in an expanding range of terrestrial biomes (Drake 2001, Lefsky et al. 2002). Lidar has only recently become available as a research tool and has yet to become widely available, but it is expected that lidar's ability to rapidly measure the three-dimensional structure of canopies can and should stimulate the development of new systems of canopy description (Lefsky et al. 2002, Parker and Brown 2000, Parker et al. 2001).

A number of authors (Hyde 2005, Popescu et al. 2004, McCombs et al. 2003, Hudak et al. 2002, Lefsky et al. 2001, Drake 2001, Dubayah et al. 2000, Lefsky et al. 1999c, Ackermann 1999) have commented on the potential synergy provided through the integration of lidar with spectral data. This product can capture strengths of both sensor technologies and improve estimates of forest stand characteristics (Popescu et al. 2004). As noted by Lefsky et al. (2001), lidar offers unique access to stand structural information that cannot be well discerned by optical remote sensing methods. If combined with data from high spectral resolution remote sensors, lidar may offer even more valuable results. Typically, in working with visible/infrared data, users rely on the spectral signature of ground targets in the image. Some vegetation species cannot be

7

separated due to their similar spectral response. Lidar images, however, contribute to the structural discrimination of similar spectral signals within the observed ground cover. Integration of lidar coverages with airborne AVIRIS hyperspectral capabilities should, therefore, potentially increase the sensitivity of the analyses.

Few studies have been published to date on the integration and/or fusion of lidar with spectral data. Hyde (2005) statistically combined LVIS data with passive optical and radar (SAR backscatter and InSAR range) data to produce broad scale maps of forest structure over the Sierra Mountain in California that are consistent and accurate relative to field data and LVIS data alone. Popescu et al. (2004) explored the feasibility of using small-footprint lidar data and multispectral imagery to estimate forest volume and biomass. They reported maximum r^2 values for estimating biomass at 0.32 for deciduous trees (RMSE = 44 Mg ha^{-1}) and 0.82 for pines (RMSE = 29 Mg ha^{-1}). The use of fused data of lidar and optical imagery, as opposed to the use of lidar data alone, always improved biomass and volume estimates for pines and, in some cases, for deciduous plots. McCombs et al. (2003) used small footprint lidar and high-resolution multispectral data sets to estimate stem counts and tree heights in a spacing study of 15-year old loblolly pine stands. Their fused dataset did improve the accuracy of tree identification over the single data set approaches. At a regional scale, Hudak et al. (2002) looked at the integration of lidar and Landsat ETM+ data for estimating and mapping forest canopy height. They found that an integrated technique of ordinary cokriging of the height residuals from an ordinary least squares regression model proved the best method for

estimating and mapping forest canopy height, and an equitable distribution of lidar

sampling points proved critical for efficient lidar-Landsat ETM+ integration.

Lim et al. (2003) are also advocates of integrated sensor data, noting:

> Lidar systems will likely become integrated with digital cameras, creating an
> effective fusion with photogrammetry. Similarly, a fusion between geometric
> laser scanning and multispectral imaging systems can be expected to make up
> for the lack of multispectral information currently available from stand-alone
> lidar systems. Therefore, by integrating lidar systems with imaging sensors,
> more robust systems will emerge, thereby, satisfying the wide range of data
> requirements of the forest practitioner at local and regional scales.

Three Papers

The capability of waveform lidar, used singly and through integration with high-

resolution spectral data, to describe and predict various aspects of the heterogeneous

structure of a northern temperate forest is explored in this dissertation through three

separate papers. Waveform lidar imagery was acquired in 1999 and 2003 over the 1000-

ha. Bartlett Experimental Forest in the White Mountains of central New Hampshire using

NASA's airborne Laser Vegetation Imaging Sensor (LVIS). High-resolution spectral

imagery from 1997 and 2003 was likewise acquired using NASA's Airborne

Visible/Infrared Imaging Spectrometer (AVIRIS). USDA Forest Service Northeastern

Research Station (USFS NERS) 2001-2003 inventory data was used to define basal area

(BA), above-ground biomass (AGBM), quadratic mean stem diameter (QMSD) and

9

proportional species abundances within each of over 400 plots. Additional field data were collected at Bartlett at the scale of LVIS footprints. Coarse woody debris data, collected and analyzed as part of a UNH master's thesis, was provided by Andy Fast and Mark Ducey.

In the first of these papers, individual LVIS waveform height metrics were correlated with coincident footprint-level field plots. This was an exercise of calibration and validation of the LVIS data sets as flown in 1999 and 2003 as part of a larger NASA effort to assess LVIS in a wide variety of biomes. Resulting regression models were used to predict forest-wide levels of AGBM and QMSD and checked for use as a general model against a USFS NERS inventory data set of over 400 plots. Restrictions set by species composition and land-use, were explored as a means to improving both the descriptive and predictive power of the regression analyses.

The second paper explored the use of a broader set of 1999 LVIS metrics, inclusive of canopy energy and ground energy variables, to look at questions of spatial patterning due to natural disturbance. Examination of higher amplitude values of 1999 LVIS ground return metrics, obtained within two years of the January 1998 ice storm, suggested that this variable appears to provide a spatial record of higher levels of canopy damage within older, unmanaged forest tracts. Analyses using USFS NERS plot compositional abundance data, 1999 LVIS metrics, unpublished Forest Service records of the 1938 hurricane damage, and a 2004 coarse woody debris data set were integrated into this study to further explore the spatial patterns that emerge in these areas of repeated natural

10

disturbance at Bartlett. LVIS height metrics were also used here to explore a statistical

relationship with extensive coarse woody debris data in areas hardest hit by the 1998 ice

storm.

The third paper is focused on the integration of waveform lidar with hyperspectral data

and the capability of the integrated data to enhance the remote description of a number of

common measures of forest structure and associated compositional abundance patterns.

The use of regression models to predict and create maps that provide results that are a

near equivalent of a field-based forest inventory was an additional objective of this work.

Literature Cited

Ackermann, F. (1999). Airborne laser scanning-present status and future expectations.
ISPRS Journal of Photogrammetry & Remote Sensing 54:64-67.

Anderson, M. (1999). Viability and spatial assessment of ecological communities in the
Northern Appalachian Ecoregion. PhD. Dissertation. University of New
Hampshire. Durham, N.H.

Bachman C.G. (1979). Laser radar systems and techniques. Norwood (MA):Artech
House.

Barker, M.G. & Pinard, M.A. (2001). Forest canopy research: sampling problems, and
some solutions. *Plant Ecology*, 153, 3-38.

Blair, J.B., Coyle, D.B., Bufton, J., & Harding, D.J. (1994). Optimization of an airborne laser altimeter for remote sensing of vegetation and tree canopies. *Proceedings of the International Geoscience and Remote Sensing Symposium* August 8-12, 1994 (pp. 939-941). Pasadena, CA.

Blair, J.B., Rabine, D.L. & Hofton, M.A. (1999). The Laser Vegetation Imaging Sensor (LVIS): A medium- altitude, digitisation-only, airborne laser altimeter for mapping vegetation and topography. *ISPRS Journal of Photogrammetry and Remote Sensing*, 54, 115-122.

Blair, J.B. &. Hofton, M.A (1999). Modeling laser altimeter return waveforms over complex vegetation using high-resolution elevation data. *Geophysical Research Letters*, 1-4.

Bormann, B.T. & Likens, G.E. (1979). *Pattern and Process in a Forested Ecosystem.* New York: Springer-Verlag.

Brokaw, N. V. L., & Lent, R. A. (1999). Vertical structure. In M. L. Hunter (ed.), Maintaining biodiversity in forest ecosystems (pp. 373 – 399). Cambridge, UK: Cambridge University Press.

Campbell, G.S. & Norman, J.M. (1989). The description and measurement of plant canopy structure. In G. Russell, B. Marshall, and P. Jarvis (Eds.), *Plant Canopies: Their Growth, Form and Function* (pp. 1-19). Cambridge, U.K.: Canbridge University Press

Caspersen, J.P., Pacala, S.W., Jenkins, J.C., Hurtt, G.C., Moorcroft, P.R., & Birdsey, R.A. (2000). Contributions of land-use to carbon accumulation in U.S. forests. *Science* 290, 1148-1151.

Christensen, N.L. (1989). Landscape history and ecological change. *Journal of Forest History*, 33, 116-124.

Christensen, N.L. (1997). Managing for heterogeneity and complexity on dynamic landscapes. In S.T.A. Pickett, R.S. Ostfeld, M. Shachak, & G.E. Likens (Eds.), *The Ecological Basis of Conservation* (pp. 167-186). New York: Chapman and Hall.

Christensen, N.L., Bartuska, A.B., Brown, J.H., Carpenter, S., D'Antonio, C., Francis, R., Franklin, J.F., MacMahon, J.A., Noss, R.F., Parsons, D.J., Peterson, C.H., Turner, M.G., & Woodmansee, R.G. (1996) . The report of the Ecological Society of America committee on the scientific basis for ecosystem management. *Ecological Applications*. 6(3), 665-691.

Cronon, W. (1983). *Changes in the Land.* New York: Hill and Wang.

Drake, J.B. (2001). Estimation of Tropical Forest Aboveground Biomass Using Large-Footprint Lidar. Doctoral Dissertation. University of Maryland.

Drake, J.B., & Weishampel, J.F. (2001). Simulating vertical and horizontal multifractal patterns of a longleaf pine savanna. *Ecological Modeling,* 145, 129-142.

Drake, J.B. & Weishampel, J.F. (2000). Multifractal analysis of canopy height measures in a longleaf savanna. *Forest Ecology and Management,* 128, 121-127.

Dubayah, R.O., Knox, R.G., Hofton, M.A., Blair, J.B. & Drake, J.B. (2000). Land surface characterization using lidar remote sensing. In M.J. Hill and R.J. Aspinall (Eds.), *Spatial Information for Land Use Management* (pp. 25-38). Australia: Gordon and Breach Science Publishers

Dubayah, R.O. and Drake, J.B. (2000). Lidar remote sensing for forestry. *Journal of Forestry,* 98, 44-46.

Foster, D., Swanson, F., Aber, J., Burke, I., Brokaw, N., Tilman, D., & Knapp, A. (2003). The importance of land-use legacies to ecology and conservation. *Bioscience,* 53(1), 77-88.

Foster, D.R. & Boose, E.R. (1992). Patterns of forest damage resulting from catastrophic wind in central New England, USA. *Journal of Ecology* 80, 79-98.

Foster, D.R., Motzkin, G., & Slater, B. (1998). Land-use history as long-term, broad-scale disturbance: regional forest dynamics in central New England. *Ecosystems,* 1, 96-119.

Franklin, J.F., Lindenmayer, D., MacMahon, J.A., McKee, A., Magnuson, J., Perry, D.A., Waide, R., & Foster. D. (2000). Threads of continuity. *Conservation Biology in Practice,* 1(1), 8-16.

Franklin, J.F. & Forman, R.T.T. (1987). Creating landscape patterns by forest cutting: ecological consequences and principles. *Landscape Ecology,* 1, 5-18.

Franklin, J.F., Spies, T.A., Van Pelt, R., Carey, A., Thornburgh, D., Berg, D.R., Lindenmayer, D., Harmon, M., Keeton, W.S., Shaw, D.C., Bible, K. & Chen. J. (2002). Disturbances and the structural development of natural forest ecosystems with some implications for silviculture. *Forest Ecology and Management,* 155, 399-423.

13

Guiterrez, R., Neuenschwander, A.L., Crawford, M.M., Schutz, B.E., Urban, T., & Liadsky, J. (2005). Comparison of GLAS and small-footprint, airborne topographic lidar waveform data from non-homogenous land cover in central Texas. *American Geophysical Union Abstract.* Fall Meeting. December 5-9, 2005.

Hagen, J.M. (Ed.) (2001). *Forest Structure: A Multilayered Conversation. Proceedings of the Forest Information Exchange.* October 25, 2001. Orono, ME.: Manomet Center for Conservation Sciences. Brunswick, ME. 78 pp.

Hagen, J.M. & Whitman, A.A. (2001). A comparison of forest structure in old-growth, even-aged, and uneven-aged forest types in Maine. In J.M. Hagan (Ed.), *Forest Structure: A Multilayered Conversation. Proceedings of the Forest Information Exchange* October 25, 2001 (pp. 72-75). Orono, ME.: Manomet Center for Conservation Sciences.

Harding, D.J., Lefsky, M.A., Parker, G.G., & Blair, J.B. (2001). Laser altimeter canopy height profiles. Methods and validation for closed-canopy, broadleaf forests. *Remote Sensing of Environment,* 76, 283-297.

Hofton, M.A., Blair, J.B., Minster, J.B., Ridgeway, J.R., Williams, N.P, Bufton, J.L., & Rabine, D.L. (2000a). An airborne scanning laser altimetry survey of Long Valley, California. *International Journal of Remote Sensing,* 21, 2413-2437.

Hofton, M.A., Minster, J.B. & Blair, J.B. (2000b). Decomposition of laser altimeter waveforms. *IEEE Transcations on Geoscience and Remote Sensing* 38, 1989-1996.

Hudak, A.T., M.A Lefsky, W.B. Cohen, & M. Berterretche. (2002). Integration of lidar and LANDSAT ETM+ data for estimating and mapping forest canopy height. *Remote Sensing of Environment,* 82, 397-416.

Hyde, P., Dubayah, R., Peterson, B., Blair, J.B., Hofton, M., Hunsaker, C., Knox, R., & Walker, W. (2005). Mapping forest structure for wildlife habitat analysis using waveform lidar: Validation of montane ecosystems. *Remote Sensing of Environment,* 96, 427-437.

Hyde, P. (2005). Measuring and mapping forest wildlife habitat characteristics using lidar remote sensing and multi-sensor fusion. PhD. Dissertation. College Park, MD: University of Maryland. 137 pp.

Irland, L.C. (1999). *The Northeast's Changing Forest.* Cambridge, MA: Harvard University Press.

14

Keeton, W.S., Strong, A.M., Tobi, D.R., & Wilmot, S. (2001). Experimental test of structural complexity enhancement in northern hardwood–hemlock forests. In J.M. Hagan (Ed.), *Forest Structure: A Multilayered Conversation. Proceedings of the Forest Information Exchange* October 25, 2001 (pp. 33-40). Brunswick, ME: Manomet Center for Conservation Sciences.

Latham, P.A., Zuuring, H.R., & Coble, D.W. (1998). A method for quantifying vertical forest structure. *Forest Ecology and Management,* 104, 157-170.

Lefsky, M.A., Cohen, W.B., Acker, S.A., Parker, G., Spies, T.A., & Harding, D. (1999a). Lidar remote sensing of the canopy structure and biophysical properties of Douglas Fir-Western Hemlock Forests. *Remote Sensing of Environment,* 70, 339-361.

Lefsky, M.A., Harding, D., Cohen, W.B., Parker, G., & Shugart, H.H. (1999b). Surface lidar remote sensing of basal area and biomass in deciduous forest of eastern Maryland, USA. *Remote Sensing of Environment,* 67, 83-98.

Lefsky, M.A., Cohen, W.B., Hudak, A., Acker S.A., & Ohmann, J. (1999c). Integration of lidar, Landsat ETM+ and forest inventory data for regional forest mapping. *International Archives of Photogrammetry and Remote Sensing,* 32, Part 3W14, 119-126.

Lefsky, M.A., Harding, D.J., Parker, G.G., Cohen, W.B., & Acker, S.A. (1999d). Progress in lidar altimeter remote sensing of stand structure in deciduous and coniferous forests using SLICER data. ISPRS Workshop: Mapping Forest Structure and Topography by Airborne and Spaceborne Laser. November 9-11. La Jolla, CA.

Lefsky, M.A., Cohen,W.B., & Spies, T.A. (2001). An evaluation of alternate remote sensing products for forest inventory, monitoring, and mapping of Douglas-fir forests in western Oregon. *Canadian Journal of Forest Research-Revue Canadienne de Recherche Forestiere,* 31, 78-87.

Lefsky, M.A., Cohen, W.B., Parker, G.G., & Harding, D.J. (2002). Lidar remote sensing for ecosystem studies. *Bioscience,* 52(1), 19-30.

Lim, K., Treitz, P.,Wulder, M., St-Onge, B., & Flood, M. (2003). Lidar remote sensing of forest structure. *Progress in Physical Geography,* 27(1), 88-106.

Lindenmayer, D.B., Margules, C.R., & Botkin, D.B. (2000). Indicators of biodiversity for ecologically sustainable forest management. *Conservation Biology*, 14, 941-950.

McCombs, J.W., Roberts, S.D., &.Evans, D.L. (2003). Influence of fusing lidar and multispectral imagery on remotely sensed estimates of stands density and mean tree height ina managed Loblolly Pine plantation. *Forest Science,* 49(3), 457-466.

McGarigal, K. & McComb, W.C. (1995). Relationships between landscape structure and breeding birds in the Oregon Coast Range. *Ecological Monographs*, 65, 235-260.

Means, J.E., Acker, S.A., Harding, D.J., Blair, J.B., Lefsky, M.A., Cohen, W.B., Harmon, M.E., & Mckee, W.A.(1999). Use of large-footprint scanning airborne lidar to estimate forest stand characteristics in the Western Cascades of Oregon. *Remote Sensing of Environment,* 67, 298-308.

Nelson, R. (1997). Modeling forest canopy heights: The effects of canopy shape. *Remote Sensing of Environment,* 60, 327-334.

Ni-Meister, W., Jupp, D.L.B., & Dubayah, R. (2001). Modeling lidar waveforms in heterogeneous and discrete canopies. *IEEE Transacations on Geoscience and Remote Sensing*, 39(9), 1943-1958.

Northern Forest Lands Council. (1994). Finding Common Ground: The Recommendations of the Northern Forest Lands Council. Northern Forest Lands Council.

Onal, H. (1997). Trade-off between structural diversity and economic objectives in forest management. *American Journal of Agricultural Economics,* 79, 1001-1012.

Parker, G.G., Lefsky, M.A., & Harding, D.J. (2001). Light transmittance in forest canopies determined using airborne laser altimetry and in-canopy quantum measurements. *Remote Sensing of Environment,* 76, 298-309.

Parker, G.G. & Brown, M.J. (2000). Forest canopy stratification-it it useful? *The American Naturalist*, 155(4), 473-484.

Parker, G.G. (1995). Structure and microclimate of forest canopies. In M. Lowman & N. Nadkarni, (Eds.), *Forest Canopies: A review of research on a biological frontier.* (pp. 73-106). San Diego, CA: Academic Press.

16

Pickett, S.T.A., Ostfeld, R.S., Shachak, M., & Likens, G.E. (Eds.) (1997). *The Ecological Basis of Conservation. Heterogeneity, Ecosystems, and Biodiversity*. New York: Chapman & Hall.

Pommerening, A. (2002). Approaches to quantifying forest structures. *Forestry, 75*, 305-324.

Popescu, S.C., Wynne, R.H., & Scrivani, J.A. (2004). Fusion of small-footprint lidar and multispectral data to estimate plot-level volume and biomass in deciduous and pine forests in Virginia, USA. *Forest Science, 50*(4), 551-565.

Runkle, J.R. (1985). Disturbance regimes in temperate forest. In S.T.A. Pickett & P.S. White (Eds.), *The Ecology of Natural Disturbance and Patch Dynamics*. (pp. 17-33). Orlando, FL:Academic Press.

Spies, T.A. (1997). Forest stand structure, composition and function. In K.A. Kohm & J.F. Franklin (Eds.), *Creating a Forestry for the 21st century*. (pp.11-30). Washington, D.C: Island Press.

Wehr, A. & Lohr, U. (1999). Airborne laser scanning-and introduction and overview. *ISPRS Journal of Photogrammetry & Remote Sensing, 54*, 68-82.

Weishampel, J.F., Ranson, K.J., & Harding, D.J. (1996). Remote sensing of forest canopies. *Selbyana, 17*, 6-14.

Weishampel, J.F., Blair, J.B., Knox, R.G., Dubayah, R., & Clark, D.B. (2000). Volumetric lidar return patterns from an old-growth tropical rainforest canopy. *International Journal of Remote Sensing, 21*, 409-415.

Whitman, A.A. & Hagen, J.M. (2001). Assessing ecological value in old-growth and managed stands in northern Maine. In J.M. Hagan (Ed.), *Forest Structure: A Multilayered Conversation. Proceedings of the Forest Information Exchange*. October 25, 2001 (pp. 70-71). Brunswick, ME: Manomet Center for Conservation Sciences.

Whitney, G.G. (1994). *From Coastal Wilderness to Fruited Plain. A History of Environmental Change in Temperate North America*. Cambridge, U.K: Cambridge University Press.

Zenner, E.K. & Hibbs, D.E. (2000). A new method for modeling the heterogeneity of forest structure. *Forest Ecology and Management, 129*, 75-87.

Zimble, D.A., Evans, D.L., Carlson, G.C., Parker, R.C., Grado, S.C., Gerard, P.D. (2003). Characterizing vertical forest structure using small-footprint airborne LiDAR *Remote Sensing of Environment,* 87, 171–182.

CHAPTER 1

THE USE OF WAVEFORM LIDAR TO MEASURE NORTHERN TEMPERATE

MIXED CONIFER AND DECIDUOUS FOREST STRUCTURE IN

NEW HAMPSHIRE

Abstract

The direct retrieval of canopy height and the estimation of aboveground biomass are two

important measures of forest structure that can be quantified by airborne laser scanning at

landscape scales. These and other metrics are central to studies attempting to quantify

global carbon cycles and to improve understanding of the spatial variation in forest

structure evident within differing biomes. Data acquired using NASA's Laser Vegetation

Imaging Sensor (LVIS) over the Bartlett Experimental Forest (BEF) in central New

19

Hampshire (USA) was used to assess the performance of waveform lidar in a northern temperate mixed conifer and deciduous forest.

Using coincident plots established for this study, we found strong agreement between field and lidar measurements of height ($r^2 = 0.80$, $p < 0.000$) at the footprint level. Allometric calculations of aboveground biomass (AGBM) and LVIS metrics (AGBM: $r^2 = 0.61$, PRESS RMSE = 58.0 Mg ha^{-1}, $p < 0.000$) and quadratic mean stem diameter (QMSD) and LVIS metrics ($r^2 = 0.54$, $p = 0.002$) also showed good agreement at the footprint level. Application of a generalized equation for determining AGBM proposed by Lefsky et al. in 2002a to footprint-level field data from Bartlett resulted in a coefficient of determination of 0.55; RMSE = 64.4 Mg ha^{-1}; $p = 0.002$. This is slightly weaker than the strongest relationship found with a the best-fit single term regression model.

Relationships between a permanent grid of USDA Forest Service inventory plots and the mean values of aggregated LVIS metrics, however, were not as strong. This discrepancy suggests that validation efforts must be cautious in using pre-existing field data networks as a sole means of calibrating and verifying such remote sensing data. Regression models established at the footprint level for AGBM and QMSD were applied to LVIS data to generate predicted values for the whole of Bartlett. The accuracy of these models was assessed using varying subsets of the USFS NERS plot data. Coefficient of determinations ranged from fair to strong with aspects of land-use history and species

20

composition influencing both the fit and the level of error seen in the predicted relationships.

Introduction

Research over the past decade has demonstrated that large footprint, waveform sampling laser altimetry (hereinafter referred to as lidar) can characterize the structural complexity and associated functional properties of natural landscapes relevant to ecological investigations by providing vertical and volumetric profiles of forest vegetation. Lidar metrics have proven useful for predicting a range of ecological variables such as canopy height and structure, the density of forest cover, biomass, and light transmittance (Dubayah et al. 2000, Drake et al. 2002, Lefsky et al. 2002b, Means et al. 1999, Harding et al. 2001, Parker et al. 2001, Hyde et al. 2005). Lidar remote sensing can also generate data that can be used to provide three-dimensional, or volumetric characterizations of vegetation structure (Weishampel et al. 2000, Lefsky et al.1999a, Harding et al. 2001). It can accurately capture spatial patterns of canopy heights (Drake and Weishampel 2000). Height data provided directly by laser altimetry sensors can serve as a surrogate estimator of stand age or successional state when coupled with species composition and site quality information (Dubayah et al. 2000). Lidar waveforms generated by medium-large footprint sensors such as LVIS, by themselves, can also be used to distinguish among

21

important land use types reflecting both historical and other environmental controls (Dubayah et al. 2000).

It is expected that lidar's ability to rapidly measure the three-dimensional structure of canopies can and should stimulate the development of new systems of canopy description (Lefsky et al. 2002b, Parker and Brown 2000, Parker et al. 2001) and provide ready means to facilitate the study of spatial variation patterning within forest structure across landscape scale tracts of land (Parker 1995, Zimble et al. 2003). According to the overview published by Lefsky et al. (2002b), current ecological applications of lidar remote sensing tend to fall within three categories: remote sensing of ground topography, measurement of three-dimensional structure and function of vegetation canopies, and prediction of forest stand structure attributes (such as aboveground biomass). The ability of lidar to predict biomass variables has been very good, as compared with non-lidar remotely sensed estimates, with six published waveform studies reporting greater than 75% of variance explained (Lefsky et al. 1999a, 1999b, Means et al. 1999, Nilsson 1996, Drake et al. 2002, Hyde et al. 2005). These initial studies have been conducted in temperate deciduous, temperate coniferous, tropical wet forest and boreal coniferous biomes. It is important, however, that the relationships between lidar metrics and directly measured forest structural characteristics be examined in an expanding range of terrestrial biomes (Drake 2001, Lefsky et al. 2002b).

To this end, we report here on a northern temperate mixed conifer and deciduous forest in central New Hampshire (USA). The objective of this study was to assess the ability of a

22

large footprint lidar to describe and predict forest structure in the variable terrain of mixed forest types typical of this region including northern hardwoods. The work was originally planned as part of the pre-launch calibration/validation of a spaceborne laser altimeter, the Vegetation Canopy Lidar (VCL). The White Mountain National Forest site was selected as a part of a series of core VCL validation sites in North and Central America, representing globally important forest and woodland biomes and exhibiting diverse canopy structures and phenologies (Knox et al. 2000). As in previous studies (Drake et al. 2002, Hyde et al. 2005), calibration and validation is accomplished by comparing spatially explicit field measurements of structure to comparable metrics derived from data collected by NASA's Laser Vegetation Imaging Sensor (LVIS; Blair et al. 1999). Few waveform-recording lidar studies assessing structural metrics have been previously reported from temperate deciduous forest (Lefsky 1997 and Lefsky et al. 1999b; tulip poplar (*Liriodendron tulipifera*) association of the coastal plain of Maryland) and only one small footprint lidar study (Lim et al. 2003) has been reported from a predominately northern hardwood forest.

Site

Over the past seventy years, the USFS Northeastern Research Station (USFS NERS) has

assembled a large volume of field data (e.g. Leak 1982, 1996, 1999, Leak and Smith

1996, 1997, Leak and Sendak 2002, Smith et al. 2002) on a variety of ecosystem

processes and forest metrics within the 1052 hectare Bartlett Experimental Forest (BEF)

located within the White Mountain National Forest in the central White Mountains, N.H.

(Figure 1.1). The landscape of this site reflects an extensive history of experimental forest

management and varied natural disturbance regimes. Deciduous and coniferous forest

types including northern hardwood [i.e. sugar maple (*Acer saccharum* Marsh), beech

(*Fagus grandifolia* Ehrh.), yellow birch (*Betula alleghaniensis* Britton)], red spruce-

balsam fir (*Picea rubens* Sarg. - *Abies balsamea* (L.) Miller), eastern hemlock (*Tsuga*

canadensis (L.) Carr.), and red oak-white pine (*Quercus rubra* L. - *Pinus strobus* L.)] are

represented on a landscape ranging in elevation from 200 m to 850 m. Slopes vary from

flat terrain to nearly vertical (rock cliff) conditions. The forest reflects a range of

successional sequences, forest patch sizes, and structural distributions. Clear-cutting,

group and individual tree selection, basal area and shelter-wood cuttings have been

undertaken on approximately 55% of the forest. Forest ages in managed stands range

from over 70 to less than 5 years old. The remaining portion of the forest serves as an

24

unmanaged, natural control. Ages for trees within this experimental forest range upwards of 100 years (Leak and Smith 1996).

Lidar Data

Lidar data was acquired on September 26, 1999 and July 18-26, 2003 over the BEF using the Laser Vegetation Imaging Sensor (LVIS; Blair et al. 1999). LVIS was used to map a swath of land approximately 5 x 60 km. in 1999 and 8 x 60 km. in 2003, extending from Bartlett, N.H. to West Thornton N.H. LVIS is an airborne imaging laser altimeter that records the time and amplitude of a laser pulse reflected off target surfaces. The sensor digitizes the vertical distribution of intercepted surfaces between the first (top of the canopy) and the last (ground) return producing a waveform record. LVIS records circular footprints of variable size; 1999 footprints had a nominal radius of 12.5 m; 2003 footprints were reduced to a nominal radius of 10 m. Additional detail on LVIS capabilities can be found in Blair et al. (1999). The 2003 LVIS flight consisted of a newly-enhanced laser altimeter instrument including digitally-recorded return waveforms, and integrated inertial navigation system (INS) and global position system (GPS) sensors that flew on the NOAA Cessna Citation aircraft at about 10 km above ground level during a one week mission (http://lvis.gsfc.nasa.gov) over New England. LVIS footprints are reported to be geo-located to within 1-2 m. (Blair and Hofton 1999; Hofton et al. 2000a).

LVIS metrics used in this study were derived from waveforms using automated algorithms based on the research of Hofton et al. 2000b. Further information on the 2003 LVIS beta data release is provided in Blair et al. (2004). Lidar canopy height was calculated by identifying two locations within the waveform; (1) where the signal initially increases above a mean noise level/threshold (the canopy top) and (2) at the center of the last Gaussian pulse (the ground return). The distance between these two locations was then calculated to derive the height metric (see Figure 1.2 adapted from Drake et al. 2002). The height of median energy metric was calculated by finding the median of the entire signal (i.e. above the mean noise level) from the waveform, including energy returned from both canopy and ground surfaces. The distance between this median location and the center of the last Gaussian pulse was then calculated to derive a height of median energy (Drake et al. 2002). Similarly, the 2003 metrics RH25 and RH75 were calculated by finding the relative height (RH), relative to the ground elevation, at which 25% and 75% respectively of the waveform energy occurs (Blair et al. 2004). Varying abbreviations for comparable lidar metrics have been published within the literature and released via on-line data sources. Within this study, the 1999 lidar canopy height abbreviation of LHT is directly comparable to the 2003 metric RH100. Similarly, the 1999 measure of height of median energy metric abbreviation of HOME is directly comparable to the 2003 metric RH50.

The number of footprints falling within the boundaries of BEF varies between the 1999 (70,496) and 2003 (62,579) LVIS flights. A substantial number of footprints (18,217 of the 70,496: 26%) of the 1999 LVIS footprints were eliminated from analysis because of

26

weak or ambiguous ground return signals. Research by Hofton et al. (2002) has noted that in some dense forest canopies, or areas of high canopy cover, the portion of the lidar signal being reflected from the ground can be weak, making ground determination ambiguous at best and indeterminable at worst. At Bartlett, this type of result may be potentially attributable to the often-dense cover of beech dominated-northern hardwoods and mixed hemlock-hardwood forests on site.

Field Data

Two separate sets of field data were available for analysis in this study. An initial set of footprint level ground plots (hereinafter referred to as the footprint level), specifically sited to be of use in the calibration and validation of individual LVIS waveforms, was created at the outset of this research in 2002. A second independent data set consisting of field plot data from the USFS NERS permanent inventory for BEF (hereinafter referred to as the USFS NERS plot level), re-sampled near in time to the original LVIS flight and coincident with the second LVIS flight, was also available to this study. These data provide a comprehensive ground inventory of standing biomass and species composition of the Bartlett Experimental Forest. Comparison of the results from each set of field data is instructive in assessing the interchangeability of pre-existing inventory data with original field data designed specific to the lidar study. The extensive nature of the second data set also allows the influence of land-use history and species composition on the relationships with waveform lidar metrics to be explored in a preliminary manner.

27

Finally, it provides a substantial amount of independent data for assessing the accuracy of predictions made using the relationships obtained from the footprint level data. Each data set and associated data analysis is described in greater detail below.

Footprint Level

Field methods followed unpublished protocols developed by NASA's VCL science team for forest structure data collection in different biomes in North and Central America. At BEF, plots were chosen to represent a range of height and habitat classes evident within the experimental forest. Twenty circular 0.07 ha (15 meter radius) plots centered on 1999 laser footprints, distributed throughout the study area, were established. Trimble Navigation Pathfinder ProXR global positioning system equipment (GPS) was used to locate the center of these circular LVIS footprints. Data was collected in a 3-D over-determined mode utilizing real-time differential correction. The position dilution of precision (PDOP) mask was set at 6 and consistent readings from a minimum of five satellites producing less than 1-meter displacement were secured before marking the plot center. The 0.07 ha footprint plots were designed to allow direct comparison of field measurements with individual lidar footprints; the plot size was slightly larger than the nominal footprint to compensate for geolocation errors, if needed (Hyde et al. 2005). Subsequent to the establishment and siting of the footprint level plots, the coordinate data defining the center points of 1999 LVIS footprints was reprocessed. This correction increased the distance between the previously located field plots and the closest 1999

28

LVIS footprints. The average distance between field plots and 1999 LVIS reprocessed position is 1.2 meters (with a maximum distance of 2.9 m). Flight lines varied between 1999 and 2003. As a result, the average distance between the center point of the same field plots and the center point of the closest 2003 footprint is 6.2 meters (with a maximum distance of 10.4 meters).

Field plot data were collected during the summers of 2002 and 2003. Laser rangefinders and sonic hypsometers were used to obtain precise tree structural data and create detailed stand maps for the GPS-sited research plots. Measurements included tree height, stem diameter (dbh), and the bearing and distance of each stem from plot center. Live and dead stems greater than 10 cm dbh were mapped. The dbh of the stem and crown radii metrics were measured with fiberglass tapes. Living stems were identified to species. A Laser Technology Inc. (LTI) Impulse series 200LR laser rangefinder (Laser Technology, Inc., Englewood, Colorado) in filter mode was used to collect tree height data. Haglof Forestor DME 201 (Forestry Suppliers Inc., Jackson, Mississippi) sonic hypsometers and sighting compasses were used to collect the horizontal distances and bearings used for stem mapping within the plot.

Stem diameters were used to calculate quadratic mean stem diameter (QMSD). QMSD was calculated as $[\Sigma D^2/n]^{1/2}$ where D is the stem diameter and n is the number of stem diameters in the plot (Curtis and Marshall 2000). Estimates of aboveground woody biomass (AGBM) were calculated from the field dbh data using established allometric equations specific to the northeastern region, which includes bole, branch and foliar

29

biomass (Hocker and Early 1983, Tritton and Hornbeck 1981, Young et al. 1980, and Whittaker et al. 1974). These equations were applied to the field data to calculate total standing AGBM for each stem (live and dead) and then summed to provide the AGBM of all stems within a plot. Whole forest averages for these metrics are seen in Table 1.1.

Statistical analyses were conducted using JMP IN® software (Sall et al. 2005). Dependent, independent variables and the regression residuals were tested for normality of their distributions using the Shapiro-Wilk W test (Shapiro and Wilk 1965) and normal quantile plots. Any variable or its transform not meeting one or more of the normality distribution tests was eliminated from regression analyses. A prediction error sum of squares root mean square error (PRESS RMSE) was calculated for each forest metric. The PRESS RMSE is computed as the square root sum of squares of the prediction residuals (Mark and Workman 1991, Hastie et al. 2001). As a validation technique, Press RMSE tests how well the current model would predict each of the points in the data set (in turn) if they were not included in the regression. Low values of PRESS RMSE usually indicate that the model is not overly sensitive to any single data point. PRESS is considered comparable to tests of independent validation (Kozak and Kozak 2003). At the footprint level, the scatter plots between field-measured maximum canopy height and the 1999 and 2003 LVIS measures of canopy height were compared (Figure 1.3). The 2003 data cloud is more accurately clustered around the 1:1 line, with less consistent bias towards underestimation than seen in the 1999 results. As a result, footprint-level regression analyses were conducted using 2003 LVIS metrics.

The subset of untransformed LVIS metrics that corresponds with the 20 footprint level

plots are highly correlated (all pairs greater than 91%). To avoid the effects of multi-

collinearity, simple linear regression was used to relate the dependent forest structural

variables of height, $QMSD^2$, or AGBM to the best single metric independent LVIS-

derived variables (RH25, RH50 and their squares, $RH75^2$, or $RH100^2$). For the footprint

level AGBM regression linear model, both dependent and independent variables were

normally distributed. For the footprint level QMSD regression model, both dependent

and independent variables were squared to meet the normality requirements of regression.

USFS NERS Plot Level

The USFS NERS originally established a regular grid of over 400 permanent research

plots at Bartlett Experimental Forest in 1931-1932. The latest re-sampling of 409 of these

0.1 ha square plots was undertaken by the USFS NERS in the 2001-2003 field seasons.

Observations recorded species and measured dbh in 1-inch (2.54 cm) dbh classes only for

trees greater than 1.5 inches (ca. 4 cm) in size. Plots fell into either managed or

unmanaged conditions (Leak and Smith 1996). QMSD and AGBM estimates were

calculated in the same manner described for the footprint-level data, although the lower

cut-off for stem size at the plot level (ca. 4 cm vs. 10 cm) should be noted. QMSD was

calculated per plot using the same dbh cutoff as with the footprint level. Whole forest

averages for these metrics can be found in Table 1.1. The relative fraction of AGBM

attributed to each tree species was calculated for each of the 409 plots used in this

31

analysis. All inventory plots have been geo-referenced to within 3-meter positional accuracy.

Given the larger number of available footprints from the 2003 LVIS flight and the coincident timing and collection of field versus flight data, plot level analyses were conducted using just the 2003 LVIS metrics. In comparison to the 0.1 ha square USFS NERS inventory plots, the 2003 LVIS circular footprints are 0.031 hectares in size. LVIS footprints whose center points were located within the bounds of USFS NERS plots were selected for analysis. Given the variable overlap of LVIS flight lines during the 2003 flight over Bartlett, any given USFS NERS plot contained the center points of from one to seventeen lidar footprints. For each of the USFS NERS plots, a set of mean values was calculated from each of the aggregated LVIS 2003 metrics (RH25, RH50, RH75 and RH100).

USFS NERS plot level measures of AGBM and QMSD were compared to the mean values of the 2003 LVIS metrics (RH25, RH50, RH75 and RH100) through stepwise mixed multiple regression. Dependent, independent variables and the regression residuals were tested for normality of their distributions using the Shapiro-Wilk W test (Shapiro and Wilk 1965) and normal quantile plots. As multiple regression results in inflation of the probability of type 1 error (Wilkinson et al. 1992), we reduced the alpha (the critical value of p) to 0.01. For each model, variables not significant at this level were eliminated. In addition, the variance inflation factor (VIF) was recorded for models with multiple predictors. VIF indicates whether multicollinearity between variables

32

inflates the variance of estimates and renders the model unstable and of less applicability to new sets of data. Variables with VIF values under 10 are indicative of models with low multicollinearity (Sall et al. 2003). Mallow's Cp statistic was also used to compare the predictive abilities of various models (Kozak and Kozak 2003). As a result, square and cross-product variables were not used in these analyses. Lastly, PRESS RMSE was calculated for each forest metric.

Forest Service categorical data made available to this study designated 158 of the BEF USFS NERS plots as being located in largely unmanaged tracts of the experimental forest (Leak and Smith 1996). Analyses using mixed stepwise regression compared the plot level metrics of AGBM and QMSD with the set of aggregated mean LVIS metrics on this subset of data. These restrictions on the data set provide an initial coarse look at the influence of land use history on these relationships.

The relative fraction of biomass attributed to individual tree species within each of the 409 USFS NERS plots was used to help assess the influence of species composition on the overall plot level relationships between plot-level AGBM and the aggregated mean LVIS metrics. The presence, absence, or dominance patterns of ten of the common tree species found at Bartlett were used to subset the data prior to regression. Subset data was analyzed using mixed stepwise multiple regressions. These included the identification of plots where certain species were absent, certain species were present in any amount, or certain species were present as a predominant species (i.e. species fraction of AGBM > 0.25 or more).

Predicted Relationships

To further assess the quality of the relationships modeled using the footprint level data, predicted AGBM and QMSD estimates for the experimental forest were created using the footprint-level models (Table 1.3; Eqs. 2 and 4) applied to the LVIS 2003 data set. The elimination of a significant number of 1999 LVIS footprints from analysis because of weak or ambiguous ground return signals means that the 2003 LVIS flight provided more comprehensive coverage of BEF through the contributions of an additional 10,300 footprints above the useable 1999 totals. Simple linear regression was used to compare these predicted values with the USFS NERS plot-level measures for AGBM and QMSD. The influence of selected aspects of species composition and management history on these results was also examined by evaluating the models' performance for selected subsets of plots. As with earlier analyses, PRESS RMSE statistics were generated and used to assess the level of error within each model.

Test of a Generalized Prediction Equation for AGBM

Lefsky et al. (2002a) have hypothesized that a single equation (AGBM = 0.342 * mean canopy height squared + 2.086 * the product of mean cover and mean canopy height; r^2 = 0.84, p <0.0001 or alternatively AGBM = 0.378 * mean canopy height squared; r^2 = 0.84, p <0.0001) can be used to relate remotely sensed canopy structure to estimated AGBM in distinctly different forested biomes. Their initial work compared temperate deciduous,

34

temperate coniferous and boreal coniferous biomes. The finding and replication of such a generalized equation across biomes would simplify modeling of forest carbon storage.

The latter version of the generalized equation was explored at both the footprint and plot levels at BEF. Lefsky et al. (2002a) define mean canopy height (MCH) as the average height of the waveforms associated with a plot. Footprint level plots at BEF compare the metrics derived from a single waveform with ground measures, while plot level data compare the mean of various waveform metrics occurring within a USFS NERS plot with ground measures. Of the 2003 LVIS waveform metrics assessed at BEF, the maximum height of the waveform (RH100) is the most comparable metric to MCH at the plot level, and differs at the footprint level only in being derived from a single waveform rather than as the average of aggregated waveforms. As such, a substitution of maximum canopy height squared ($RH100^2$) for mean canopy height squared was made to the generalized equation proposed for the prediction of AGBM at BEF. This provided an approximate, but reasonably close assessment of the relationship described by the generalized equation.

As above, simple linear regression was used to compare these predicted values with the USFS NERS plot-level measures for AGBM and QMSD. The influence of selected aspects of species composition and management history on these results was also examined by evaluating the models' performance for selected subsets of plots. As with earlier analyses, PRESS RMSE statistics were generated.

35

Field Data

Across BEF as a whole, forest structural metrics as derived from footprint level measurements were comparable to results from plot level measurements (Table 1.1). Plot level data from 2001-2003 of 409 (0.1 ha) plots had a mean AGBM of 241.9 Mg ha^{-1} and 24.8 cm for QMSD. This compared well with the totals from the footprint level data established for this study: 230.4 Mg ha^{-1} for AGBM and 25.4 cm for QMSD of all 20 (0.07 ha) footprint level plots. It should be noted that USFS NERS plot data extensively samples the upper end of the biomass spectrum at Bartlett leaving only 12 of 409 plots used in this study with total AGBM estimates under 100 Mgha^{-1}.

Footprint Level

Regression results are summarized in Table 1.2. The mean of the maximum canopy height metrics derived from the 2003 LVIS data was most comparable to results from footprint level measurements (Table 1.1). At the footprint level, metrics from the 2003 LVIS data were able to estimate the structural attributes of AGBM and QMSD throughout the range of conditions at Bartlett. The height at which 50% of the waveform energy occurs (RH50) was a significant predictor of total biomass at the footprint level

for the 2003 LVIS metrics, explaining 61% of the variation. This result was compared to those derived from application of a generalized AGBM equation (Table 1.2:eq. 3) proposed by Lefsky et al. (2002a). Use of the 2003 LVIS metric of $RH100^2$ produced a coefficient of determination of 0.55 with slightly higher error than the best-fit model from the footprint data. The 2003 LVIS metric of canopy height squared ($RH100^2$) was also a good predictor of the square of QMSD explaining 54% of the variation. Scatter plots with best fit lines are found in Figure 1.4.

USFS NERS Plot Level

USFS NERS plot level regression results are summarized in Table 1.3. Relationships between plot level AGBM and QMSD estimates and LVIS 2003 metrics showed less overall agreement than those seen at the footprint level. While the coefficients of determination were not strong, improvement in the fit of the relationships and reduced levels of error were seen in the models derived from plots located in largely unmanaged forest conditions.

For this data set, the species composition of a plot did exert influence on the relationship between AGBM and LVIS metrics (Table 1.4). For example, when the percentage of red spruce biomass was relatively high within a plot, the data showed good agreement between aboveground biomass and the LVIS metric of canopy height. The presence of white pine at any level resulted in a strong relationship between estimated AGBM and

37

LVIS metrics. The absence of the common components of northern hardwood forests,

particularly yellow birch and American beech, within the plots also led to fairly strong

agreement between aboveground biomass and certain LVIS metrics. Three-quarters of

the relationships explored here were best predicted, alone or in combination, by the sub-

canopy LVIS RH50 metric. When the predominance of a species was used to select plots,

half of the relationships tended to be better predicted, alone or in combination, by the

LVIS RH100 metric reflecting highest canopy height.

Predicted Relationships

Relationships between AGBM and QMSD, predicted using relationships established at

the footprint level, and USFS NERS plot level measures are found in Table 1.5 and

Figures 1.5 & 1.6. The influence of selected aspects of species composition and

management history was also examined through varying restrictions on plot selection.

Overall relationships for predicted AGBM and QMSD across all plots ranged from fair to

strong. As seen earlier in the plot level relationships, coefficients of determination and

levels of error associated with the predictions of AGBM tended to improve when the

northern hardwood species of yellow birch and beech were not present. Unmanaged

conditions and the predominance of spruce also improved the predicted relationships.

These effects were more pronounced in the relationships with AGBM versus those seen

with the QMSD models.

Error was also reduced when plot selection was restricted by species composition and/or plots were sited in forest tracts with little recent management activity. The lowest PRESS RMSE error of 33.13 Mg ha^{-1} (Table 1.5) reported for a footprint-level AGBM regression model is approximately 14% of the mean USFS NERS plot level AGBM value of 241.9 reported in Table 1.1. The lowest PRESS RMSE error of 2.17 cm (Table 1.5) reported for a footprint-level QMSD regression model is approximately 9% of the mean USFS NERS plot level QMSD value of 24.8 reported in Table 1.1.

Discussion

Footprint Level Relationships

The relationships between lidar metrics and field-derived forest structural measures at the footprint scale are generally strong. Single term equations (Table 1.2, eqs.2 and 4) derived through linear regression using the 2003 LVIS metrics explain up to 80% of the variation in maximum canopy height, 61% of the variation in estimated AGBM, and 54% of the variation in QMSD, across the range of conditions sampled in this northern temperate forest landscape.

Some of the residual error may well reflect the increasing distance between the actual location of the footprint level field plots and the center of the closest LVIS footprints as flown in 2003. Additionally, the nominal size of the 2003 footprints is less than half the area of the footprint level field plots. Footprint level field plots were originally located using Trimble GPS to be within one meter of 1999 LVIS footprint coordinates, but 2003 LVIS flight lines vary of necessity from those flown in 1999, resulting in less overlap between the closest 2003 LVIS footprints and the footprint level plots. The size of the footprint level field plots was also originally determined by the larger nominal footprint size of the 1999 flight.

Footprint level results from this research can be compared to the one other published study (Lefsky et al. 1999b) using waveform lidar on a temperate deciduous site in eastern Maryland. Mean AGBM figures are comparable for the two sites (NH: 241.9 Mg ha^{-1}; MD: 235.9 Mg ha^{-1}). Lefsky et al. (1999b) reported that a height index developed for their study, quadratic mean canopy height (QMCH) predicted 80% of the variance in aboveground biomass. Standard deviation of the residuals resulting from this linear regression was reported as 75.1 Mg ha^{-1}. Although a different predictor is used with the Bartlett data, the results are somewhat lower with a predicted variance of 61% for AGBM. Error, however, was generally lower at Bartlett with PRESS RMSE calculated at 58.03 Mg ha^{-1}.

At Bartlett, application of a modified version of Lefsky et al.'s (2002a) generalized equation (AGBM = 0.378 * maximum canopy height squared) to footprint level data

40

resulted in a coefficient of determination of 0.55; RMSE = 64.41 Mg ha^{-1}; N=20; p = 0.0002. This is only slightly weaker than the strongest relationship found with the 2003 LVIS metrics and estimated AGBM at the footprint level (Table 1.2). Lefsky et al. (2002a) reported r^2 values of 65% for temperate deciduous plots using both the generalized equation and an individual site equation.

USFS NERS Plot Level Relationships

Plot level relationships between AGBM and QMSD and LVIS 2003 metrics show less overall agreement (Table 1.3) than those established at the footprint level. The use of aggregated footprint metrics coincident within a larger plot does not provide as strong a fit as the more precisely matched footprint-level data set. The results may also reflect on some limitations of the Forest Service data set in sampling low biomass areas within the experimental forest. Without the full range of conditions sampled, the variability seen in total AGBM of mature forest types at BEF swamps the narrower range of LVIS metrics. The same patterns hold true for QMSD. The footprint data reflect a wider distribution of conditions.

The improvement seen in the fit and error of the relationships measured in unmanaged forest conditions likely reflects on the size and type of disturbance typically encountered at BEF and its' interaction with geo-location errors. The majority of recent management actions at BEF are small operations, ranging from clear-cuts and group selection cuts of a

41

few hectares to shelterwood and individual tree selection cuts within management

compartments that may cover from 10 to 50 hectares. As a result, the maximum tree

height of a given area can change dramatically within a few meters within or near the

edges of these managed tracts. Such small scale edge effects, especially in areas of partial

cutting, may confound relationships between LVIS footprints and nearby USFS NERS

plots, even with relatively small spatial registration errors. The level of error seen in the

regression models for each of the forest metrics consistently dropped in unmanaged forest

conditions.

The most notable improvement in the fit of the relationship between Forest Service plot-

level biomass measurements and LVIS metrics was seen when species composition of the

plots was also factored into the analysis (Table 1.4). In particular, the absence of certain

species with dense crown architecture tended to improve the relationship between plot

estimates of AGBM and LVIS metrics. This was most apparent within unmanaged forest

tracts at Bartlett. The total absence of American Beech or Yellow Birch within the plots

demonstrated strong agreement between aboveground biomass and certain LVIS metrics.

Beech is very effective at intercepting light in the understory. Studies from Hubbard

Brook Experimental Forest (HBEF) (Siccama; unpublished data cited in Hane 2003) give

an indication of the tremendous stem density that is currently achieved by beech in

certain northern hardwood forests. Between 1965 and 1997, the number of beech in the

understory (trees < 10 cm. dbh) within northern hardwood tracts at HBEF has exploded

by nearly fivefold; a response to the impact of beech bark disease on that forest following

42

its arrival in the 1970's (Hane 2003). A similar response is documented for the Bartlett Forest (Leak and Smith 1996).

Beech is a dominant species in forest communities where light intensities are typically quite low (Curtis 1959). Its clonal nature, particularly following disturbance, further augments the density of its cover in the understory. But the absence of beech in the forests at Bartlett is common in the higher elevation ridgeline coniferous forests on BEF's western boundary. Here, the predominance of red spruce in these plots may be just as important as the absence of beech in explaining the strong relationship between biomass and LVIS metrics. Over 62% (15 of 24) of the plots selected at Bartlett as having a high fraction of spruce biomass were also selected as plots where beech is absent. Similarly, over 70% (24 of 34) of the plots selected at Bartlett where white pine is present were also selected as plots where yellow birch is absent.

Predicted Relationships

As suggested by the low coefficients of determination, the overall ability to predict AGBM and QMSD using the footprint level regression models across all of the forest conditions at BEF appears weak. Coefficients of determination between actual versus predicted measures of AGBM and QMSD were 0.27 and 0.20, respectively.

Yet, under selected conditions, notable and potentially useful improvements were seen. In this northern temperate mixed conifer and deciduous forest, predictions made in areas relatively untouched by recent management operations were particularly good at producing results with lower levels of error. In addition, given some level of pre-existing knowledge of species composition (i.e. presence, absence, or predominance patterns), strong predictive models with associated strong reductions in error were produced for some forest types. For example, forest stands dominated by red spruce at BEF were more readily predicted. The distinctiveness of such stands, given their shorter stature at the higher elevations of Bartlett, likely contributed to the success of modeling them with LVIS metrics. Forest tracts dominated by the typical northern hardwoods species of yellow birch and American beech were the most difficult to model at BEF. Of the hardwoods, only sugar maple, where found in high abundance, provided relatively good results from the predictive models. The explanation behind this successful modeling of stands with high abundance of sugar maple may be complex, involving the history of natural disturbance over the past century and its relationship with broad environmental conditions at Bartlett. Further work on this question is underway. These findings augment those of other lidar researchers, such as Popescu et al. (2004), who have noted that differentiation of forest types will result in the improvement of regression models aimed at estimating forest parameters.

Application of a modified version of Lefsky et al.'s (2002a) generalized equation (AGBM = 0.378 * maximum canopy height squared) to the plot level data provided weaker results than the best fit model derived from the footprint level data, although the

44

predictions did show the same trend towards improvement when analyses were restricted to plots with relatively unmanaged conditions or by species composition. The scatter plots and regression lines shown in Figure 1.7 show the tendency for the generalized equation to overestimate AGBM.

Conclusions

Metrics derived from an airborne waveform lidar sensor were significantly correlated with forest structural characteristics at the footprint level in a structurally variable northern temperate mixed conifer and deciduous forest. Single-term regression models were derived for AGBM without transformation of the dependent and independent variables. At the level of individual LVIS footprints, the relationships between lidar metrics and forest structural characteristics were weakened by problems of geo-location. In addition, height measures were more consistently underestimated by 1999 LVIS metrics than by 2003 LVIS metrics. As a result, predicted values for AGBM or QMSD used to map overall forest spatial patterning at Bartlett were more accurate when utilizing models derived from 2003 LVIS metrics.

USFS NERS plot level lidar metrics, however, were strongly correlated with forest structural characteristics only under more limited conditions in the same forest. With the

45

majority of the field-measured forest structural data coming from the high-end of the biomass spectrum at Bartlett, the relationships between instrument metrics and field measures were more weakly correlated; impacting their use as a calibration and validation data set. These relationships could be selectively improved, however, when characteristics of land-use and species composition were taken into consideration. As a result, spatial patterning and variation seen in canopy height, QMSD and biomass can be mapped at a landscape scale; producing unique data sets for use in operations extending from ecological modeling and inventory to conservation planning and forest management. While data on species composition is not easily retrieved from lidar sensors alone, other sources of remote sensing data providing spectral information could complement lidar data in this respect. This will be a focus of future research.

A modification of the generalized biomass equation proposed by Lefsky et al. (2002a) met mixed success in this study. At the more precise scale of LVIS footprints, the equation was only slightly weaker in fit and error than the best-fit model derived from the associated field data. At the larger plot scale, the relationships between predicted and actual were relatively weak.

This study confirms earlier published findings on waveform lidar and adds further perspective on the workings of lidar sensors under conditions of high canopy closure in northern temperate mixed conifer and deciduous forests. Augmenting existing findings for discrete return lidar in northern hardwoods (Lim et al. 2003), it also demonstrates that

46

waveform lidar can be used to estimate key biophysical properties of northern hardwood and associated forest types.

Acknowledgements

Blair, J.B. & Hofton, M.A. (1999). Modeling laser altimeter return waveforms over complex vegetation using high-resolution elevation data. *Geophysical Research Letters*, 1-4.

Blair, J.B., Rabine, D.L., & Hofton, M.A. (1999). The Laser Vegetation Imaging Sensor (LVIS): A medium- altitude, digitisation-only, airborne laser altimeter for mapping vegetation and topography. *ISPRS Journal of Photogrammetry and Remote Sensing*, 54, 115-122.

Blair, J.B., Hofton, M.A., & Rabine, D.L. (2004). Processing of NASA LVIS elevation and canopy (LGE, LCE and LGW) data products, version 1.0. (http://lvis.gsfc.nasa.gov).

Curtis, J.T. (1959). *The Vegetation of Wisconsin*. Madison, WI: University of Wisconsin Press, 657 pp.

Curtis, R.O. & Marshall, R.O. (2000). Why Quadratic Mean Diameter? *Western Journal of Applied Forestry*, 15(3), 137-139.

Drake, J.B. (2001). Estimation of Tropical Forest Aboveground Biomass Using Large Footprint Lidar. Doctoral Dissertation, College Park, MD: University of Maryland.

Drake, J.B., Dubayah, R.O., Clark, D.B., Knox, R.G., Blair, J.B., Hofton, M.A., Chazdon, R.L., Weishampel, J.F., & Prince, S.D. (2002). Estimation of tropical forest structural characteristics using large-footprint lidar. *Remote Sensing of Environment*, 79, 305-319.

Drake, J.B. & Weishampel, J.F. (2000). Multifractal analysis of canopy height measures in a longleaf savanna. *Forest Ecology and Management*, 128, 121-127.

Dubayah, R.O., Knox, R.G., Hofton, M.A., Blair, J.B., & Drake, J.B. (2000). Land surface characterization using lidar remote sensing. In M.J. Hill and R.J. Aspinall (Eds.), *Spatial Information for Land Use Management* (pp.25-38). Australia: Gordon and Breach Science Publishers.

Hane, E. N. (2003). Indirect effects of beech bark disease on sugar maple seedling survival. *Canadian Journal of Forest Research*, 33, 807-813.

Harding, D.J., Lefsky, M.A., Parker, G.G., & Blair, J.B. (2001). Laser altimeter canopy height profiles. Methods and validation for closed-canopy, broadleaf forests. *Remote Sensing of Environment*, 76, 283-297.

Hastie, T., Tibshirani, R. & Friedman, J. (2001). *The Elements of Statistical Learning: Data Mining, Inference and Prediction.* Springer-Verlag. 536. pp.

Hocker, H.W. & Early, D.J. (1983). Biomass and leaf equations for northern forest species. Research Report 102, Durham, N.H.: New Hampshire Agricultural Experiment Station.

Hofton, M.A., Blair, J.B., Minster, J.B., Ridgeway, J.R., Williams, N.P., Bufton, J.L., & Rabine, D.L. (2000a). An airborne scanning laser altimetry survey of Long Valley, California. *International Journal of Remote Sensing*, 21, 2413-2437.

Hofton, M.A., Minster, J.B., & J.B. Blair. 2000b. Decomposition of laser altimeter waveforms. IEEE *Transactions on Geoscience and Remote Sensing*, 38(4), 1989-1996.

Hofton, M., Rocchio, L., Blair, J.B., & Dubayah, R. (2002). Validation of vegetation canopy lidar sub-canopy topography measurements for a dense tropical forest. *Journal of Geodynamics*, 34(3-4), 491-502.

Hyde, P., Dubayah, R., Peterson, B., Blair, J.B., Hofton, M., Hunsaker, C., Knox, R., & Walker, W. (2005). Mapping forest structure for wildlife habitat analysis using waveform lidar: Validation of montane ecosystems. *Remote Sensing of Environment*, 96, 427-437.

Kozak, A. & Kozak, R. (2003). Does cross validation provide additional information in the evaluation of regression models? *Canadian Journal of Forest Research*, 33, 976-987.

Knox, R.G., Dubayah, R., Blair, J.B., Hofton, M.A., Peterson, B., Drake, J.B., Weishampel, J.F., & Clark, D.B. (2000). A ground validation network for remote sensing of forest canopy structure. Ecological Society of America, Annual Meeting. Snowbird, Utah.

Leak, W.B. (1982). Habitat mapping and interpretation in New England. *USDA Forest Service. Forest Service Research Paper* NE-496. 28 pp.

Leak, W.B. (1996). Long-term structural change in uneven-aged northern hardwoods. *Forest Science*, 42, 160-165.

Leak, W.B. (1999). Species composition and structure of a northern hardwood stand after 61 years of group/patch selection. *Northern Journal of Applied Forestry,* 16(3), 151-153.

Leak, W.B. & Sendak, P.E. (2002). Changes in species, grade, and structure over 48 years in a managed New England northern hardwood stand. *Northern Journal of Applied Forestry,* 19(1), 25-27.

Leak, W.B. & Smith, M.L. (1996). Sixty years of management and natural disturbance in a New England forested landscape. *Forest Ecology and Management,* 81, 63-73.

Leak, W.B. & Smith, M.L. (1997). Long-term species and structural changes after cleaning young even-aged northern hardwoods in New Hampshire, USA. *Forest Ecology and Management,* 95, 11-20.

Lefsky, M.A. (1997). Application of lidar remote sensing to the estimation of forest canopy and stand structure. PhD. Dissertation. Charlottesville, VA: University of Virginia.

Lefsky, M.A., Cohen, W.B., Acker, S.A., Parker, G., Spies, T.A., & Harding, D. (1999a). Lidar remote sensing of the canopy structure and biophysical properties of Douglas Fir-Western Hemlock Forests. *Remote Sensing of Environment,* 70, 339-361.

Lefsky, M.A., Harding, D., Cohen, W.B., Parker, G., & Shugart, H.H. (1999b). Surface lidar remote sensing of basal area and biomass in deciduous forest of eastern Maryland, USA. *Remote Sensing of Environment,* 67, 83-98.

Lefsky, M.A., Cohen, W.B., Harding, D.J., Parker, G.G., Acker, S.A., & Gower, S.T. (2002a). Lidar remote sensing of above-ground biomass in three biomes. *Global Ecology & Biogeography,* 11, 393-399.

Lefsky, M.A., Cohen, W.B., Parker, G.G., & Harding, D.J. (2002b). Lidar remote sensing for ecosystem studies. *Bioscience,* 52(1), 19-30.

Lim, K., Treitz, P., Baldwin, K., Morrison, I., & Green, J. (2003). Lidar remote sensing of biophysical properties of tolerant northern hardwood forests. *Canadian Journal of Remote Sensing,* 29(5), 658-678.

Mark, H. & Workman, J. (1991). *Statistics in Spectroscopy.* San Diego, CA.: Academic Press, Inc.

Means, J.E., Acker, S.A., Harding, D.J., Blair, J.B., Lefsky, M.A., Cohen, W.B., Harmon, M.E., & Mckee, W.A. (1999). Use of large-footprint scanning airborne lidar to estimate forest stand characteristics in the Western Cascades of Oregon. *Remote Sensing of Environment*, 67, 298-308.

Nilsson, M. (1996). Estimation of tree heights and stand volume using an airborne lidar system. *Remote Sensing of Environment*, 56, 1-7.

Parker, G.G. (1995). Structure and microclimate of forest canopies. In M. Lowman and N. Nadkarni (Eds.), *Forest Canopies: A Review of Research on a Biological Frontier* (pp. 73-106). San Diego, CA.: Academic Press.

Parker, G.G. & Brown, M.J. (2000). Forest canopy stratification-it it useful? *The American Naturalist*, 155(4), 473-484.

Parker, G.G., Lefsky, M.A., & Harding, D.J. (2001). Light transmittance in forest canopies determined using airborne laser altimetry and in-canopy quantum measurements. *Remote Sensing of Environment*, 76, 298-309.

Popescu, S.C., Wynne, R.H., & Scrivani, J.A. (2004). Fusion of small-footprint lidar and multispectral data to estimate plot-level volume and biomass in deciduous and pine forests in Virginia, USA. *Forest Science*, 50(4), 551-565.

Sall, J., Creighton, L. & Lehman, A. (2005). *JMP Start Statistics* (3rd edition). SAS Institute, Inc. Toronto, Canada: Thomson, Brooks/Cole.

Shapiro, S.S. & Wilk, M.B. (1965). An anlysis of variance test for normality (complete samples). *Biometrika* 52(3-4): 591-611.

Smith, M.L., Ollinger, S.V., Martin, M.E., Aber, J.D., Hallett, R.A., & Goodale, C.L. (2002). Direct estimation of aboveground forest productivity through hyperspectral remote sensing of canopy nitrogen. *Ecological Applications*, 12, 1286-1302.

Tritton, L.M. & Hornbeck, J.W. (1981). Biomass equations for major tree species of the Northeast. USDA Forest Service General Technical Report NE-69. Broomall, PA: Northeast Forest Experiment Station.

Weishampel, J.F., Blair, J.B., Knox, R.G., Dubayah, R., & Clark, D.B. (2000). Volumetric lidar return patterns from an old-growth tropical rainforest canopy. *International Journal of Remote Sensing*, 21, 409-415.

Whittaker, R.H., Bormann, F.H., Likens, G.E., & Siccama, T.G. (1974). The Hubbard Brook Ecosystem Study: Forest Biomass and Production. *Ecological Monographs,* 44(2), 233-254.

Wilkinson, L., Hill, M.A., & Vang, E. (1992). *SYSTAT: Statistics.* Version 5.2. Evanston, IL.: Systat Inc. 724 pp.

Young, H.E., Ribe, J.H., & Wainwright, K. (1980). Weight tables for tree and shrub species in Maine. Miscellaneous Report 230. Life Sciences and Agricultural Experiment Station, University of Maine at Orono. 84 pp.

Zimble, D.A., Evans, D.L., Carlson, G.C., Parker, R.C., Grado, S.C., & Gerard, P.D. (2003). Characterizing vertical forest structure using small-footprint airborne LiDAR. *Remote Sensing of Environment,* 87,171–182.

Data Sources and Types	N	Plot or Footprint Size (ha)	Mean of Maximum Canopy Height (standard deviation) (m)	Mean QMSD (standard deviation) (cm)	Mean AGBM (standard deviation) (Mg ha⁻¹)
Footprint - Level Plots	20	0.07	26.3 (7.6)	25.4 (8.0)	230.4 (88.4)
USFS NERS Inventory Plots	409	0.1		24.8 (3.6)	241.9 (65.7)
LVIS 1999 Footprints within BEF	52279	0.049	22.9 (4.7)		
LVIS 2003 Footprints within BEF	62579	0.031	25.4 (4.8)		

Table 1.1 Measures of forest structure for Bartlett Experimental Forest

54

Forest Metric	r^2	PRESS RMSE	Equation using 2003 LVIS metrics	N	P
Height	0.80	3.49 m	(1) HT = 1.094 (RH100) − 1.537	20	< 0.0001
AGBM	0.61	58.03 Mg ha^{-1}	(2) AGBM = 29.954 + 14.297 (RH50)	20	< 0.0001
AGBM (generalized equation from Lefsky et al. 2002a)	0.55	64.41 Mg ha^{-1}	(3) AGBM = 0.378* (RH100^2)	20	0.0002
QMSD^2	0.54	235.65	(4) QMSD^2 = 68.825 + 0.928 (RH100^2)	20	0.0002

Table 1.2 Relationships between 2003 LVIS metrics and selected measures of forest structure. Single-term regression equations were developed at the footprint-level.

55

Forest Metric	r² or adj. r²	PRESS RMSE	LVIS 2003 Metrics used in Regression Model	VIF	N	P
AGBM	0.27	56.51 Mg ha⁻¹	Mean of RH50	1	409	< 0.0001
ABGM (Unmanaged)	0.41	46.94 Mg ha⁻¹	Mean of RH50	1	158	< 0.0001
QMSD	0.22	3.23 cm	Mean of RH25 & Mean of RH75	< 2	409	< 0.0001
QMSD (Unmanaged)	0.31	2.62 cm	Mean of RH100	1	158	< 0.0001

Table 1.3 Relationships between aggregated 2003 LVIS metrics and USFS NERS inventory plot measures.

56

Species presence/absence and species fraction of AGBM in USFS NERS inventory plots	r^2 or adj. r^2	PRESS RMSE (Mg ha^{-1})	LVIS 2003 Metrics Used in Regression Model	VIF	N	alpha	P
Yellow Birch (sp. is absent from plots)	0.77	34.29	Mean of RH50 & Mean of RH75	< 4	48	0.01	< 0.0001
Yellow Birch (sp. is present in plots)	0.17	56.56	Mean of RH50	1	361	0.01	< 0.0001
Yellow Birch (sp. fraction of AGBM > 0.25)	0.14	48.45	Mean of RH100	1	39	0.05	0.0185
American Beech (absent)	0.67	41.51	Mean of RH50	1	27	0.01	< 0.0001
American Beech (present)	0.21	57.14	Mean of RH50	1	382	0.01	< 0.0001
American Beech (> 0.25)	0.20	56.23	Mean of RH50 & Mean of RH100	< 2	227	0.01	< 0.0001
Sugar Maple (absent)	0.44	45.06	Mean of RH75	1	120	0.01	< 0.0001
Sugar Maple (present)	0.22	59.52	Mean of RH50 & Mean of RH100	< 2	289	0.01	< 0.0001
Sugar Maple (>0.25)	0.54	56.11	Means of RH25, RH50 & RH100	< 9	62	0.01	< 0.0001
Red Maple (absent)	0.35	59.74	Mean of RH50	1	87	0.01	< 0.0001
Red Maple (present)	0.24	55.93	Mean of RH50	1	322	0.01	< 0.0001
Red Maple (>0.25)	0.35	45.93	Mean of RH25	1	120	0.01	< 0.0001
Eastern Hemlock (absent)	0.33	62.29	Mean of RH50	1	69	0.01	< 0.0001
Eastern Hemlock (present)	0.26	55.31	Mean of RH50 & Mean of RH100	< 2	340	0.01	< 0.0001
Eastern Hemlock (> 0.25)	0.25	44.86	Mean of RH50	1	56	0.01	< 0.0001
Paper Birch (absent)	0.34	56.15	Mean of RH50 & Mean of RH100	< 2	202	0.01	< 0.0001
Paper Birch (present)	0.25	54.04	Mean of RH75	1	207	0.01	< 0.0001
Paper Birch (> 0.25)	0.32	51.60	Mean of RH75	1	19	0.01	0.0069
Red Spruce (absent)	0.21	60.15	Mean of RH50	1	226	0.01	< 0.0001
Red Spruce (present)	0.32	52.18	Mean of RH25	1	183	0.01	< 0.0001
Red Spruce (>0.25)	0.55	42.03	Mean of RH100	1	24	0.01	< 0.0001
White Ash (absent)	0.25	53.64	Mean of RH50	1	278	0.01	< 0.0001
White Ash (present)	0.28	62.87	Mean of RH50	1	131	0.01	< 0.0001
White Ash (> 0.25)	0.22	45.38	Mean of RH50	1	21	0.05	0.0338
White Pine (absent)	0.23	57.02	Mean of RH50	1	375	0.01	< 0.0001
White Pine (present)	0.75	33.37	Mean of RH50	1	34	0.01	< 0.0001
Pin Cherry (absent)	0.30	53.26	Mean of RH50 & Mean of RH100	< 2	391	0.01	< 0.0001
Pin Cherry (present)	0.46	48.92	Mean of RH50	1	18	0.01	0.0019

Table 1.4   Species composition effects on plot-level relationships of AGBM with aggregated LVIS 2003 metrics.

57

Predicted AGBM AGBM = 29.954 + (14.297 * RH50)	r²	PRESS RMSE	N	P
AGBM – all plots	0.27	56.51 Mg ha⁻¹	409	< 0.0001
AGBM - plots located within relatively unmanaged forest tracts	0.41	46.94 Mg ha⁻¹	158	< 0.0001
AGBM - American Beech is not present within plots	0.67	41.51 Mg ha⁻¹	27	< 0.0001
AGBM - Red Spruce fraction of AGBM within plots > 0.25	0.50	45.74 Mg ha⁻¹	24	0.0001
AGBM - Yellow Birch is not present within plots	0.74	36.99 Mg ha⁻¹	48	< 0.0001
AGBM – White Pine is present within plots	0.75	33.37 Mg ha⁻¹	34	< 0.0001
AGBM - Yellow Birch is not present within plots sited in unmanaged forest tracts	0.79	33.13 Mg ha⁻¹	34	< 0.0001

Predicted QMSD	r²	PRESS RMSE	N	P
QMSD - all plots	0.20	3.28 cm	409	< 0.0001
QMSD - plots located within relatively unmanaged forest tracts	0.31	2.62 cm	158	< 0.0001
QMSD - American Beech is not present within plots	0.37	2.77 cm	27	0.0008
QMSD - Red Spruce fraction of AGBM within plots > 0.25	0.33	3.06 cm	24	0.0033
QMSD - Yellow Birch is not present within plots	0.31	2.97 cm	48	< 0.0001
QMSD - Yellow Birch is not present within plots sited in unmanaged forest tracts	0.55	2.17 cm	34	< 0.0001

Table 1.5   Relationships between predicted AGBM and QMSD and USFS NERS plot level forest measures. Predicted values of AGBM and QMSD were calculated using 2003 LVIS metrics and equations derived from 2003 footprint level regression models (Table 2). The influence of selected aspects of species composition and management history on the prediction relationships was examined through the restriction of plot selection.

Predicted AGBM AGBM = 0.378 * RH100^2	r^2	PRESS RMSE	N	P
AGBM - all plots	0.08	63.27 Mg ha^{-1}	409	< 0.0001
AGBM - plots located within relatively unmanaged forest tracts	0.22	54.25 Mg ha^{-1}	158	< 0.0001
AGBM - American Beech is not present within plots	0.56	47.46 Mg ha^{-1}	27	< 0.0001
AGBM - Red Spruce fraction of AGBM within plots > 0.25	0.52	44.15 Mg ha^{-1}	24	< 0.0001
AGBM - Yellow Birch is not present within plots	0.16	67.68 Mg ha^{-1}	48	< 0.0048
AGBM - White Pine is present within plots	0.31	57.38 Mg ha^{-1}	34	0.0006
AGBM - Yellow Birch is not present within plots sited in unmanaged forest tracts	0.35	61.73 Mg ha^{-1}	34	0.0002

Table 1.6   Relationships between predicted AGBM using a generalized model and USFS NERS plot level estimated AGBM. Predicted values of AGBM were calculated using 2003 LVIS metrics and a generalized regression model patterned after Lefsky et al. (2002a). The influence of selected aspects of species composition and management history on the prediction relationships was examined through the restriction of plot selection.

59

Figure 1.1   Location of Bartlett Experimental Forest, showing established plot network.

60
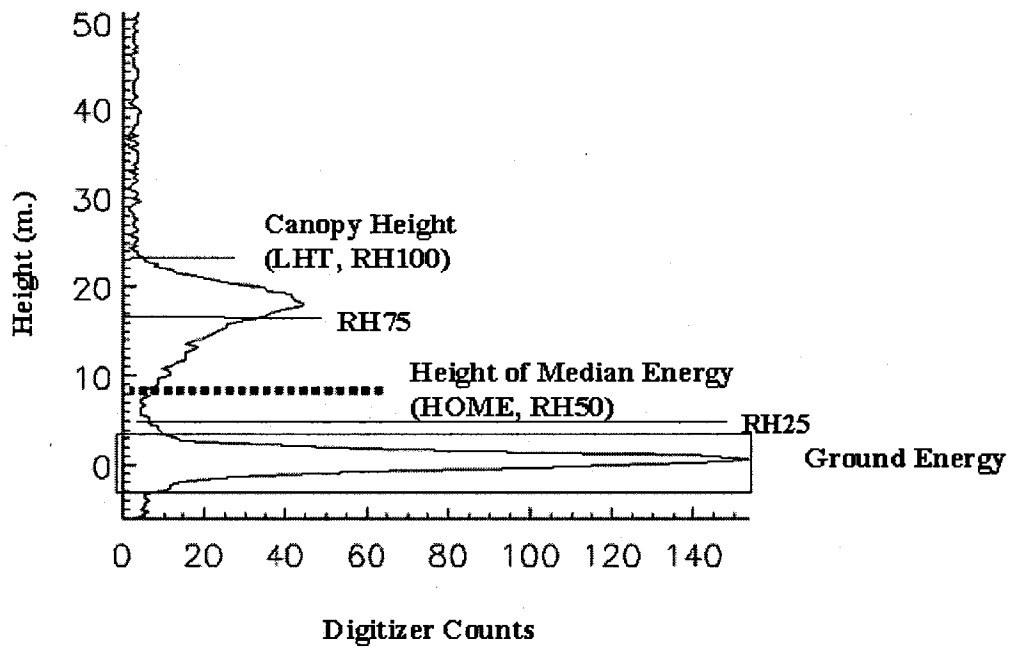
Figure 1.2 Metrics derived from lidar waveforms. Adapted from Drake et al. 2002.

61
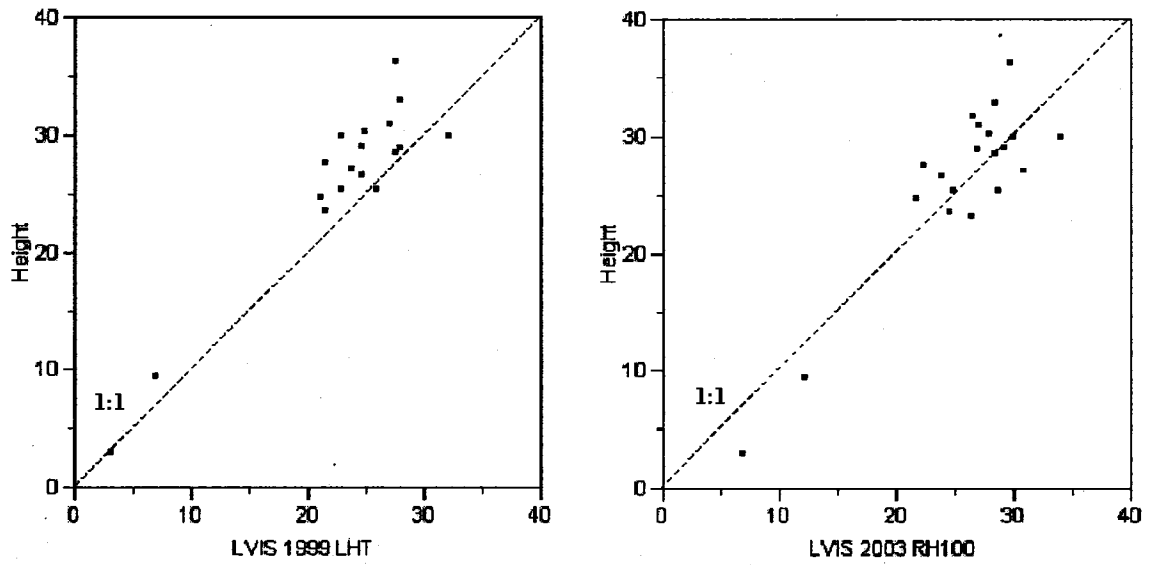
Figure 1.3   Footprint-level scatter plots of 1999 and 2003 LVIS height metrics vs. maximum canopy height. Note overall trend in the 1999 LVIS height metrics towards underestimation of maximum canopy height. Dashed lines indicate 1:1 correspondence.

62
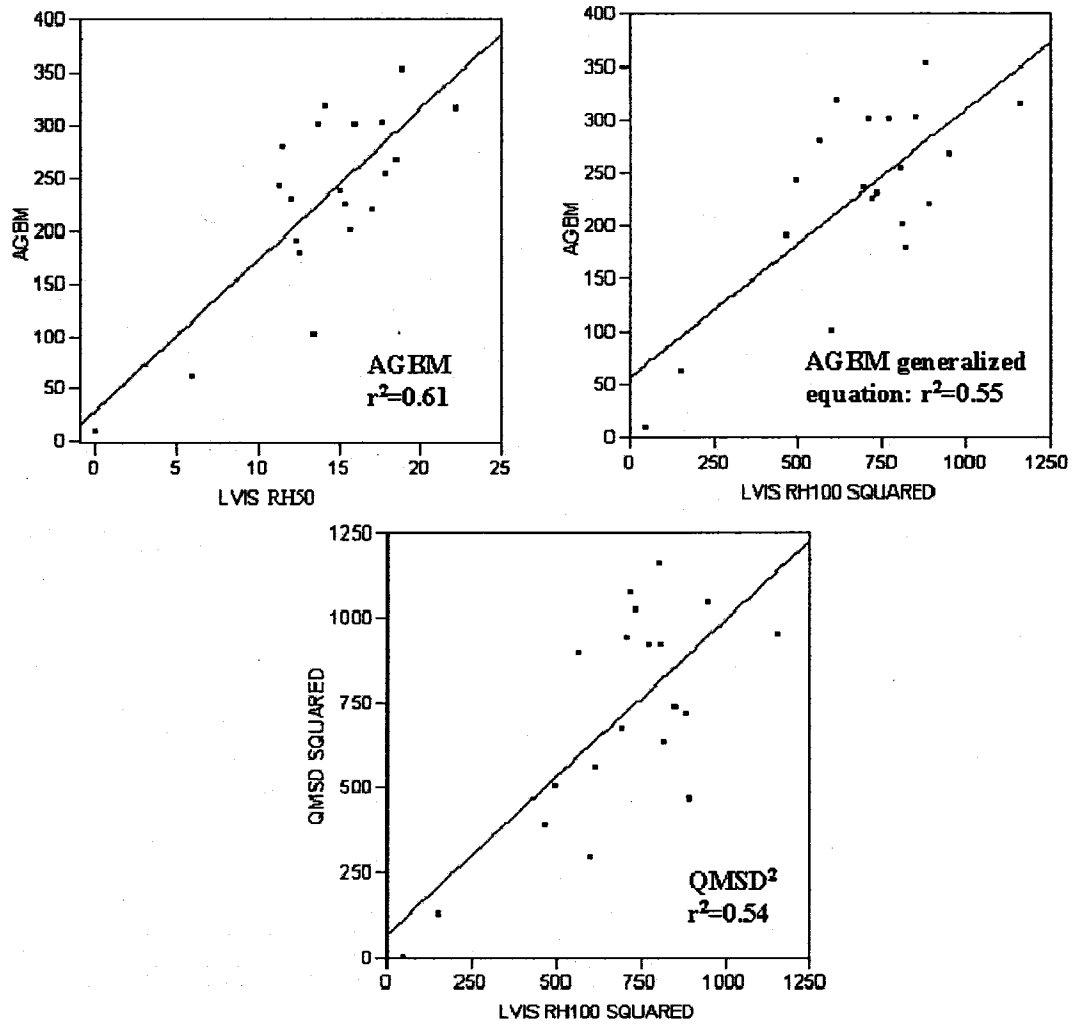
Figure 1.4 Footprint-level scatter plots of 2003 LVIS metrics and forest measurements. Regression equations are found in Table 1.2.

63
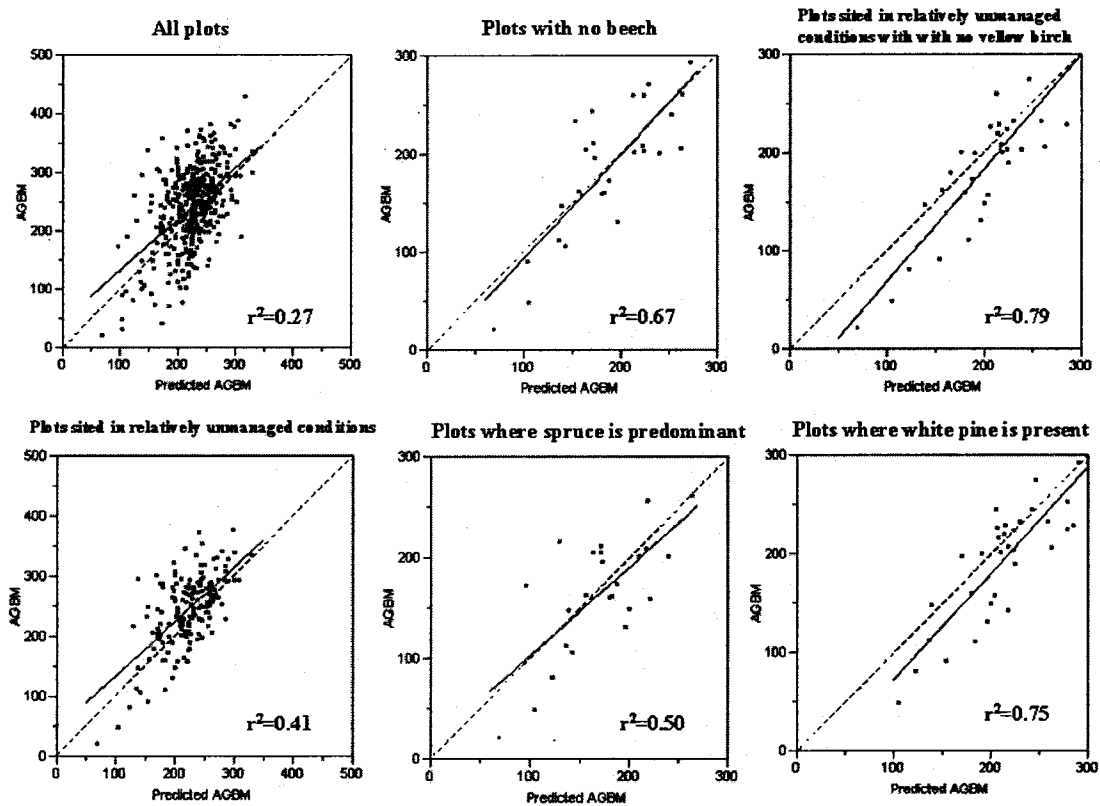
Figure 1.5   Actual versus predicted AGBM (Mg ha⁻¹) scatter plots. Predicted regression equation from Table 1.2 applied to 2003 LVIS metrics. The influence of selected aspects of species composition and management history on the prediction relationships was examined through the restriction of plot selection.

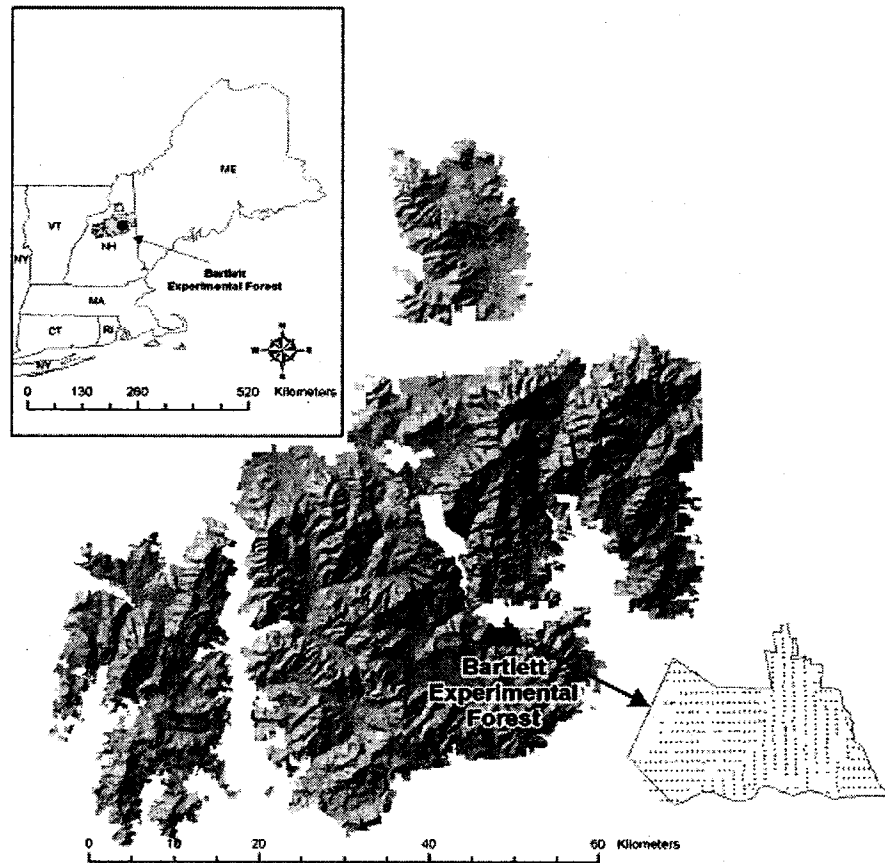64
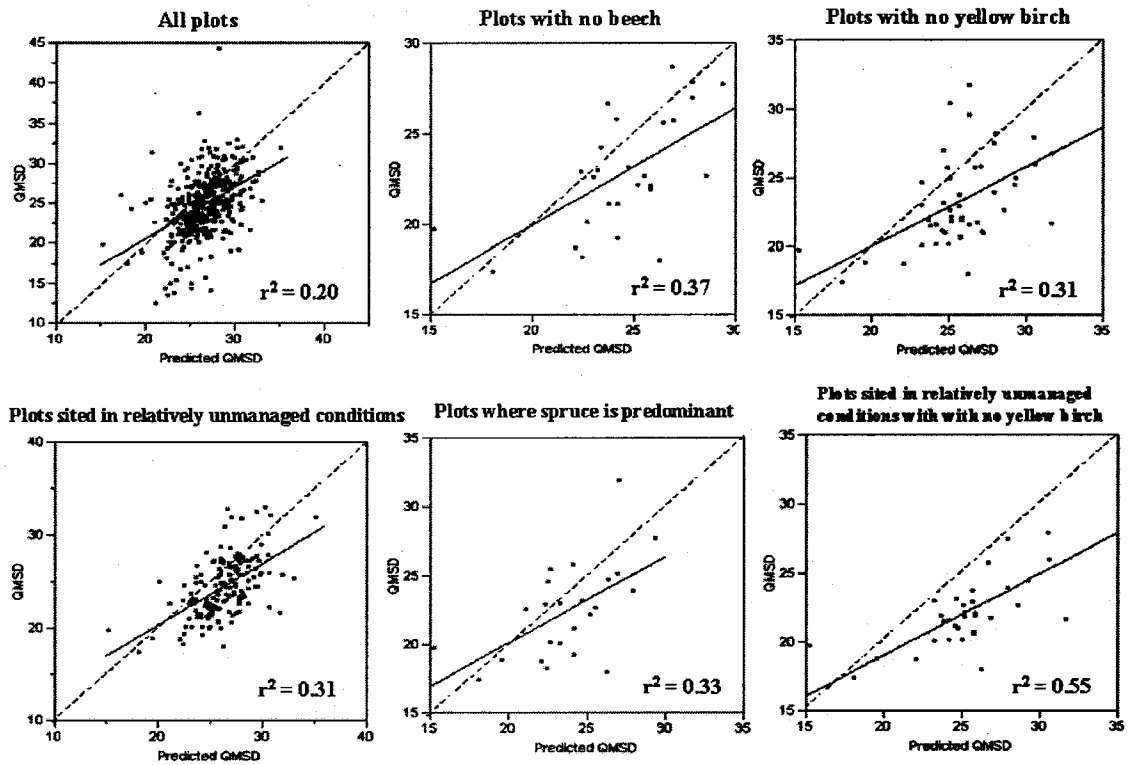
Figure 1.6 Actual versus predicted scatter plots of QMSD.
Predicted regression equation from Table 1.2 (footprint-level) applied to 2003 LVIS metrics.

65
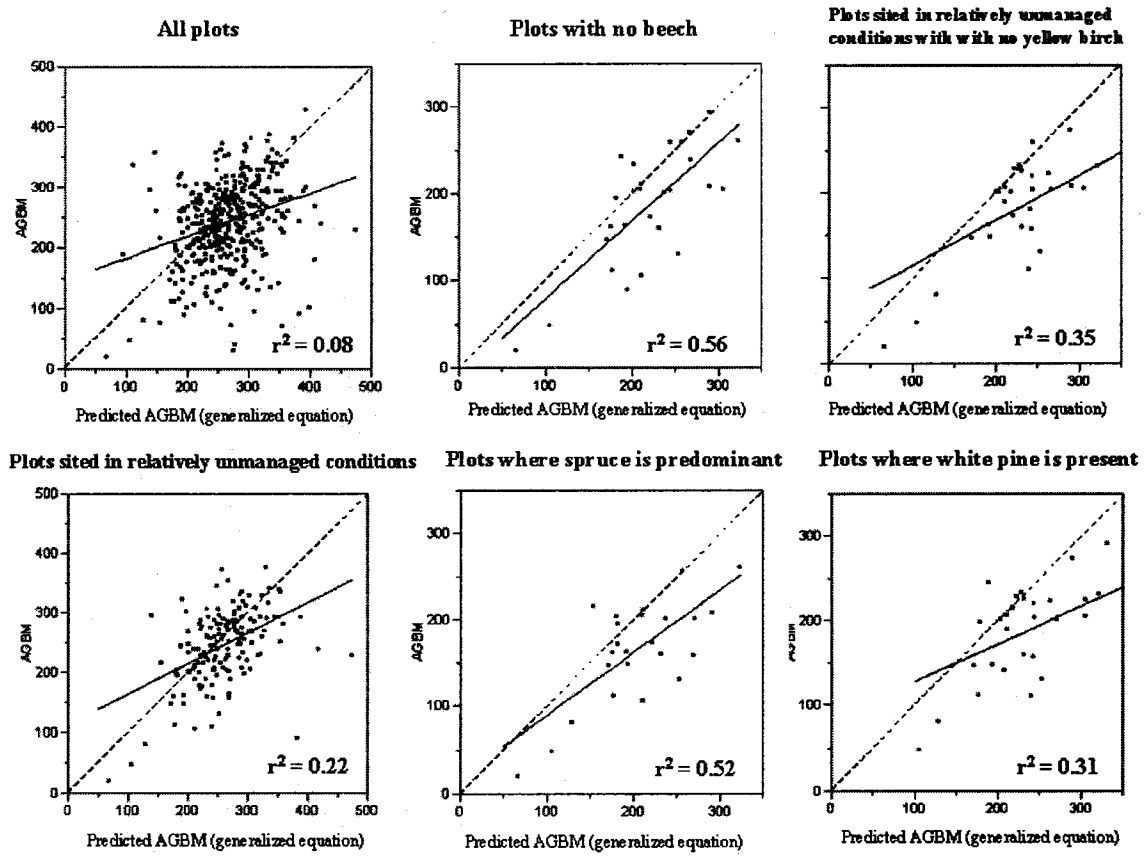
Figure 1.7 Actual versus predicted scatter plots of AGBM using generalized equation. Generalized equation of Lefsky et al. (2002a) was applied to 2003 LVIS metrics.

CHAPTER 2

REMOTE INVENTORY FOR A NORTHERN TEMPERATE FOREST INTEGRATING WAVEFORM LIDAR WITH HYPERSPECTRAL REMOTE SENSING IMAGERY

Abstract

It has been suggested that attempts to use remote sensing to map the spatial and structural

patterns of individual tree species abundances in heterogeneous forests, such as those

found in northeastern North America, may benefit from the integration of hyperspectral

or multi-spectral information with other active sensor data such as lidar. Towards this

end, we describe the combined ability of individual waveform lidar metrics and

hyperspectral data to correlate with three common forest measurements: basal area (BA),

above-ground biomass (AGBM) and quadratic mean stem diameter (QMSD) and to also

discriminate the distribution and abundance patterns of five common and often dominant

67

tree species in a northern temperate mixed conifer and deciduous forest. Waveform lidar imagery was acquired in July 2003 over the 1000-ha. Bartlett Experimental Forest (BEF) in central New Hampshire (USA) using NASA's airborne Laser Vegetation Imaging Sensor (LVIS). High spectral resolution imagery was likewise acquired in August 2003 using NASA's Airborne Visible/Infrared Imaging Spectrometer (AVIRIS). Sensor data were analyzed with field data from over 400 plots of USDA Forest Service Northeastern Research Station (USFS NERS) 2001-2003 inventory.

Results suggest that the integrated data sets of hyperspectral and waveform lidar do improve the outcomes in evaluating BA, AGBM and QMSD for a given site over use of either data set alone. This level of improvement from use of integrated data doesn't hold, however, for detection of the proportional abundance patterns created by the common and dominant tree species of this forest. Nonetheless, results of value to traditional forest inventory efforts can be obtained in these northern temperate forest tracts through separate analyses, as well as combined use of the two data sets. AVIRIS data alone, and in combination with LVIS data, does correlate well with certain compositional abundance patterns determined by species fraction of biomass. When further registered with QMSD data, derived from LVIS data sets, maps predicting species-level abundance patterns and coincident patterns of stem size can be created for several of the dominant tree species of this region. The results provide a unique species-based remote inventory of potential benefit to both forestry and conservation biology planning efforts.

Keywords: waveform lidar, LIDAR, LVIS, laser altimetry, AVIRIS, high spectral resolution imagery, hyperspectral, biomass, basal area, quadratic mean stem diameter, canopy structure, height, tree species distribution

Introduction

In northeastern North America, the spatial variation in forest structure across large tracts of land is driven by a heterogeneous mix of deciduous and coniferous species and enhanced by the complexity of species interactions with ecological factors such as topography, soils and disturbance history. These temperate forests are recognized as important components of the global carbon cycle. Yet, a comprehensive understanding of the overall spatial patterns of structural variation seen in these large landscapes is still largely lacking. The integration of optical sensor data, such as that obtained from hyperspectral imaging spectroscopy, with the structural information readily obtained from active sensors, such as lidar, is believed to hold great promise for improving the accuracy of forest inventory and ecological modeling at a landscape scale. Images from lidar and optical sensors offer the possibility of combining very detailed information from both vertical and horizontal spatial planes (Hudak et al. 2002, Popescu et al. 2004, Lefsky et al. 1999, Treuhaft et al. 2002, McCombs et al. 2003). It has been suggested, as such, that each of these sensors brings complementary and potentially synergistic capabilities

69

to land-cover classification and estimation of stand structure (Ackermann 1999, Dubayah et al. 2000, Lim et al. 2003).

In recent years, hyperspectral remote sensing has been used to ascertain species-level abundance patterns in a variety of biomes (Roberts et al. 1998, Ustin and Xiao 2001, Plourde et al. in press). The advantage of hyperspectral remote sensing in detecting differences in species-level abundance patterns is found in the over-determined nature of spectral response (i.e. hundreds of narrow, contiguous spectral channels). Reducing the dimensionality of the data in order to discern the most meaningful spectral response has been the inherent challenge (Plourde et al. in press, Underwood et al. 2003, Williams and Hunt 2002, Haskett and Sood 1998). To complement the advantages provided by hyperspectral imagery in detailing species abundance patterns, waveform lidar imagery can provide direct measures of canopy height. Strong indirect relationships between canopy and sub-canopy lidar metrics and traditional forest measures, such as biomass, can also be established at a landscape scale (Dubayah et al. 2000, Lefsky et al. 2002).

Plourde et al. (in press) have noted that given the inherent spatial and temporal variability of northern temperate forests and attendant problems with classification, measures of species' relative abundances across a forest landscape may provide a more functional representation of ground conditions than classification of discrete forest type classes.

70

By adding information on forest structure to such compositional data, the combination of remotely acquired detailed distribution patterns reflecting both species abundance and aspects of size could provide essential information to pressing issues of management and research.

Several studies (Plourde et al. in press, Ollinger and Smith 2005, Anderson et al. in revision) conducted at the Bartlett Experimental Forest (BEF) in north central New Hampshire (USA) have already separately assessed the validity of using airborne hyperspectral data for the classification of individual tree species, prediction of forest growth and mapping of abundance patterns, as well as the use of airborne waveform lidar to describe and predict various forest metrics. Here we describe the advantage conferred by combining structural information with spectral approaches to quantify individual species abundances and associated physical metrics in a heterogeneous temperate forest using integrated data from both sensor types.

71

Study Area and Field Data

Bartlett Experimental Forest (44.06°N, 71.3°W) is located within the White Mountain National Forest, a heavily forested and mountainous region in north central New Hampshire (Figure 2.1). Established by the USDA Forest Service in 1931, the BEF is a 1052-ha field site for the study of secondary deciduous and coniferous forest dynamics and ecology. Major tree species include American beech (*Fagus grandifolia* Ehrn.), red maple (*Acer rubrum* L.), eastern hemlock (*Tsuga canadensis* L. Carr.), sugar maple (*Acer saccharum* L.), yellow birch (B*etula alleghaniensis* Britt.), paper birch (*Betula papyrifera* Marsh.), red spruce (*Picea rubens* Sarg.) and balsam fir (*Abies balsamea* (L.) Mill.), with some localized small stands of eastern white pine (*Pinus strobus* L.). Arrayed in a regular grid across the BEF are over 400 intensively sampled 0.1 ha plots (see http://www.fs.fed.us/ne/durham/4155/bartlett.htm), measured in 2.54 cm diameter classes, most recently in 2001-03. All inventory plots have been geo-referenced to within 3-meter positional accuracy. Plot elevations range from approximately 200 to 800 m.

Basal area (BA) and dry weight biomass (AGBM: bole, branch, and foliar) by species for each inventory plot was calculated using regionally developed allometric equations based on stem diameter measurements (Jenkins et al. 2004). Fraction of biomass by species per

plot was calculated from the most recent BEF survey data. Stem diameters were also used

to calculate quadratic mean stem diameter (QMSD). QMSD was calculated as $[\Sigma D^2/n]^{1/2}$

where D is the stem diameter and n is the number of stem diameters in the plot (Curtis &

Marshall 2000). Two minimum values were used to calculate separate measures of

QMSD. $QMSD_{10}$ calculated the average stem diameter using all trees with dbh measured

as greater than 10 cm. $QMSD_5$ calculated the average stem diameter using all stems with

dbh measured as greater than 5 cm.

The descriptive statistics of the field data were calculated as follows: mean BA was 39.5

m^2ha^{-1} with a standard deviation of 10.1 m^2ha^{-1}; mean AGBM was 243 $Mgha^{-1}$ with a

standard deviation of 64.8 $Mgha^{-1}$; and mean $QMSD_{10}$ was 24.8 cm with a standard

deviation of 3.44 cm. All data were stored in a geographic information system, referenced

to NH State Plane feet (NAD83, GRS1980).

AVIRIS Data

On August 24, 2003, NASA's Airborne Visible/Infrared Imaging Spectrometer (AVIRIS)

was flown on the ER-2 platform (Green et al. 1998; see http://aviris.jpl.nasa.gov) and

collected cloud-free data in a 11 km wide swath centered over the BEF. AVIRIS is a

"whisk broom" scanner that captures upwelling spectral radiance in 224 contiguous

spectral bands for wavelengths from 400 to 2500 nm with a 10nm nominal bandwidth.

The ER-2 flies at approximately 20 km above sea level, resulting in a pixel size of about

73

16-17 m. The AVIRIS imagery was delivered by NASA JPL as calibrated radiance data (gain*μW/cm^2/nm/steradian) and stored as 16-bit signed integers (IEEE) in BIP format.

In order to minimize a view-angle brightness gradient in the AVIRIS image, the mean and standard deviation of each column of raster data was normalized to the overall mean and standard deviation. The image was atmospherically corrected with ImSpec LLC's Atmospheric COrrection Now (ACORN) (v. 4.14) software (http://www.imspec.com) and geometrically corrected with a second order polynomial based on reference points collected from 1992 digital orthophotoquads (DOQ) with 1-m nominal spatial resolution acquired from the New Hampshire Geographically Referenced Analysis and Information Transfer System (NH GRANIT; http://www.granit.sr.unh.edu), registered to NH State Plane feet (NAD83, GRS1980).

The AVIRIS image was transformed with a forward minimum noise fraction transform (MNF) rotation (ENVI $^{©}$ v. 3.6, Research Systems, Inc. 2002) to reduce data dimensionality. Twenty-four bands with eigenvalues above 2.5 were retained for analysis.

LVIS Data

Lidar data were acquired on July 19-26, 2003 over the BEF using NASA's Laser Vegetation Imaging Sensor (Blair et al. 1999). Multiple flight lines were completed

74

between Bartlett and West Thornton, N.H. LVIS is an airborne imaging laser altimeter that records the time and amplitude of a laser pulse reflected off target surfaces. The sensor digitizes the vertical distribution of intercepted surfaces between the first (top of the canopy) and the last (ground) return producing a waveform record. LVIS records circular footprints of variable size; 2003 footprints had a nominal radius of 10 m. Additional detail on LVIS capabilities can be found in Blair et al. (1999).

LVIS data for this site were beta released in September 2004 (see http://lvis.gsfc.nasa.gov). LVIS metrics used in this study were derived from the waveforms using an automated algorithm (M. Hofton, personal communication). Lidar canopy height (RH100) was calculated by identifying two locations within the waveform (1) where the signal initially increases above a mean noise level/threshold (the canopy top); and (2) at the center of the last Gaussian pulse (the ground return). The distance between these two locations was then calculated to derive the height metric (Figure 2.2). The height of median energy (RH50) was calculated by finding the median of the entire signal (i.e. above the mean noise level) from the waveform, including energy returned from both canopy and ground surfaces. The location of the median energy was then referenced to the center of the last Gaussian pulse to derive a height (Drake et al. 2002). Similarly RH25 and RH75 were calculated by finding the relative height (RH), relative to the ground elevation, at which 25% and 75%, respectively, of the waveform energy occurs (http://lvis.gsfc.nasa.gov).

75

Integration of AVIRIS and LVIS Data

A roughly 6.9 km by 6.2 km region surrounding the Bartlett Experimental Forest was defined and used to establish a subset of the AVIRIS and LVIS imagery for further analysis. Individual LVIS circular footprints with a nominal resolution of 20 m were converted to raster format using an inverse distance weighted algorithm (power = 3) (ArcGIS v.8.3, ESRI 2003). Pixel size was set at 15.8 m to match the nominal resolution of the AVIRIS data. AVIRIS and LVIS imagery were aligned geometrically to establish coincident pixels.

Values from each of the 24 AVIRIS MNF bands and 4 LVIS metrics were extracted and standardized (i.e. subtract the mean and divide by the standard deviation) from the locations of the USFS NERS inventory plots. Each plot (0.1 ha; roughly 30 by 30 m) encompassed portions of four to six pixels. Pixel data were aggregated and summarized as mean values.

Data Analysis

The relationships between the measured USFS NERS plot data (dependent variables) and the mean values of 28 standardized LVIS and AVIRIS MNF metrics (independent variables) were explored through stepwise mixed linear regression techniques. Analyses conducted using only LVIS metrics were explored through simple linear regression or

two-term multiple regressions, limited to three pairs of less correlated LVIS metrics (RH25 & RH75; RH25 & RH100; and RH50 & RH100) as the independent variables. Statistical analyses were conducted using JMP IN® software (SAS Institute Inc. 2005). Dependent, independent variables and the regression residuals were tested for normality of their distributions using the Shapiro-Wilk W test (Shapiro and Wilk 1965) and normal quantile plots. For each regression, variables with clearly non-normal distributions were eliminated. An arcsine square root transform was used to improve the normality of the distribution of the species-level proportional abundance data. The critical value of P (alpha) was set at 0.05 for all analyses. Prediction error sum of squares root mean square errors (PRESS RMSE) were calculated for each forest metric. PRESS RMSE is computed as the square root sum of squares of the prediction residuals (Mark and Workman 1991, Hastie et al. 2001). As an out-of-sample validation technique, PRESS RMSE tests how well the current model would predict each of the points in the data set (in turn) if they were not included in the regression. Low values of PRESS RMSE usually indicate that the model is not overly sensitive to any single data point. In addition, the variance inflation factor (VIF) was assessed for models with multiple predictors. VIF indicates whether multi-collinearity between variables inflates the variance of estimates and renders the model unstable and of less applicability to new sets of data. Variables with VIF values under 10 are indicative of models with low multi-collinearity (Sall et al. 2003). Regression results are summarized in Tables 2.1 - 2.3. Maps were analyzed and produced using ENVI® v. 4.2 (Research Systems, Inc. 2005), ERDAS Imagine® v. 8.7 (ERDAS 2004), and ArcGIS ® v. 8.3 (ESRI 1999-2002) software.

BA, AGBM, QMSD

Overall relationships between inventory and combined sensor data were fair (Table 2.1): (BA: adj. r^2 = 0.47; Press RMSE = 7.5 m^2 ha^{-1}); (AGBM: adj. r^2 = 0.39; PRESS RMSE = 51.1 Mg ha^{-1}); ($QMSD_{10}$: adj. r^2 = 0.33; PRESS RMSE = 2.86 cm). AGBM results (AGBM: adj. r^2 = 0.55; PRESS RMSE = 41.0 Mg ha^{-1}) improved notably when analysis was restricted to plots located in forest tracts not subject to any recent management activity. Best results were obtained using both AVIRIS and LVIS metrics in combination as compared to the use of either set of sensor data alone. Comparatively, AVIRIS variables alone explained more of the basal area variation seen within all plots, while LVIS variables alone explained more of the variation seen within the $QMSD_{10}$ data where stems greater than 10 cm dbh were used as a lower cutoff of measurement. Relatively similar amounts of AGBM variance and error were explained by stepwise linear regressions using AVIRIS and LVIS data separately.

78

Species Abundance Proportional to AGBM

USFS NERS field measures of fractional AGBM (transformed as an arcsine square root value) specific to five tree species were compared to the mean values of standardized 2003 AVIRIS MNF variables and LVIS metrics through stepwise mixed multiple regression (Table 2.2). Relationships were explored between ground measures and sensor data only in those plots where the given species being modeled was present (AGBM fraction > 0 or 0.01). Therefore the value of N varied from a low of 138 plots (red maple in unmanaged conditions) to a high of 379 plots (beech) amongst the five species studied. For four of five species, good linear relationships between the transformed species fraction of AGBM and varying combinations of AVIRIS and LVIS metrics were found (beech: adj. r^2 = 0.65; red maple: adj. r^2 = 0.61; eastern hemlock: adj. r^2 = 0.57; sugar maple: adj. r^2 = 0.51). PRESS RMSE errors were generally consistent, ranging from a low of 0.12 (hemlock) to a high of 0.16 (beech) across these four species. AVIRIS variables were the sole predictors for the beech and hemlock proportional relationships, while the other species were best modeled through a combination of AVIRIS and LVIS metrics. In each case, however, the AVIRIS variables explained almost all of the variance in the models. The information content represented, in particular, by the number of AVIRIS MNF variables needed to model species' abundances proportional to AGBM was large and the individual AVIRIS MNF variables chosen as predictors varied between species. Both AVIRIS and LVIS metrics had poor relationships with species fraction of AGBM for yellow birch.

QMSD under Varying Restrictions of Species Composition and Abundance

The use of species composition and abundance to select varying subsets of USFS NERS inventory plots for analyses tended to improve the relationships found with overall plot measures of QMSD for three of the species examined (Table 2.3). USFS NERS field measures of $QMSD_{10}$ and $QMSD_5$ were compared to the mean values of LVIS metrics. In this instance, relationships were explored between the ground measures and the sensor data only in those plots where a given species was present at higher levels of abundance and in the case of the maples, situated in relatively unmanaged conditions. For each subset of plots examined, the adjusted r^2 increased to over 0.4, while the associated error decreased to less than 2.25 cm.

Combined Analyses for Inventory

Three of the tree species (eastern hemlock, red maple, and sugar maple) with the strongest relationships to proportional patterns of abundance (Table 2.2 and Figure 2.3), also had overall QMSD relationships (Table 2.3 and Figure 2.3) that were strong enough at higher levels of species abundance to allow for the creation of combined abundance/size maps for these individual species within the forest as a whole. As a consequence, tree maps detailing the predicted abundance of individual species (Figures

80

2.4 – 2.6) were coupled with predicted measures of average tree diameter (defined as QMSD) in areas of high abundance (Figures 2.7 – 2.9).

Discussion

Relationships with BA, AGBM, QMSD and Species Abundance Proportional to AGBM

While examples of data integration within the broad realm of remote sensing are relatively common, access to the unique combination of coincident airborne hyperspectral and waveform lidar data at a landscape scale is rare. The promise posed by this type of integration of data sets to meet operational requirements for forest inventory and ecological modeling at varying scales has been noted repeatedly within the remote sensing literature (Ackermann 1999, Dubayah et al. 2000, Drake 2001, Hudak et al. 2002, Popescu et al. 2004, Lefsky et al. 2002, Truehaft et al. 2002, 2003 McCombs et al. 2003, Ollinger and Smith 2005, and Lim et al. 2003).

Integration of data from multiple sources attempts to gain more knowledge about an observed phenomenon than can be acquired from the data sources independently, and ideally, should serve to increase the reliability of the interpretation (McCombs et al. 2003, Pohl and Van Genderen 1998). By these standards, the integration of airborne

81

hyperspectral and waveform lidar over the Bartlett Experimental Forest achieved these objectives as seen in the increase in the coeffiecients of determination and reduction in the measures of error for each of the relationships with traditional forest inventory measures (i.e. BA, AGBM, and QMSD; Table 1). This improvement is seen despite relatively low r^2 values overall. While these improvements were modest, they were achieved with only a limited number of structural metrics from the LVIS sensor. Data relative to canopy closure from LVIS metrics determined via measures of ground and canopy energy, in particular, were unavailable for this study. Relationships established between sensor data and plot metrics in forests tracts with relatively little recent active management were even stronger, generally increasing the coefficients of determination, especially for AGBM, and universally reducing error. The low to fair r^2 results also reflect some limitations of the USFS NERS data set in sampling low biomass areas within the experimental forest. Only 11 of 406 sampled plots have biomass estimates under 100 Mgha^{-1}. While BEF actually has relatively little acreage in early successional status, expansion of field data to represent the full range of conditions present at BEF could potentially improve both the fit and error estimates of these relationships.

Hyyppä et al. (2000) and Hyyppä and Hyyppä (2001) have previously reported that a typical standwise forest inventory is carried out with a 15% error concerning main forest attributes, calculated as the percentage value of the standard error of regression (i.e. RMSE) divided by the mean value of the stand attribute data. Foster and Townsend (2004) also point out that forest inventory data used for validation are prone to error and may be only about 80% accurate. By these approximate guidelines, 15%-20% errors for

field-measured AGBM at BEF range from 36.5 Mgha^{-1} to 48.6 Mgha^{-1}. Similarly, 15%-20% errors for field-measured BA range from 5.9 m^{2}ha^{-1} to 7.9 m^{2}ha^{-1}. Lastly, 15%-20% errors for field-measured QMSD$_{10}$ range from 3.7 cm to 5.0 cm. The lowest PRESS RMSE values reported for predicted AGBM and BA in this study (Table 2.1) are within this error range. The lowest PRESS RMSE values reported for predicted QMSD$_{10}$ using both AVIRIS MNF and LVIS metrics in this study (Table 2.1) exceed those standards by over 4 percentage points.

By the same standards for data integration described above, the integration of airborne hyperspectral and waveform lidar used to examine patterns of species abundance proportional to biomass within the BEF did not achieve much, if any, improvement in the relationships with five common tree species over the use of AVIRIS data alone. Presumably, the lack of sufficiently contrasting height attributes across these five species reduced the contribution of LVIS in distinguishing species level patterns. Data were insufficient in this study to add results for red spruce and white pine. Both of these conifers, however, as mature components in the canopy of a northern temperate forest can present emergent and/or distinct structural attributes that may be more uniquely detected by LVIS waveforms and thus, worth further study at another site.

The scatter plots reflecting predicted versus actual abundance patterns for hemlock and sugar maple each tend to over-estimate at low abundance levels and under-estimate at high abundance levels (Figure 2.3). Part of the error in these relationships results from the close proximity of species to one another relative to the pixel size of the instruments used

83

to detect them. Individual pixels of the size referenced here for both AVIRIS and LVIS often include fine scale mixtures of species. Furthermore, in this study, the AVIRIS and LVIS metrics used in the regressions were mean values calculated from the aggregation of four to six pixels associated with a USFS NERS plot, further increasing the potential for error from admixed species compositions.

Four of five tree species examined had coefficients of determination above 0.5, suggesting good relationships with the AVIRIS MNF and LVIS metrics, alone (in the case of beech and hemlock) or in combination. In previous work using spectral mixture analysis (SMA), Plourde et al. (in press) noted that predictions of American beech abundance ($r^2 = 0.36$; RMSE = 0.18; N = 200) derived from 2001 AVIRIS data were less reliable overall than predictions of sugar maple ($r^2 = 0.49$; RMSE = 0.09; N=150). Using different techniques in this study, those relationships were reversed ($r^2 = 0.65$ and 0.51 respectively) with beech (Figure 2.10) showing a much stronger correlation with the sensor data.

Relationships with QMSD under Varying Restrictions of Species Composition and Abundance

Species composition did influence the strength of the relationships with mean QMSD for three species under limited conditions. At higher levels of abundance, particularly in areas of the forest that have not seen recent management, relationships between QMSD

84

and LVIS metrics for eastern hemlock, red maple and sugar maple improved in both fit and reduction of error. PRESS RMSE values were determined to be less than 2.25 cm for each of the species studied under these restrictions. Reported as a percentage of the mean value for QMSD across all 406 plots, this measure of error is 11% or less for both $QMSD_{10}$ (24.8 cm: 9%) and $QMSD_5$ (19.9 cm: 11%) values.

Combined Analyses for Inventory

As Plourde et al. (in press) recently discussed, estimation and mapping of species abundances represents an important approach that may be more suitable to the purposes of forest inventory than discrete type classification in heterogeneous forests such as those found at Bartlett. Analyses conducted in this study uncovered information from both AVIRIS and LVIS metrics, alone and in combination, useful to the remote inventory of several, often dominant, tree species for this region; most notably for Eastern hemlock, red maple and sugar maple. These three tree species, having the strongest relationships to proportional patterns of abundance (Table 2.2), also had associated QMSD relationships with the highest coefficients of determination seen in this study and low error (Table 2.3). The maps resulting from use of these regression models, have value, at a local level, for forest inventory and planning efforts.

Increasingly over the past several years, reports of operational or near-operational use of newer forms of remote sensing for forest inventory are being published in the scientific

85

literature (Hyyppä and Hyyppä 2001). Much of this perspective is emanating from Scandanavia and Canada in regions dominated by coniferous forests (Holmgren 2003, Næsset 2002). While the derivation of biophysical parameters from a wide range of sensors at regional to global scales is still a matter of intensive research, this study adds to the argument that the inventory of traditional forest parameters, inclusive of mixed coniferous and deciduous conditions, at local to landscape scales, can be accomplished remotely.

Conclusions

Results here suggest that the integrated data sets of hyperspectral and waveform lidar do improve the outcomes in evaluating BA, AGBM and QMSD for a given site over use of either data set alone. This echoes similar findings reported in Popescu et al. (2004) for fused small footprint lidar and multispectral data sets used to estimate common forest parameters. This level of improvement doesn't hold, however, for detection of the proportional composition patterns created by the common and dominant tree species of this northern forest.

Nonetheless, results of value to traditional forest inventory efforts can be obtained in these northern temperate forest tracts through separate analyses, as well as combined use

86

of the two data sets. AVIRIS data alone, and in combination with LVIS data, does

correlate well with compositional abundance patterns determined by species fraction of

biomass. When further registered with QMSD data, derived from LVIS data alone, maps

predicting species-level abundance patterns and coincident patterns of stem size and/or

height can be created for several of the dominant tree species of this region.

Acknowledgments

87

Literature Cited

Ackermann, F. (1999). Airborne laser scanning-present status and future expectations *ISPRS Journal of Photogrammetry & Remote Sensing*, 54,64-67.

Anderson, J.E., Martin, M.E., Smith, M.L., Dubayah, R.O., Hofton, M., Hyde, P., Peterson, B., Blair, J.B., and Knox, R. (2006). The Use of Waveform Lidar to Measure Northern Temperate Mixed Conifer and Deciduous Forest Structure in New Hampshire. *Remote Sensing of Environment*, (in revision).

Blair, J.B., D.L. Rabine, & Hofton, M.A. (1999). The Laser Vegetation Imaging Sensor (LVIS): A medium- altitude, digitisation-only, airborne laser altimeter for mapping vegetation and topography. *ISPRS Journal of Photogrammetry and Remote Sensing*, 54, 115-122.

Blair, J.B., Hofton, M.A. & Rabine. D.L. (2004). Processing of NASA LVIS elevation and canopy (LGE, LCE and LGW) data products, version 1.0. (http://lvis.gsfc.nasa.gov).

Curtis, R.O. & Marshall, D.D. (2000). Why Quadratic Mean Diameter? *Western Journal of Applied Forestry,* 15(3), 137-139.

Drake, J.B. 2001. Estimation of Tropical Forest Aboveground Biomass Using Large-Footprint Lidar. Doctoral Dissertation. University of Maryland.

Drake, J.B., Dubayah, R.O., Clark, D.B., Knox, R.G., Blair, J.B., Hofton, M.A., Chazdon, R.L.,Weishampel, J.F., & Prince, S.D. (2002). Estimation of tropical forest structural characteristics using large-footprint lidar. *Remote Sensing of Environment,* 79, 305-319.

Dubayah, R.O., Knox, R.G., Hofton, M.A., Blair, J.B., & Drake, J.B. (2000). Land surface characterization using lidar remote sensing. In M.J. Hill & R.J. Aspinall (Eds.), *Spatial Information for Land Use Management* (pp.25-38). Australia: Gordon and Breach Science Publishers.

Foster, J.R., & Townsend, P.A. (2004). Linking hyperspectral imagery and forest inventories for forest assessment in the central Appalachians, Proceedings of the 14th Central Hardwood Forest Conference, 16-19 March 2004, Wooster, Ohio (U.S. Department of Agriculture, Forest Service, Northeastern Research Station Gen. Tech. Rep. NE-316, Newtown Square, Pensylvania), pp. 76–86.

Green, R.O., Eastwood, M.L., Sarture, C.M., Chrien, T.G., Aronsson, M., Chippendale, B.J., Faust, J.A., Pavri, B.E., Chovit, C.J., Solis, M. 1998. Imaging Spectrometry and the Airborne Visible/Infrared Imaging Spectrometer (AVIRIS). *Remote Sensing of Environment,* 65, 227-248.

Haskett, H.T. & Sood, A.K. (1998). Trade-off studies of detection performance versus the number of reflective spectral bands in hyperspectral imagery, Proceedings of the SPIE Conference on Algorithms for Multispectral and Hyperspectral Imagery IV, April 1998, Orlando, Florida (SPIE Vol. 3372), pp. 26-42.

Hastie, T., Tibshirani, R. & Friedman, J. (2001). *The Elements of Statistical Learning: Data Mining, Inference and Prediction.* Springer-Verlag. 536. pp.

Holmgren, J. (2003). *Estimation of forest variables using airborne lidar scanning.* Doctoral thesis. Swedish University of Agricultural Sciences. Umea, Sweden.

Hudak, A.T., Lefsky, M.A ,Cohen, W.B., & Berterretche, M. (2002). Integration of lidar and LANDSAT ETM+ data for estimating and mapping forest canopy height. *Remote Sensing of Environment*, 82, 397-416.

Hyyppä, J., Hyyppä, H., Inkinen, M., Engdahl, M., Linko, S., & Zhu,Y-H. (2000). Accuracy comparison of various remote sensing data sources in the retrieval of forest stand attributes. *Forest Ecology and Management*, 128, 109-120.

Hyyppa, H. J. & Hyyppa, J. M. (2001). Effects of stand size on the accuracy of remote sensing-based forest inventory. *IEEE Transactions on Geoscience and Remote Sensing*, 39(12), 2613-2621.

Jenkins, J.C., Chojnacky, D.C., Heath, L.S., & Birdsey, R.A. (2004). Comprehensive database of diameter-based biomass regressions for North American tree species. Gen. Tech. Rep. NE-319. Newtown Square, PA: U.S. Department of Agriculture, Forest Service, Northeastern Research Station. 45 p. [1 CD-ROM].

Lefsky, M.A., Cohen, W.B., Acker, S.A., Parker G., Spies, T.A., & Harding, D. (1999). Lidar remote sensing of the canopy structure and biophysical properties of Douglas Fir-Western Hemlock Forests. *Remote Sensing of Environment*, 70, 339-361.

Lefsky, M.A., Cohen, W.B., Parker, G.G., & Harding. D.J.(2002). Lidar remote sensing for ecosystem studies. *Bioscience*, 52(1), 19-30.

Lim, K., Treitz, P., Baldwin, K., Morrison, I., & Green, J. (2003). Lidar remote sensing of biophysical properties of tolerant northern hardwood forests. *Canadian Journal of Remote Sensing*, 29(5), 658-678.

Mark, H. & Workman, J. (1991). *Statistics in Spectroscopy*. San Diego, CA: Academic Press, Inc.

McCombs, J.W., Roberts, S.D., & Evans, D.L. (2003). Influence of fusing lidar and multispectral imagery on remotely sensed estimates of stands density and mean tree height ina managed Loblolly Pine plantation. *Forest Science*, 49(3), 457-466.

Naesset, E. (2002). Estimating tree height and crown properties using airborne scanning laser in a boreal nature reserve. *Remote Sensing of Environment*, 79(1), 105–115.

Ollinger, S.V. & Smith, M-L (2005). Net primary production and canopy nitrogen in a temperate forest landscape: An analysis using imaging spectroscopy, modeling, and field data, *Ecosystems*, 8:760-778.

Pohl, C. & Van Genderen, J.L. (1998). Multisensor image fusion in remote sensing: concepts, methods, and applications. *International Journal of Remote Sensing,* 19(5), 823-854.

Plourde, L., Martin, M.E., Smith M-L, & Ollinger, S.V. (2006). Estimating species abundance in a northern temperate forest using spectral mixture analysis. *Photogrammetric Engineering and Remote Sensing,* (in press).

Popescu, S.C., Wynne, R.H., & Scrivani, J.A. (2004). Fusion of small-footprint lidar and multispectral data to estimate plot-level volume and biomass in deciduous and pine forests in Virginia, USA. *Forest Science,* 50(4), 551-565.

Research Systems, Inc. (2002). ENVI (Version 3.6) User's Guide.

Roberts, D.A., Gardner, M., Church, R., Ustin, S., Scheer, G., and Green, R.O. (1998). Mapping chaparral in the Santa Monica mountains using endmember spectral mixture models, *Remote Sensing of Environment,* 65, 267-279.

Sall, J., Creighton, L. & Lehman, A. (2005). *JMP Start Statistics* (3rd edition). SAS Institute, Inc. Toronto, Canada: Thomson, Brooks/Cole.

Shapiro, S.S. & Wilk, M.B. (1965). An anlysis of variance test for normality (complete samples). *Biometrika* 52(3-4): 591-611.

Treuhaft, R.N., Asner, G.P., Law, B.E., & Van Tuyl, S. (2002). Forest leaf area density profiles from the quantitative fusion of radar and hyperspectral data. *Journal of Geophysical Research-Atmospheres,* 107: 4568.

Treuhaft, R. N.; Asner, G. P., and Law, B. E. Structure-Based Forest Biomass From Fusion of Radar and Hyperspectral Observations. Geophysical Research Letters. 2003 May 8; 30(9).

Underwood, E., Ustin, S., & DiPietro, D. (2003). Mapping nonnative plants using hyperspectral imagery. *Remote Sensing of Environment,* 86, 150-161.

Ustin, S.L. & Xiao, Q.F. (2001). Mapping successional boreal forests in interior central Alaska. *International Journal of Remote Sensing,* 22(6), 1779-1797.

Williams, A.P. & Hunt, Jr., E. R. (2002). Estimation of leafy spurge cover from hyperspectral imagery using mixture tuned matched filtering, *Remote Sensing of Environment,* 83, 446-456.

AVIRIS & LVIS

Forest Metric	adj. r^2	Press RMSE	N	Number of AVIRIS MNF 2003 and LVIS 2003 Model Predictors	VIF	Alpha	P
BA	0.47	7.51 m^{2}ha^{-1}	406	7 AVIRIS MNF and 1 LVIS	< 3	0.05	< 0.0001
AGBM	0.39	51.10 Mg ha^{-1}	406	7 AVIRIS MNF and 1 LVIS	< 2	0.05	< 0.0001
QMSD	0.33	2.86 cm	406	8 AVIRIS MNF and 2 LVIS	< 3	0.05	< 0.0001
BA - (unmanaged)	0.45	7.02 m^{2}ha^{-1}	158	4 AVIRIS MNF and 1 LVIS	< 2	0.05	< 0.0001
AGBM - (unmanaged)	0.55	41.03 Mg ha^{-1}	158	2 AVIRIS MNF and 1 LVIS	< 2	0.05	< 0.0001
QMSD - (unmanaged)	0.32	2.61 cm	158	2 AVIRIS MNF and 1 LVIS	< 2	0.05	< 0.0001

AVIRIS ONLY

Forest Metric	adj. r^2	Press RMSE	N	Number of AVIRIS MNF 2003 Model Predictors	VIF	Alpha	P
BA	0.39	8.08 m^{2}ha^{-1}	406	11 AVIRIS MNF	< 3	0.05	< 0.0001
AGBM	0.30	55.27 Mg ha^{-1}	406	13 AVIRIS MNF	< 2	0.05	< 0.0001
QMSD	0.17	3.18 cm	406	10 AVIRIS MNF	< 2	0.05	< 0.0001
BA - (unmanaged)	0.40	7.26 m^{2}ha^{-1}	158	3 AVIRIS MNF	< 2	0.05	< 0.0001
AGBM - (unmanaged)	0.45	45.27 Mg ha^{-1}	158	4 AVIRIS MNF	< 2	0.05	< 0.0001
QMSD – (unmanaged)	0.19	2.84 cm	158	3 AVIRIS MNF	< 2	0.05	< 0.0001

LVIS ONLY

| Forest Metric	adj. r^2	Press RMSE	N	Number of LVIS 2003 Model Predictors	VIF	Alpha	P
BA	0.16	9.35 m^{2}ha^{-1}	406	1 LVIS (RH25)	1	0.05	< 0.0001
AGBM	0.27	55.52 Mg ha^{-1}	406	1 LVIS (RH50)	1	0.05	< 0.0001
QMSD	0.25	3.00 cm	406	2 LVIS (RH25 and RH75)	< 2	0.05	< 0.0001
BA - (unmanaged)	0.25	8.05 m^{2}ha^{-1}	158	1 LVIS (RH50)	1	0.05	< 0.0001
AGBM - (unmanaged)	0.36	48.75 Mg ha^{-1}	158	1 LVIS (RH50)	1	0.05	< 0.0001
QMSD – (unmanaged)	0.29	3.00 cm	158	1 LVIS (RH100)	1	0.05	< 0.0001

Table 2.1 Relationships between 2003 AVIRIS MNF and LVIS metrics and selected measures of forest structure

Forest Metrics	adj. r^2	Press RMSE	N	Number of AVIRIS MNF 2003 & LVIS 2003 Model Predictors	VIF	Alpha	p
Arcsine Square Root of American Beech AGBM Fraction	0.65	0.16	379	7 AVIRIS MNF	< 2	0.05	< 0.0001
Arcsine Square Root of Red Maple AGBM Fraction (Red Maple AGBM fraction > 0.01 in unmanaged forest)	0.61	0.13	138	5 AVIRIS MNF & 1 LVIS	< 2	0.05	< 0.0001
Arcsine Square Root of Red Maple AGBM Fraction (Red Maple AGBM fraction > 0.01 in unmanaged forest)	0.52	0.14	138	5 AVIRIS MNF	< 2	0.05	< 0.0001
Arcsine Square Root - Eastern Hemlock AGBM Fraction	0.57	0.12	337	8 AVIRIS MNF	< 2	0.05	< 0.0001
Arcsine Square Root of Sugar Maple AGBM Fraction (Sugar Maple AGBM fraction > 0.01)	0.51	0.14	256	10 AVIRIS MNF & 1 LVIS	< 2	0.05	< 0.0001
Arcsine Square Root of Sugar Maple AGBM Fraction (Sugar Maple AGBM fraction > 0.01)	0.49	0.14	256	10 AVIRIS MNF	< 2	0.05	< 0.0001
Arcsine Square Root of Yellow Birch AGBM Fraction	0.25	0.14	358	8 AVIRIS & 1 LVIS	< 2	0.05	< 0.0001

Table 2.2 Relationships between 2003 AVIRIS MNF and LVIS metrics and species composition proportional to AGBM

93

Forest Metric	r^2 or adj. r^2	Press RMSE (cm)	N	LVIS 2003 Model Predictors	VIF	Alpha	P
QMSD$_H$ (Eastern Hemlock AGBM fraction > 0.3)	0.46	1.93	38	RH 25 & RH75	< 2	0.05	< 0.0001
QMSD$_R$ (Red Maple AGBM fraction > 0.33 in unmanaged forest)	0.43	2.22	55	RH100	1	0.05	< 0.0001
QMSD$_S$ (Sugar Maple AGBM fraction > 0.1 in unmanaged forest)	0.40	1.85	27	RH75	1	0.05	0.0004

Table 2.3 Relationships between 2003 LVIS metrics and QMSD

94
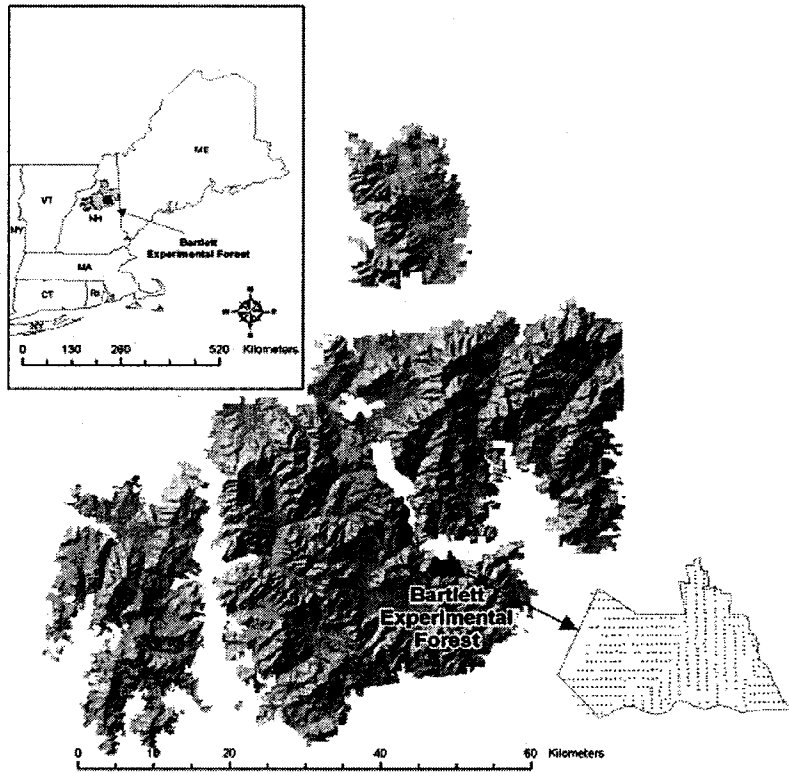
Figure 2.1 Location of Bartlett Experimental Forest, showing established plot network.

95
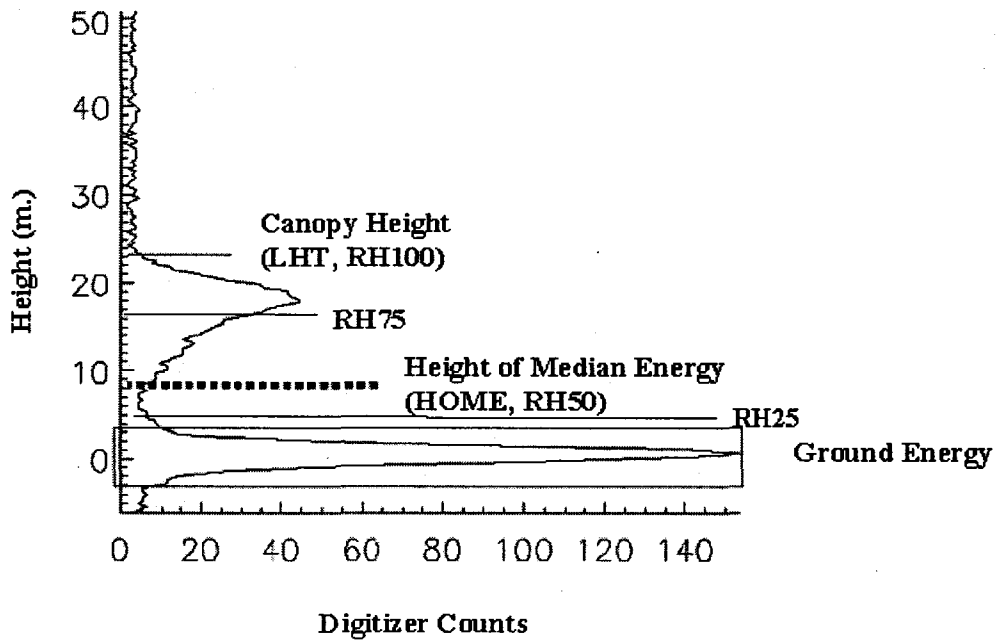
Figure 2.2   Metrics derived from lidar waveforms. Adapted from Drake et al. 2002.
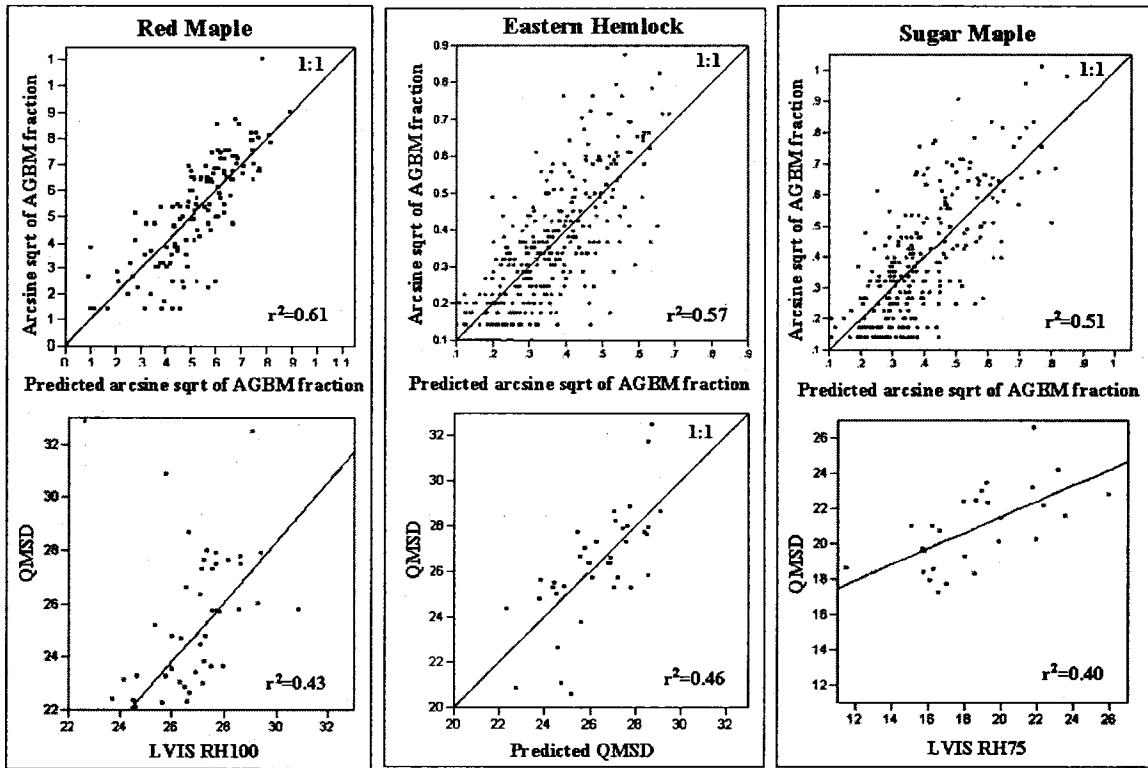
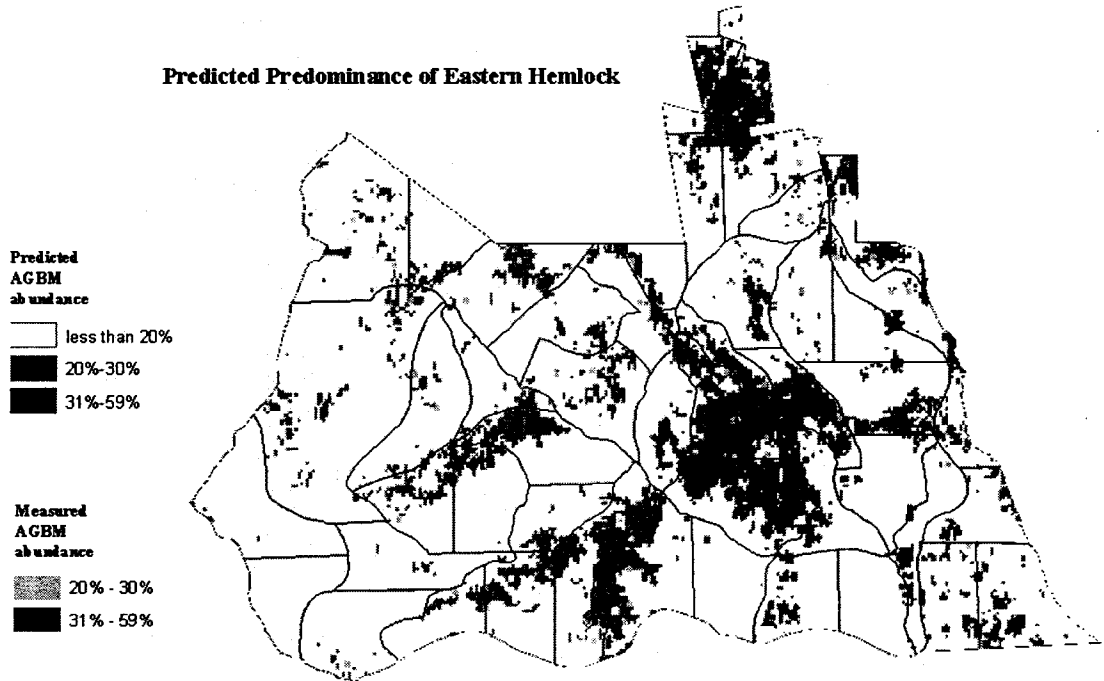**Figure 2.3 Scatter plots of predicted abundance patterns and QMSD relationships for selected species. Restrictions on plot selections and resulting regression models are found in Tables 2.2 and 2.3.**

97

Predicted Predominance of Eastern Hemlock

Predicted
AGBM
abundance

- less than 20%
- 20%-30%
- 31%-59%

Measured
AGBM
abundance

- 20% - 30%
- 31% - 59%

Figure 2.4   Predicted areas of eastern hemlock predominance (AGBM fraction > 0.2) in BEF. Black shading is predicted to encompass more than 30% hemlock AGBM. Lighter gray shading is predicted to encompass from 20% to 30% hemlock AGBM. The model generated the following parameters: adj. r^2 = 0.57; Press RMSE = 0.12; p < .0001; N=337 for points where hemlock AGBM > 0, using 8 AVIRIS variables as predictors. The model is derived from stepwise regression of 25 standardized LVIS and AVIRIS MNF metrics obtained from flights conducted in 2003. An overlay of USFS NERS plot data indicating hemlock abundance (dark red squares > 0.3; pale red squares < 0.3 and > 0.2) measured in 2001-2003 is also presented.

98

Predicted Predominance of Red Maple

Predicted
AGBM
abundance

less than 20%
20%-30%
30%-80%

Measured
AGBM
abundance

20% - 30%
31% - 80%
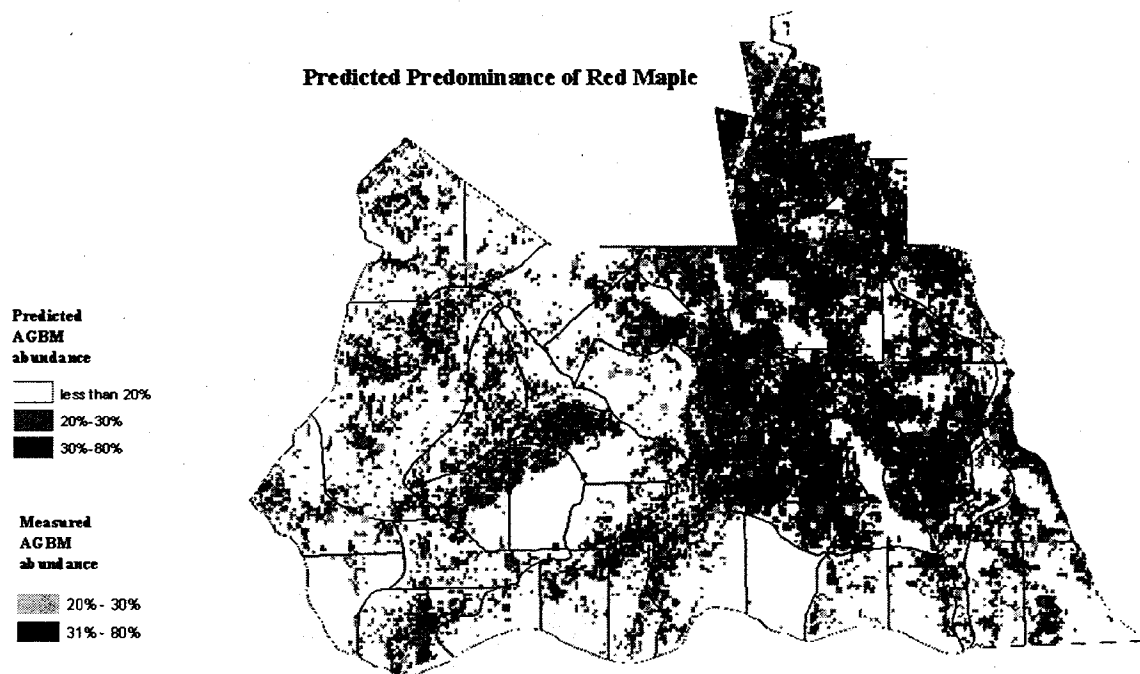
Figure 2.5 Predicted areas of red maple predominance in the BEF. Black shading is predicted to encompass more than 30% red maple AGBM. Gray shading is predicted to encompass from 20% to 30% red maple AGBM. The model generated the following parameters: adj. r^2 = 0.61; Press RMSE = 0.13; p < .0001; N=138 for points where red maple AGBM > 0.01 in relatively unmanaged conditions, using 5 AVIRIS variables and 1 LVIS metric as predictors. The model is derived from stepwise regression of 24 LVIS and AVIRIS MNF metrics obtained from flights conducted in 2003. An overlay of USFS NERS plot data indicating red maple abundance (dark red squares > 0.30; pale red squares < 0.3 and > 0.2) measured in 2001-2003 is also presented.

99

Predicted Predominance of Sugar Maple
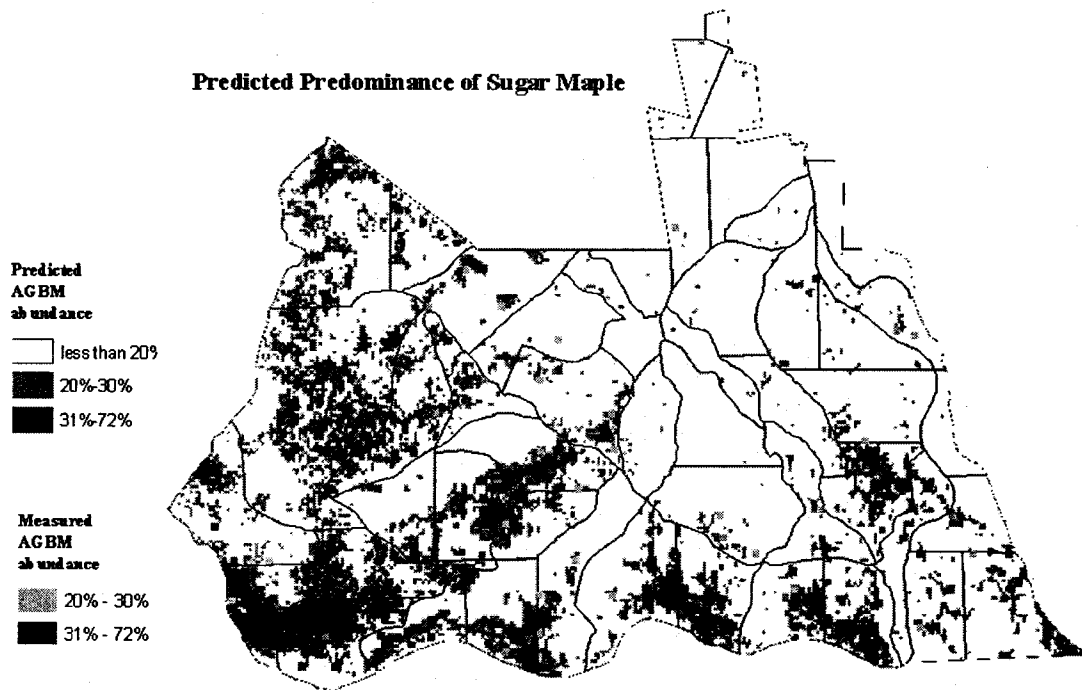

Figure 2.6   Predicted areas of sugar maple predominance in BEF. Black shading is predicted to encompass more than 30% sugar maple AGBM. Gray shading is predicted to encompass from 20% to 30% sugar maple AGBM. The model generated the following parameters: adj. r^2 = 0.51; Press RMSE = 0.14; p < .0001; N=256 for points where sugar maple AGBM > 0.01, using 10 AVIRIS variables and 1 LVIS metric as predictors. The model is derived from stepwise regression of 26 LVIS and AVIRIS MNF metrics obtained from flights conducted in 2003. An overlay of USFS NERS plot data indicating sugar maple abundance (dark red squares > 0.30; pale red squares < 0.3 and > 0.2) measured in 2001-2003 is also presented.

100

Remote Inventory (AVIRIS and LVIS) of Eastern Hemlock

Predicted QMSD (cm)

- 0
- 1 - 15
- 16 - 20
- 21 - 22
- 23 - 24
- 25 - 26
- 27 - 28
- 29 - 30
- 31 - 35
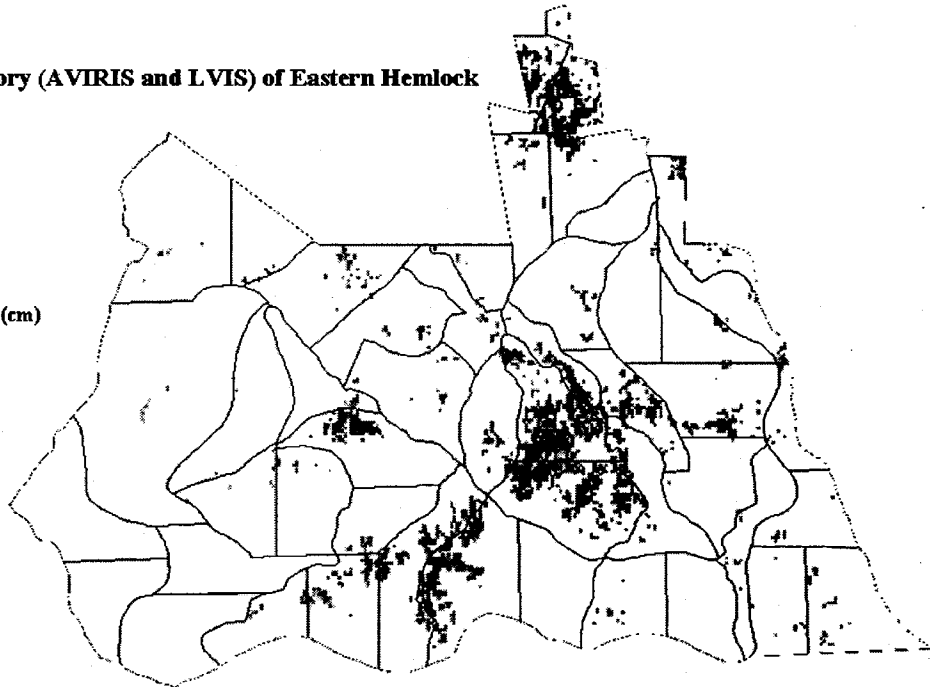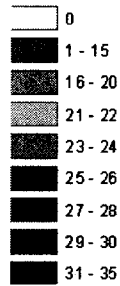
Figure 2.7 Two prediction models are combined in this map. Levels of predicted quadratic mean stem diameter (QMSD; cm) are shown within regions of the BEF that are predicted to encompass more than 30% Eastern Hemlock AGBM. The abundance model is derived from stepwise regression of 25 LVIS and AVIRIS MNF metrics obtained from flights conducted in 2003. The model predicting eastern hemlock abundance generated the following parameters: adj. r^2 = 0.57; Press RMSE = 0.12; p < 0.0001; N=337 for points where Eastern Hemlock AGBM > 0, using 8 AVIRIS variables as predictors. The model predicting QMSD (stems > 10 cm) generated the following parameters: adj. r^2 = 0.46; Press RMSE = 1.93 cm; p < .0001; N= 38 for points where Eastern Hemlock AGBM fraction > 0.30, using 2 LVIS metric as predictors.

101

Remote Inventory (AVIRIS and LVIS) of Red Maple

Predicted
QMSD
(cm)

- 1-5
- 6-10
- 11-15
- 16-20
- 21-25
- 26-30
- 31-35
- 36-40
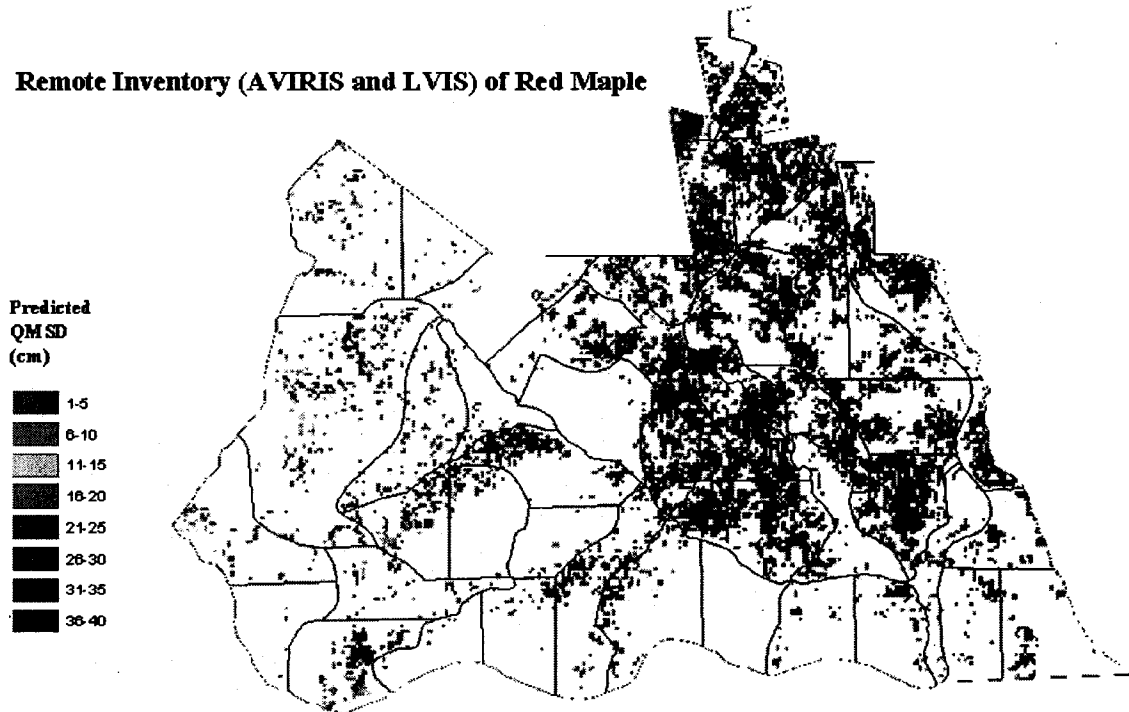
Figure 2.8   Two prediction models are combined in this map. Levels of predicted quadratic mean stem diameter (QMSD; cm) are shown within regions of the BEF that are predicted to encompass more than 30% red maple AGBM. The abundance model is derived from stepwise regression of 24 LVIS and AVIRIS MNF metrics obtained from flights conducted in 2003. The model predicting red maple abundance generated the following parameters: adj. r^2 = 0.61; Press RMSE = 0.13; p < 0.0001; N=138 for points where red maple AGBM > 0.01 in relatively unmanaged conditions, using 5 AVIRIS variables and 1 LVIS metric as predictors. The model predicting QMSD (stems > 10 cm) generated the following parameters: adj. r^2 = 0.43; Press RMSE = 2.22 cm; p < .0004; N= 55 for points where red maple AGBM fraction > 0.33, using 1 LVIS metric as a predictor.

Remote Inventory (AVIRIS and LVIS) of Sugar Maple

Predicted
QMSD
(cm)

- 13 - 14
- 15 - 16
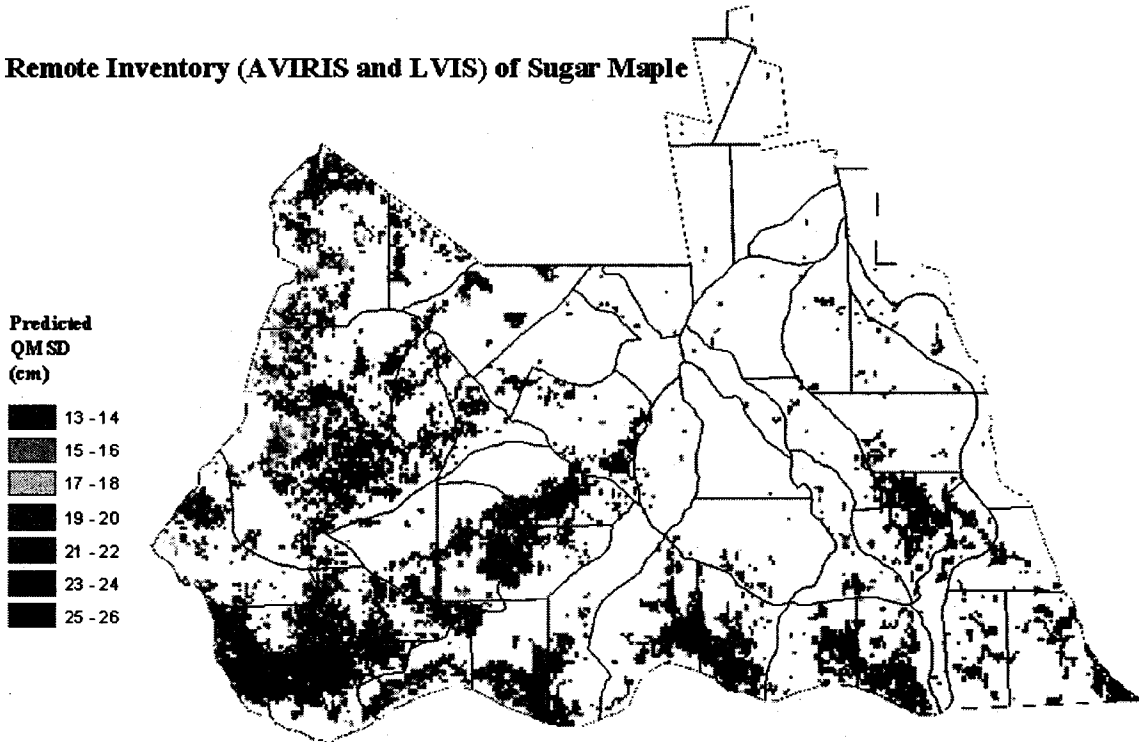- 17 - 18
- 19 - 20
- 21 - 22
- 23 - 24
- 25 - 26

Figure 2.9 Two prediction models are combined in this map. Levels of predicted quadratic mean stem diameter (QMSD; cm) are shown within regions of the Bartlett Experimental Forest that are predicted to encompass more than 20% sugar maple AGBM. The abundance model is derived from stepwise regression of 26 LVIS and AVIRIS MNF metrics obtained from flights conducted in 2003. The model predicting suagr maple abundance generated the following parameters: adj. r^2 = 0.51; Press RMSE = 0.14; p < 0.0001; N=256 for points where sugar maple AGBM > 0.01, using 10 AVIRIS variables and 1 LVIS metric as predictors. The model predicting QMSD (stems > 5 cm) generated the following parameters: adj. r^2 = 0.40; Press RMSE = 1.85 cm; p < .0004; N= 27 for points where sugar maple AGBM fraction > 0.1, using 1 LVIS metric as a predictor.

103
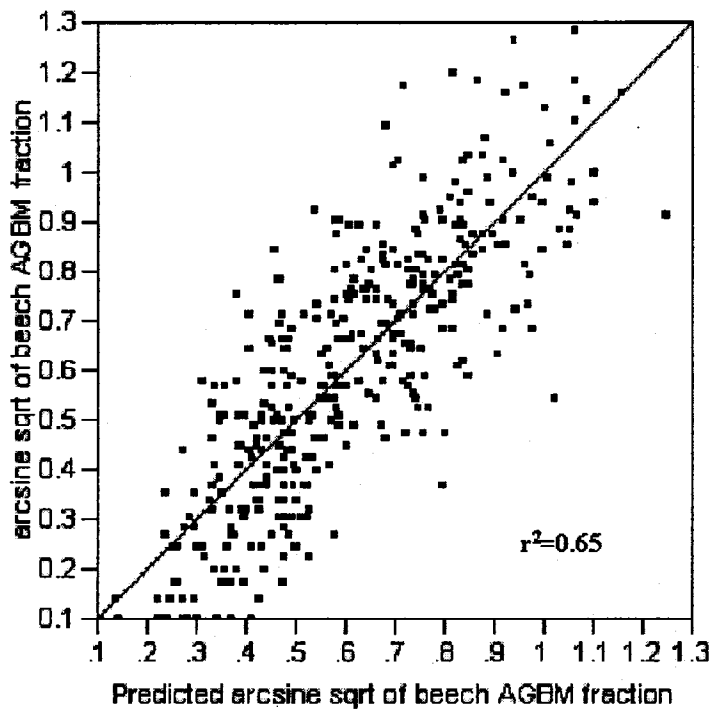
Figure 2.10 Scatter plot of predicted abundance pattern for American beech. Regression model is found in Table 2.2.

104

CHAPTER 3

THE USE OF WAVEFORM LIDAR AND HYPERSPECTRAL SENSORS TO ASSESS THE SPATIAL, COMPOSITIONAL, AND STRUCTURAL PATTERNS ASSOCIATED WITH RECENT AND REPEAT DISTURBANCE

Abstract

Waveform lidar imagery was acquired on September 26, 1999 over the 1000-ha. Bartlett Experimental Forest (BEF) in central New Hampshire (USA) using NASA's airborne Laser Vegetation Imaging Sensor (LVIS). This flight occurred 20 months after an extensive ice storm damaged millions of acres of forestland in northeastern North America. Lidar measurements of the amplitude and intensity of ground returns appeared to readily detect areas of moderate to severe ice storm damage within the BEF and revealed environmental patterning associated with the worst damage. Southern through eastern aspects on side slopes were particularly susceptible to higher levels of damage in

105

this forest, in large part overlapping tracts of forest that had also suffered the highest levels of wind damage from the 1938 hurricane. The highest levels of sugar maple (*Acer saccharum*) basal area and biomass within the BEF, determined through analysis of 1997 Airborne Visible/Infrared Imaging Spectrometer (AVIRIS) high resolution spectral imagery and ongoing inventory of USFS Northeastern Research Station (NERS) field plots, are located within the same tracts of forest. Site susceptibility to repeated natural disturbance of intermediate severity occurring over a period of decades may be influencing the species composition of these tracts. The percentage of sugar maple coarse woody debris (CWD), adjusted to represent the amount of dead wood of 3 in. (7.6 cm.) diameter size or greater fallen throughout BEF since the 1998 ice storm, is only 4% of the total despite sugar maple comprising 11% of the total biomass of BEF. We found log normal agreement between field measurements of coarse woody debris greater than 7.6 cm dbh and the LVIS metrics of mean canopy height ($r^2 = 0.57$; $p = 0.000$) in areas that had been subjected to moderate-to-severe ice storm damage.

Keywords: lidar, LIDAR, LVIS, laser altimetry, AVIRIS, high resolution spectral imagery, hyperspectral, end member analysis, canopy, structure, height, biomass, ground energy, ice storm, hurricane, site susceptibility to natural disturbance; coarse woody debris, sugar maple, *Acer saccharum*

Introduction

In regions prone to catastrophic wind events, it has been suggested by Foster et al. (1998) that persistent landscape-scale variation in site susceptibility can strongly influence patterns of forest damage and may, as a consequence of the frequency and intensity of disturbance, also control such ecological characteristics as canopy structure, the spatial pattern and traits of successional and old-growth forests, and primary production. It has also been increasingly recognized that in addition to major wind events, ice storm damage is a significant factor in the structuring of forests; under certain conditions, reaching levels of biomass and basal area damage that rival or even exceed the magnitude of damage seen with major hurricanes (Hooper et al. 2001). Factors controlling the pattern of forest damage from such disturbances include gradients of wind velocity, topographic exposure, site condition, composition, structure and history (Foster et al. 1998).

For parts of northern New England, two of the most significant, wide-ranging natural disturbances of the past century were the September 1938 hurricane and the January 1998 ice storm. These storms occurred 60 years apart and impacted some of the same landscape, particularly in north-central New Hampshire. Information on the characteristic distribution and legacies of these natural disturbances over time and space has been reported and simulated in the northeast from a few well-studied sites (Boose et al. 1994,

Foster 1988a, 1988b, Foster & Boose 1992, Peart et al.1992, Rhoads et al. 2002), but the demand for agencies charged with forest management to remotely and repeatedly document the spatial extent and magnitude of such events on a broader scale has been increasing over time (Schwarz et al. 2003, Millward and Kraft 2004). Knowledge of the variability found within these patterns is also important to efforts to accurately model carbon balances worldwide.

Waveform-recording lidar (hereinafter lidar) can readily detect the spatial patterns of large, infrequent disturbance (Boutet and Weishampel 2003). As a remote sensing tool with excellent ability to characterize various aspects of forest structure and light patterning, as well as elevation (Dubayah et al. 2000, Parker et al. 2001), it can be used to reveal environmental controls on patterns that are specific to particular types of disturbance. Relationships between lidar metrics and the magnitude of coarse woody debris (CWD) found in forested areas subjected to recent disturbance have not been previously studied. But such findings, especially when combined with compositional data revealed through spectral imagery, could increase the possibilities to remotely map and quantify the overall impacts resultant from site susceptibility to repeated natural disturbance events.

In New England, severe damage from the 1938 hurricane has been characteristically, but not exclusively, reported on south-to-east facing slopes (Boose et al. 1994, Foster 1988a, Peart et al. 1992). Similarly, Lafon et al. (1999) described ice storm impacts from two successive storms in Virginia where the heaviest forest damage occurred on mountain

108

slopes facing south and east, while Millward and Kraft (2004) reported that damage from the January 1998 ice storm in the Adirondacks was concentrated at locations with a landscape orientation facing eastward and ranging between northwest and southeast. They also reported impacts concentrated at elevations ranging from 200 to 600 m. Rhoads et al. (2002) have documented the effect of the January 1998 ice storm on the northern hardwood canopy at Hubbard Brook. They reported that damage in the 60 to 120 year old south-facing watersheds was greatest in trees >30 cm diameter at breast height and at elevations above 600 m. Of the dominant tree species within that northern hardwood forest, beech was the most damaged, sugar maple was the most resistant, and yellow birch was intermediate.

Canham et al. (2001) have noted that periodic storms of intermediate severity allow interspecific differences in canopy tree survival to play a strong role in succession, with forests becoming progressively wind-firm and less susceptible to wind disturbance in the absence of catastrophic events. Their findings in mature northern hardwood forests report that yellow birch and sugar maple have the lowest levels of windthrow; accounting in part for their relatively high abundance in old-growth forests (Woods and Cogbill 1994). While the return intervals for extreme catastrophic disturbance of northern temperate forests may be measured over centuries, historical records also suggest that storms with winds or ice sufficient to damage a significant fraction of canopy trees in a stand occur at frequencies measured in decades to scores of years (Canham et al. 2001).

109

Ruffner and Abrams (2003) provide further data on the return time between such moderate-to-severe natural disturbances and comparable links between disturbance frequency and compositional status of northeastern hemlock-northern hardwoods forests. Disturbance intensity was directly related to site elevation and exposure, decreasing from the upland to riparian sites. Upland sites (stand age approximately 350 years) experienced medium-intensity disturbances (>20% canopy damage) nearly every 30 years with four decades exhibiting heavy (severe) disturbances (>40% canopy damage), resulting in higher importance of early successional taxa on uplands. The side slope site (stand age 350 years) experienced medium-intensity disturbances every decade with only one severe intensity disturbance. The riparian site (stand age 250 years) was impacted by medium-intensity disturbances every 80 years with no severe disturbances in the last 250 years, resulting in the dominance of these sites by later successional hemlock and beech. Recruitment patterns were affected by disturbance intensity, with successional hardwood species such as yellow birch and red maple recruiting only after medium-to-heavy intensity disturbances, and later successional hemlock and beech recruiting successfully with low-intensity disturbances.

Significant canopy damage was inflicted on the Bartlett Experimental Forest in north-central New Hampshire (USA) by both the 1938 hurricane and the 1998 ice storm (Forest Service records, M.L. Smith, personal communication). Airborne remote sensors collecting both spectral and physical attribute data were flown over Bartlett relatively close to the timeframe of the 1998 storm. The close juxtaposition of the heaviest damage from both storm events over the same tracts of northern temperate mixed deciduous

110

forest at Bartlett provides an opportunity to look for emergent structural properties that may result from repeat exposure to storms of intermediate severity using the tools of remote sensing. It is the intent of this paper to assess the use of waveform lidar and hyperspectral sensor data to locate the spatial, compositional and structural patterns that emerge as the legacies of repeat disturbances at this specific site within the White Mountain National Forest.

Methods

Site

Over the past seventy years, the USFS Northeastern Research Station (NERS) has assembled a large volume of field data (e.g. Leak 1982, 1996, 1999, Leak and Smith 1996, 1997, Leak and Sendak 2002, Smith et al. 2002) on a variety of ecosystem processes and forest metrics within the 1052-hectare Bartlett Experimental Forest (BEF) located within the White Mountain National Forest in the central White Mountains (Figure 3.1 and Table 3.1). The landscape of this site reflects an extensive history of experimental forest management and varied natural disturbance regimes. Deciduous and coniferous forest types including northern hardwood [e.g. sugar maple (*Acer saccharum* Marsh), beech (*Fagus grandifolia* Ehrh.), yellow birch (*Betula alleghaniensis* Britton),

111

red spruce-balsam fir (*Picea rubens* Sarg.-*Abies balsamea* (L.) Miller), eastern hemlock (*Tsuga canadensis* (L.) Carr.), and red oak-white pine (*Quercus rubra* L - *Pinus strobus* L.)] are represented on a site ranging in elevation from 200 m to 850 m. Slopes vary from flat terrain to nearly vertical (rock cliff) conditions. The forest reflects a range of successional sequences, forest patch sizes, and structural distributions. Clear-cutting, group and individual tree selection, basal area and shelter-wood cuttings have been undertaken on approximately 55% of the forest. Forest ages in managed stands range from more than 70 to less than 5 years old. Half of the forest serves as an unmanaged, natural control, characterized by natural forest disturbance regimes, with ages ranging upwards of 100 years (Leak and Smith 1996).

Aspect

For this study, aspect (Figure 3.2) was determined using a digital elevation model derived from the bilinear interpolation of a USGS national elevation data set. (Ingraham 2004). Eight classes, each encompassing a range of 45° plus an additional class for flat terrain were established using tools within the spatial analyst extension of ArcGIS (v. 8.3) (ESRI 1999-2002). Eastern through southern aspects specifically range from 67.5° - 202.5°.

112

The USFS NERS originally established a regular grid of approximately 500 permanent research plots at Bartlett Experimental Forest in 1931-1932 (Figure 3.1). Re-sampling of over 400 of these 0.1 ha square plots was undertaken by the USFS NERS in the 2001-2003 field seasons. Measurements tally species and dbh in 1-inch (2.54 cm) dbh classes for trees greater than 1.5 inches (.ca 4 cm.) in size. Stem diameters were used to calculate basal area. Estimates of total standing aboveground biomass (AGBM) were calculated from the field DBH data at footprint and larger scales using established allometric equations specific to the northeastern region and inclusive of bole, branch and foliar biomass (Hocker and Early 1983, Tritton and Hornbeck 1981, Young et al. 1980, and Whittaker et al. 1974). These equations were applied to the field data to calculate total standing (aboveground) biomass for each stem (live and dead) and then summed to provide the biomass of all stems within a plot. The relative fraction of basal area and biomass attributed to each tree species was calculated for each of the inventoried plots. All inventory plots have been geo-referenced to within 3-meter positional accuracy. These data provide a comprehensive ground inventory of standing biomass and species composition of the Bartlett Experimental Forest (Table 3.1).

113

Lidar Data

Lidar data was acquired on September 26, 1999 over the BEF using NASA's Laser

Vegetation Imaging Sensor (Blair et al. 1999). Nine flight lines were completed between

Bartlett and West Thornton, N.H. (M. Hofton, personal comm.). LVIS is an airborne

imaging laser altimeter that records the time and amplitude of a laser pulse reflected off

target surfaces. The sensor digitizes the vertical distribution of intercepted surfaces

between the first (top of the canopy) and the last (ground) return producing a waveform

record. LVIS records circular footprints of variable size; 1999 footprints had a nominal

radius of 12.5 m. Additional detail on LVIS capabilities can be found in Blair et al.

(1999).

LVIS metrics used in this study were derived from the waveforms using an automated

algorithm (Hyde et al. 2005). Lidar canopy height (LHT) was calculated by identifying

two locations within the waveform where (1) the signal initially increases above a mean

noise level/threshold (the canopy top) and (2) at the center of the last Gaussian pulse (the

ground return). The distance between these two locations was then calculated to derive

the height metric (Figure 3.3) The height of median energy (HOME) was calculated by

finding the median of the entire signal (i.e. above the mean noise level) from the

waveform, including energy returned from both canopy and ground surfaces. The

location of the median energy was then referenced to the center of the last Gaussian pulse

to derive a height (Drake et al. 2002). The ground energy return metric (GRND) was

114

determined by taking the total intensity (i.e. number of digitizer counts) contained in all

approximately 30 cm vertical bins contained in the last Gaussian peak (Hofton et al.

2000); (Figure 3.3). Canopy energy (CAN_E) is calculated as the total intensity of the

entire waveform minus the ground return energy (GRND).

Coarse Woody Debris

Line-intercept sampling (Warren and Olsen 1964, Beers and Miller 1976, Husch et al.

2003) was utilized to collect coarse woody debris data on 190 transects within the Bartlett

Experimental Forest in 2004. Each transect was approximately 100 meters in length

originating at the primary corner of a USFS NERS permanent inventory plot. Dead wood

greater than 3 inches (7.62 cm.) was recorded. Measurements included log length, end of

log diameters, and orientation of fall. Logs were identified to species or

hardwood/softwood categories where possible.

Logs were assigned to one of eight decay classes in the field with decay class I containing

the most recently fallen debris. Decay classes were established based on methods used by

C. Cogbill (personal correspondence to A. Fast) and Pyle and Brown (1998 and 1999).

The range in years since mortality encompassed within any given decay class of fallen

logs was classified based on analysis of an ongoing tree silvics study established at BEF

in 1963 and 1964 (Leak and Solomon 1975, Solomon 1977a, Solomon 1977b). All trees

within 48 one-third acre plots were identified, tagged, and mapped; plots were

115

inventoried every 2-6 years: 1967, 1969, 1972, 1974, 1980, 1985, 1989, 1991, 1995, 2000 and 2004. This data allowed a range of time each log has been on the ground to be determined. Logs were assigned to decay classes in 2004 and cross-tabulated with time since mortality. The cumulative percentage of logs of a given age within any decay class was subsequently calculated (Fast 2005). For example, decay class I and II encompass hardwood logs that have been on the ground for anywhere from 1 to 13 years with 89% of the logs in decay class I having been on the ground for six years or less and 44% of the logs from decay class II having been on the ground for six years or less (Fast 2005).

For this study, log volume per acre figures were adjusted to reflect the amount of CWD on the ground that had fallen within the six-year time frame since the occurrence of the 1998 ice storm.

Initial volume calculations follow the equations provided below:

Volume per log was calculated as $V_{Tot} = D^2 / [b_0 + (b_1/H)]$ (Honer 1967) where:

V_{Tot} = Total volume in ft^3

D = diameter outside bark (inches) measured at breast height (4.5. ft)

H = total height (ft)

b_0 and b_1 are species specific regression coefficients derived from Honer (1967).

Volume per acre was calculated as 43,560 $ft^2/(w_i \times T)$ ft^2 (Tritton 1980) where:

116

T = transect length (330 ft. or 100.58 meters)

S_i = sample$_i$

P_i = projections (feet or meters)

$W_i = P_i + P_i$ (effective plot width for S_i)

AVIRIS

Sugar maple (*Acer saccharum*) abundance classification was derived from high spectral resolution imagery (Figure 3.4). Image data were acquired using NASA's Airborne Visible/Infrared Imaging Spectrometer (AVIRIS). AVIRIS records data in 224 contiguous spectral bands covering the spectral range of 0.4-2.4 μm with a spectral resolution of 10 nm. The spatial resolution of AVIRIS data is 20 m with a full scene covering 10 x 10 km. (Vane and Goetz 1988). Cloud-free AVIRIS imagery was obtained for the entire White Mountain National Forest in New Hampshire in August 1997. A subset of this image data set was created to include only BEF. This image was then atmospherically corrected using ATREM 3.1 (Gao et al. 1992) and geometrically corrected with ERDAS Imagine v. 8.5. Wavelength channels were evaluated in the AVIRIS image using the ENVI™ (v. 3.6) animation tool, and those with strong water absorption features and low signal-to-noise were excluded from further analysis. The AVIRIS image was then transformed with a minimum noise fraction (MNF) transform rotation to reduce data dimensionality in preparation for spectral unmixing.

117

Inventory data collected for more than 400 plots in Bartlett Experimental Forest in the early 1990s provided the basis for estimates of sugar maple abundance. Regions of interest (ROIs) were created in the AVIRIS image using relative sugar maple abundance calculated from basal area for 163 of the plots. The endmembers from these ROIs were then applied to a mixture tuned matched filtering (MTMF™) algorithm (Research Systems, Inc. 2002) to map six classes of sugar maple abundance: 1 to 10%; 11 to 20%; 21 to 30%; 31 to 40%; 41 to 50%; and greater than 50%.

Data Analysis

Sugar Maple Abundance and LVIS Metrics

USFS NERS inventory plot data for the Bartlett Experimental Forest was used to examine relationships between sugar maple abundance, aspect and 1999 LVIS measures of ground return energy. In comparison to the 0.1 ha square USFS NERS inventory plots, the 1999 LVIS circular footprints are 0.049 hectares in size. Given the variable overlap of LVIS flight lines during the 1999 flight over Bartlett, any given USFS NERS plot contained the center points of from one to ten lidar footprints. For each of these plots, mean values were calculated for the 1999 LVIS metrics (e.g. elevation and ground return

118

energy) derived from footprints with center points located within the bounds of USFS

NERS plots. Analysis was restricted to 145 plots where sugar maple was present

at elevations above 325 m with mean tree height exceeding 19 m. Plots were then

aggregated by aspect and mean values on sugar maple abundance and mean ground

energy generated for each group.

Coarse Woody Debris and LVIS Metrics

For this analysis, the CWD data for Bartlett was adjusted to use log volume

measurements per acre that reflect the fraction of volume derived from logs that were

considered to be six years or less in age since mortality. This six year period corresponds

to the time frame between CWD data collection and the last major natural disturbance

within this forest; the ice storm of January 1998. A 20 meter by 100 meter polygon

(hereinafter called the CWD plot) originating from the USFS Northeastern Research

Station (NERS) primary plot corner was used to encompass each CWD transect and to

define an area from which the center points of the 1999 LVIS footprints that fall within

the plot could be extracted.

Given the variable overlap of LVIS flight lines during the 1999 flight over Bartlett, any

given CWD plot contained the center points from between one to eighteen lidar footprints

(Figure 3.5). For each of the 190 CWD transects, mean values and their squares were

calculated for the LVIS 1999 metrics (LHT, HOME, GRND, CAN_E) derived from

119

footprints with center points located within the bounds of the CWD plots. The CWD

metrics of volume per log per acre within the most recent six year mortality class were

also aggregated and summed for each CWD transect.

To find relationships specific to those areas of Bartlett that contain mature, northern

hardwood forest with open or damaged canopy, three restrictions were imposed on the

dataset. Sites were chosen where the LVIS measure of the intensity of ground return

energy was relatively high (mean ground energy > 2250), mean elevation exceeded 325

m and where LVIS canopy height reflected the height of mid-successional forest (mean

height > 19 m; Figure 3.6). The latter restrictions removed from consideration those sites

at Bartlett that have been subject to recent forest management and gave emphasis to

sloped forest tracts comprised largely of northern hardwood species. Eighteen CWD plots

met these restrictions (Figure 3.6).

The relationships between the measured CWD data (dependent variables) and the mean

values of 4 LVIS (LHT, HOME, GRND_E and CAN_E) (independent variables) were

explored through stepwise mixed linear regression techniques. Statistical analyses were

conducted using JMP IN® software (SAS Institute Inc. 2005). Dependent, independent

variables and the regression residuals were tested for normality of their distributions

using the Shapiro-Wilk W test (Shapiro and Wilk 1965) and normal quantile plots. A

natural log transform was used to improve the normality of the distribution. The critical

value of P (alpha) was set at 0.05. Prediction error sum of squares root mean square

errors (PRESS RMSE) were calculated for each forest metric. PRESS RMSE is

computed as the square root sum of squares of the prediction residuals (Mark and Workman 1991, Hastie et al. 2001). As an out-of sample validation technique, Press RMSE tests how well the current model would predict each of the points in the data set (in turn) if they were not included in the regression. Low values of PRESS RMSE usually indicate that the model is not overly sensitive to any single data point. Regression results are summarized in Figure 3.9. Maps were analyzed and produced using ENVI® v. 4.2 (Research Systems, Inc. 2005), Imagine® v. 8.7 (ERDAS 2004), and ArcGIS ® v. 8.3 (ESRI, 1999-2002) software.

Results

Sugar Maple Abundance and LVIS Metrics

A strong association between areas supporting greater than 30% basal area of sugar maple with the higher values of 1999 LVIS ground energy metrics is visually apparent in Figure 3.7. The overlap is particularly striking on forest tracts with southern through eastern aspects. USFS NERS field data (Figure 3.8) also indicates that plots located on southeastern aspects at Bartlett support a higher abundance of sugar maple and higher levels of measured ground return energy. Analysis of variance of 1999 LVIS mean ground energy metrics versus aspect was significant ($p < 0.000$) for all 411 plots sampled

121

by the Forest Service, as well as for the smaller subsets of 277 plots where sugar maple was present and 145 plots restricted to mature forests above elevations of 325 m. The distribution of sugar maple abundance was non-normal and Kruskal-Wallis analysis of sugar maple abundance versus aspect was significant at $p < 0.007$ (N=145) and $p < 0.000$ (N=277 and 411). Sugar maple CWD from decay classes I and II is virtually non-existent within these same areas with only 8 logs out of 437 (2%) logs found within those two decay classes in the forest as a whole (Figure 3.7). Sugar maple CWD from decay classes I-III accounted for only 4% of the downed logs within the forest.

Coarse Woody Debris and LVIS metrics

The restrictions described above resulted in the selection of eighteen plots in the western half of Bartlett. Of these, seventeen are largely hardwood sites, with beech predominant as CWD (Table 3.2). Sixteen of these eighteen plots are located on southern, southeastern or eastern aspects (Figure 3.7). All transects were located within the area of Bartlett that suffered the heaviest amounts of damage from the 1998 ice storm. Under these restrictions, the relationship between the log value of the sum of CWD log volumes (adjusted to reflect a per acre figure for logs that have fallen within the past six years) per CWD transect with the mean canopy height of aggregated 1999 LVIS height metrics was good ($R^2 = 0.58$; p= 0.003; Figure 9). The PRESS RMSE error of 0.44 was 9% of the mean distribution value (5.12) of the natural log of the CWD values.

Discussion

If the premise described by Foster et al. (1998) of persistent landscape-scale variation in site susceptibility is correct, then spatial, compositional and structural patterns should emerge as the legacies of such repeat events. Two of the largest impact disturbances at Bartlett over the past century have been the hurricane of September 1938 and the ice storm of January 1998. Unpublished data (M.L. Smith personal communication; Forest Service records) on moderate-to-severe tree damage sustained from both events largely overlap over the western end of the experimental forest (Figure 3.7). These same areas generally support higher levels of northern hardwood species compared to lower elevation sites at Bartlett (Plourde et al. in press), with sugar maple reaching some of the highest levels of basal area and biomass within the entire forest on these sites. These side slope sites are located generally above 350 meters in elevation and coincide with some of the only east- and southeast-facing aspects on the landscape at Bartlett.

LVIS ground energy metrics have utility in mapping the spatial pattern of damaged forest canopy, particularly in unmanaged tracts. Relatively high values of ground energy are recorded as larger numbers of photons reach the ground in areas where canopy cover has been damaged and opened to greater light penetration. At Bartlett, only areas of recent active forest management and tracts of forest subject to the most damage from the 1998 ice storm were revealed by these higher values of measured ground energy. Once

123

restricted to reflect only largely unmanaged forest conditions at higher elevations (above 325 m), the overall correspondence of high ground energy metrics with both southern through eastern aspects and the distribution of higher levels of sugar maple biomass and basal area at Bartlett is striking. The pattern suggests the possibility that repeat disturbance events on southern through eastern aspects have helped shape the hardwood composition of these forests.

Where natural disturbances or environmental conditions have increased the openness of the canopy within this older, largely unmanaged forest, a relationship between CWD and LVIS structural metrics can be established. In this situation, LVIS metrics are likely recording a structural configuration of the canopy that has been shaped by the same disturbance events that also largely define the amount of CWD on the ground. Although the canopy configuration of older trees is certainly not the result of just one disturbance event, the relationship between LVIS metrics and CWD improves if the CWD totals are adjusted to levels that correspond with the timeframe of the most recent significant natural disturbance. At Bartlett, the 1998 ice storm has both significantly impacted canopy configuration and contributed to the current levels of CWD. The 1999 LVIS flight captured the damage within 2 years of the January 1998 storm and before salvage operations were undertaken within sections of the experimental forest. CWD data collected even six years later appears to correlate well.

In general, the relationship found between the LVIS metrics and CWD followed the well-established ecological pattern of taller trees (and hence often larger trees) corresponding

with larger amounts of CWD. This trend became more noticeable as tree height began to exceed the mean value (~ 23 m) seen in the forest as a whole (Table 1). Rhoads et al. (2002) discuss two factors, amount of decay and surface area of crown, as possible determinants in the differential susceptibility to damage seen between larger and smaller trees. Decay can weaken the mechanical properties of the wood in older (and often larger) trees while larger crowns accumulate heavier loads of ice or wind stress; both factors increasing the likelihood of damage from ice or wind events. Hagen and Whitman (2001) have similarly noted that differences in volumes of downed dead wood among comparable forest types in Maine were being driven by the density of large living trees, with large-diameter living trees creating an ecological cascade of structure.

Conclusions

LVIS metrics obtained within two years following the January 1998 ice storm provided two notable findings for the forest at Bartlett: (1) Higher amplitude values of LVIS ground return metrics provided a spatial record of higher levels of canopy damage within older, unmanaged forest tracts; and (2) Within those largely unmanaged forest tracts identified as having open and/or damaged canopy, LVIS height metrics can be used to establish a statistical relationship with CWD data. Future replication or expansion of the

dataset may allow prediction of such variables for other similar forest tracts within the region.

The general patterns from natural disturbances of intermediate severity reported elsewhere in New Hampshire (Foster 1988a, Rhoades et al. 2002, Peart et al. 1992) are upheld at Bartlett, with damage from hurricane and ice storm being particularly evident on south to east facing slopes, higher elevations of the forest showing greater levels of damage, and coarse woody debris being dominated by beech, red spruce, and other hardwoods with little contribution from sugar maple.

A previously unreported factor influencing the abundance of higher levels of sugar maple within the Bartlett Experimental Forest appears to be landscape scale adaptation to sites subject to moderate-to-severe natural disturbances every few decades. The general resistance of sugar maple to the levels of canopy damage and associated levels of CWD seen in contrast to other associated northern hardwood species appears to support to this response.

The ability to examine the spatial, compositional and structural patterns revealed by waveform lidar and hyperspectral data in conjunction with other physical landscape patterns may allow information on the characteristic distribution of these events in time and space to be more broadly recognized on the landscape. Determination and recording of such spatial patterning is critical as ecologists increasingly recognize that the legacies of natural disturbance and land-use continue to influence ecosystem structure and

126

function for decades or even centuries into the future (Foster et al. 1998, Foster et al. 2003).

Acknowledgements

Literature Cited

Beers, T.W. & Miller, C.I. (1976). Line sampling for forest inventory. *Agric.Exp. Sta. Res. Bull. 934*. West Lafayette, IN: Perdue University.

Blair, J.B., Rabine, D.L. & Hofton, M.A. (1999). The Laser Vegetation Imaging Sensor (LVIS): A medium- altitude, digitisation-only, airborne laser altimeter for mapping vegetation and topography. *ISPRS Journal of Photogrammetry and Remote Sensing*, 54, 115-122.

Boose, E.R., Foster, D.R. & Fluet, M. (1994). Hurricane impacts to tropical and temperate forest landscapes. *Ecological Monographs*, 64(4), 369-400.

Boutet, Jr., J.C. & Weishampel, J.F. (2003). Spatial pattern analysis of pre-and post-hurricane forest canopy structure in North Carolina, USA. *Landscape Ecology*, 18(6), 553-559.

Canham, C.D., Papaik, M.J., & Latty, E.F. (2001). Interspecific variation in susceptibility to windthrow as a function of tree size and storm severity for northern temperate tree species. *Canadian Journal of Forest Research*, 31(1), 1-10.

Drake, J.B., Dubayah, R.O., Clark, D.B., Knox, R.G., Blair, J.B., Hofton, M.A., Chazdon, R.L., Weishampel, J.F., Prince, S.D. (2002). Estimation of tropical forest structural characteristics using large-footprint lidar. *Remote Sensing of Environment*, 79, 305-319.

Dubayah, R.O., Knox, R.G. Hofton, M.A., Blair, J.B, & Drake, J.B. (2000). Land surface characterization using lidar remote sensing. pp.25-38 In: M.J. Hill & R.J. Aspinall (Eds.), *Spatial Information for Land Use Management.* Australia: Gordon and Breach Science Publishers.

Fast, A. (2005). A comparison of endemic and catastrophic wind damage in Bartlett Experimental Forest, New Hampshire. Master's Thesis. Durham, N.H.:University of New Hampshire.155 pp.

Foster, D.R. (1988a). Disturbance history, community organization and vegetation dynamics of the old-growth Pisgah Forest, south-western New Hampshire, USA. *Journal of Ecology,* 76, 105-134.

Foster, D.R. (1988b). Species and stand response to catastrophic wind in central New England, USA. *Journal of Ecology,* 76, 135-151.

Foster, D.R. & Boose, E.R. (1992). Patterns of forest damage resulting from catastrophic wind in central New England, USA. *Journal of Ecology,* 80, 79-98.

Foster, D.R., Knight, D.H., & Franklin, J.F. (1998). Landscape patterns and legacies resulting from large, infrequent forest disturbances. *Ecosystems,* 1(6), 497-510.

Foster, D., Swanson, F., Aber, J., Burke, I., Brokaw, N., Tilman, D., & Knapp, A. (2003). The importance of land-use legacies to ecology and conservation. *Bioscience,* 53(1), 77-88.

Gao, B-C., Heidebrecht, K.B., & Goetz, A.F.H. (1992). Atmospheric Removal Program (ATREM) User's Guide. Center for the Study of Earth from Space, Cooperative Institute for Research in Environmental Sciences, University of Colorado, Boulder.

Hagen, J.M. & Whitman, A.A. (2001). A comparison of forest structure in old-growth, even-aged, and uneven-aged forest types in Maine. In J.M.Hagan (Ed.), *Forest Structure: A Multilayered Conversation. Proceedings of the Forest Information Exchange.* October 25, 2001 (pp. 72-75). Brunswick, ME: Manomet Center for Conservation Sciences.

Hastie, T., Tibshirani, R. & Friedman, J. (2001). *The Elements of Statistical Learning: Data Mining, Inference and Prediction.* Springer-Verlag. 536. pp.

Hocker, H.W. & D.J. Early. (1983). Biomass and leaf equations for northern forest species. Research Report 102. New Hampshire Agricultural Experiment Station, Durham, N.H.

Hofton, M.A., Minster, J.B. & Blair, J.B. (2000). Decomposition of laser altimeter waveforms. *IEEE Transactions on Geoscience and Remote Sensing, 38,* 1989-1996.

Hooper, M.C., Arii, K., & Lechowicz, M.J.(2001). Impact of a major ice storm on an old growth hardwood forest. *Canadian Journal of Botany, 79,* 70-75.

Honer, T.G. (1967). Standard volume tables and merchantable conversion factors for the commercial tree species of central and eastern Canada. Canadian .Department of Forestry. Rural Development, Forest Management Research and Service Institute Information Report. FMR-X-5.

Husch, B., Beers, T.W., &. Kershaw, J.A. (2003). *Forest Mensuration 4th ed.* John Wiley & Sons Inc., Hoboken, New Jersey.

Hyde, P., Dubayah, R., Peterson, B., Blair, J.B., Hofton, M., Hunsaker, C., Knox, R., & Walker, W. (2005). Mapping forest structure for wildlife habitat analysis using waveform lidar: Validation of montane ecosystems. *Remote Sensing of Environment, 96,* 427-437.

Ingraham, P.A. (2004). Detecting rich mesic forest: A remote sensing and geographic information systems approach. Master's Thesis. Durham, N.H: University of New Hampshire.

Lafon, C.W., Graybeal, DY., & Orvis, K.H. (1999). Patterns of ice accumulation and forest disturbance during two ice storms in southwestern Virginia. *Physical Geography,* 20 (2), 97-115.

Leak, W.B. (1982). Habitat mapping and interpretation in New England. *USDA Forest Service. Forest Service Research Paper* NE-496. 28 pp.

Leak, W.B. (1996). Long-term structural change in uneven-aged northern hardwoods. *Forest Science,* 42, 160-165.

Leak, W.B. (1999). Species composition and structure of a northern hardwood stand after 61 years of group/patch selection. *Northern Journal of Applied Forestry,*16(3), 151-153.

Leak, W.B. & Sendak, P.E. (2002). Changes in species, grade, and structure over 48 years in a managed New England northern hardwood stand. *Northern Journal of Applied Forestry,* 19(1), 25-27.

Leak, W.B, & Solomon, D.S. (1975). Influence of residual stand density on regeneration of northern hardwoods. USDA Forest Service Northeastern Forest Experiment Research Paper NE-310.

130

Leak, W.B. & Smith, M.L. (1996). Sixty years of management and natural disturbance in a New England forested landscape. *Forest Ecology and Management,* 81, 63-73.

Leak, W.B. & Smith, M.L. (1997). Long-term species and structural changes after cleaning young even-aged northern hardwoods in New Hampshire, USA. *Forest Ecology and Management,* 95, 11-20.

Lemon, P.C. (1961). Forest ecology of ice storms. *Bulletin of the Torrey Botanical Club,* 88(1), 21-29.

Mark, H. & Workman, J. (1991). *Statistics in Spectroscopy.* San Diego, CA.: Academic Press, Inc.

Millward, A.A. & Kraft, C.E. (2004). Physical influences of landscape on a large-extent ecological disturbance: the northeastern North American ice storm of 1998. *Landscape Ecology,* 19(1), 99-111.

Parker, G.G., Lefsky, M.A., & Harding, D.J. (2001). Light transmittance in forest canopies determined using airborne laser altimetry and in-canopy quantum measurements. *Remote Sensing of Environment,* 76, 298-309.

Peart, D.R., Cogbill, C.V., & Palmiotto, P.A. (1992). Effects of logging history and hurricane damage on canopy structure in a northern hardwoods forest. *Bulletin of the Torrey Botanical Club,* 199(1), 29-38.

Plourde, L., Ollinger, S.V., Smith, M.L., & Martin, M.E. (2006). Species classification for a northern temperate forest using spectral unmixing of hyperspectral remote sensing imagery. *Photogrammetric Engineering and Remote Sensing.* In press.

Pyle, C. & Brown, M.M. (1998). A rapid system of decay classification for hardwood logs of the eastern deciduous forest floor. *Journal of the Torrey Botanical Society,* 125, 237-245.

Pyle, C. & Brown, M.M. (1999). Heterogeneity of wood decay classes within hardwood logs. *Forest Ecology and Management,* 114, 253-259.

Research Systems, Inc. (2002). ENVI (Version 3.6) User's Guide.

Rhoads A.G., Hamburg, S.P., Fahey, T.J., Siccama, T.G, Hane, E.N., Battles, J., Cogbill, C., Randall J., Wilson, G. (2002). Effects of an intense ice storm on the structure of a northern hardwood forest. *Canadian Journal Of Forest Research-Revue Canadienne De Recherche Forestiere,* 32(10), 1763-1775.

Ruffner, C.M. & Abrams, M.D. (2003). Disturbance history and stand dynamics along a topographic gradient in old-growth hemlock-northern hardwood forests of the Alleghany Plateau, USA. *Natural Areas Journal,* 23(2), 98-113.

Sall, J., Creighton, L. & Lehman, A. (2005). *JMP Start Statistics* (3rd edition). SAS Institute, Inc. Toronto, Canada: Thomson, Brooks/Cole.

Schwarz, M., Steinmeier, C., Holecz, F., Stebler, O., & Wagner, H. (2003). Detection of windthrow in mountainous regions with different remote sensing data and classification methods. *Scandanavian Journal of Forest Research,* 18, 525-536.

Shapiro, S.S. & Wilk, M.B. (1965). An anlysis of variance test for normality (complete samples). *Biometrika* 52(3-4): 591-611.

Smith, D.M. (1946). *Storm damage in New England forests.* M.S. thesis. Yale University.

Smith, M.L., Ollinger, S.V., Martin, M.E., Aber, J.D., Hallett, R.A., & Goodale, C.L. (2002). Direct estimation of aboveground forest productivity through hyperspectral remote sensing of canopy nitrogen. *Ecological Applications,* 12, 1286-1302.

Solomon, D.A. (1977a). Growth rates of northern hardwoods under uneven-age management. *The Northern Logger,* 25(8), 18-38.

Solomon, D.A. (1977b). The influence of stand density and structure on growth of northern hardwoods in New England. U.S. Department of Agriculture. Forest Service Northeastern Station Research Paper NE-362. 13 pp.

Tritton, L.M. (1980). *Dead wood in the northern hardwood ecosystem.* Ph.D.Dissertation. Yale University. New Haven, CT. 172 pp.

Tritton, L.M. & Hornbeck, J.W. (1981). Biomass equations for major tree species of the Northeast. USDA Forest Service General Technical Report NE-69. Broomall, PA: Northeast Forest Experiment Station.

Vane, G. & Goetz, A.F.H. (1988). Terrestrial imaging spectroscopy. *Remote Sensing of Environment,* 24, 1-29.

Warren, W.G. & Olsen, P.F. (1964). A line intersect technique for assuming logging waste. *Forest Science,* 10, 267-276.

Whittaker, R.H., Bormann, F.H., Likens, G.E., & Siccama, T.G. (1974). The Hubbard Brook Ecosystem Study: Forest Biomass and Production. *Ecological Monographs,* 44(2), 233-254.

Woods, K.D. & Cogbill, C.V. (1994). Upland old-growth forests of Adirondack Park, New York, USA. *Natural Areas Journal*, 14, 241-257.

Young, H.E., Ribe, J.H. & Wainwright, K. (1980). Weight tables for tree and shrub species in Maine. Life Sciences and Agricultural Experiment Station. University of Maine at Orono.Miscellaneous Report 230. 84 pp.

| Data Sources and Types	N	Plot or Footprint Size (ha)	Mean of Maximum Canopy Height [standard deviation] (m)	Mean QMSD [standard deviation] (cm)	Mean AGBM [standard deviation] (Mg ha^{-1})	Mean BA [standard deviation] (m^2 ha^{-1})
LVIS 1999 Footprints within BEF	52279	0.049	22.9 [4.7]			
USFS NERS Inventory Plots at BEF	413	0.1		24.9 [3.7]	242.4 [63.7]	39.5 [10.3]

Table 3.1 Measures of Forest Structure for Bartlett Experimental Forest

Transect Name	# of LVIS footprints	# logs > 3 in. diameter	Species (BE =American Beech; RS= Red Spruce; SM = Sugar Maple; EH = Eastern Hemlock; YB = Yellow Birch; WB = Paper Birch; RM = Red Maple; BF = Balsam Fir; ST = Striped Maple)	Mean LVIS Height (m.)	Sum of CWD Volume fallen since 1998 Ice Storm (ft³/ac)
7D-e	5	13	6 unknown; 2 SM; 2 RM; 1 YB; 1 WB; 1 ST	23.62	133.65
12H-w	8	21	10 ST; 3 BE, 3 SM, 3 unknown; 1 RS; 1 YB	23.11	164.05
18C-n	5	12	7 BE; 2YB; 2 ST; 1 unknown	25.36	172.97
11F-w	4	13	6 BE; 4 unknown; 1 SM; 1 RM; 1 YB	23.98	194.39
12T-w	4	17	7 YB; 2 BE; 1 EH; 1 SM; 1 ST; 5 unknown	25.77	214.33
18L-w	5	13	9 BE; 1 YB; 1 WA; 1 ST; 1 unknown	25.42	214.78
10N-e	9	28	19 BE; 3 RM; 2 YB; 1 SM; 1 ST; 2 unknown	24.81	228.74
7F-w	5	21	9 BE; 10 unknown; 2 YB	24.10	231.66
10L-w	3	16	7 BE; 2 EH; 2 ST; 1 YB; 1 WB; 3 unknown	23.88	245.18
11P-e	5	21	17 BE; 3 Unknown; 1 SM	23.26	259.21
9F-w	6	22	13 BE; 7 unknown; 2 SM	26.17	331.78
8H-w	7	35	17 BE; 9 unknown; 6 SM; 2 RS; 1 YB	25.43	449.30
14J-e	7	22	16 BE; 5 unknown, 1 YB	26.85	462.81
10P-w	3	26	14 BE; 4 SM; 4 unknown; 2 WB; 1 RS; 1YB	22.78	495.57
12F-e	5	17	3 BE; 3 YB; 2 RM; 2 WB; 2 RS; 1 EH; 1 SM; 1 ST; 2 unknown	25.71	546.20
4F-e	6	22	15 BE; 5 unknown; 1 RM; 1 WB	28.22	673.39
9z-e	1	29	17 RS; 6 EH; 6 unknown	28.77	833.08
12X-w	1	20	11 BE; 3 WB; 4 unknown, 1 SM; 1 BF	29.97	1157.84

Table 3.2 Detail of CWD and associated 1999 LVIS data for selected transects at Bartlett Experimental Forest.

135
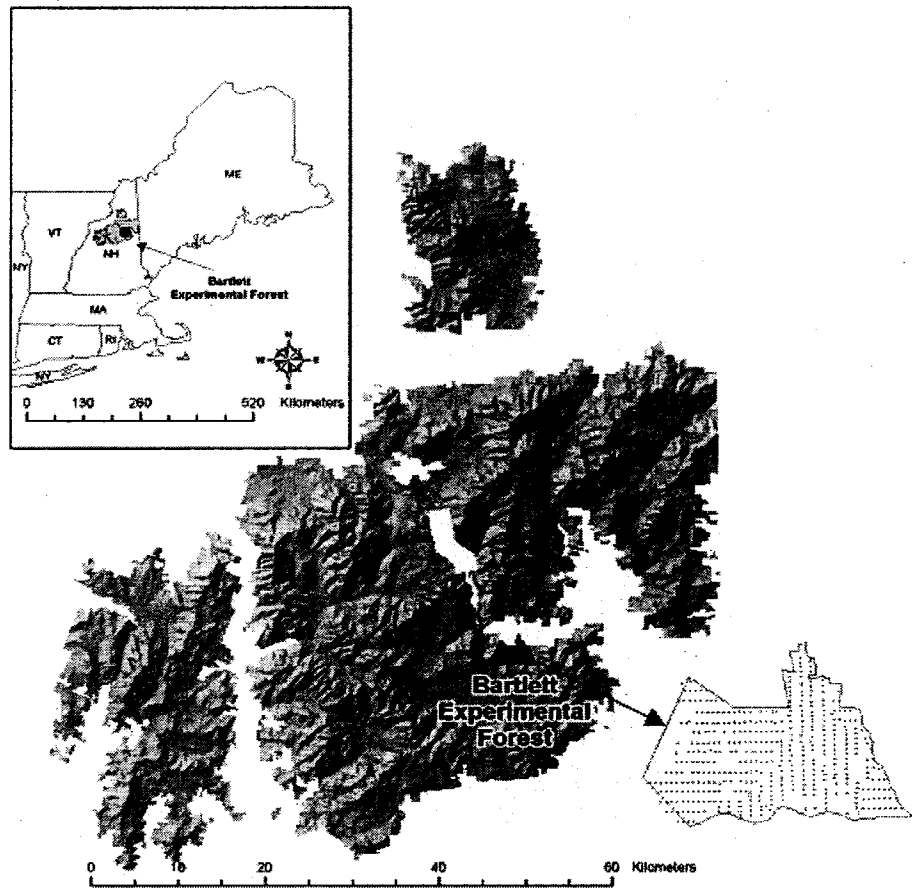
Figure 3.1 Location of Bartlett Experimental Forest, showing established plot network.

136
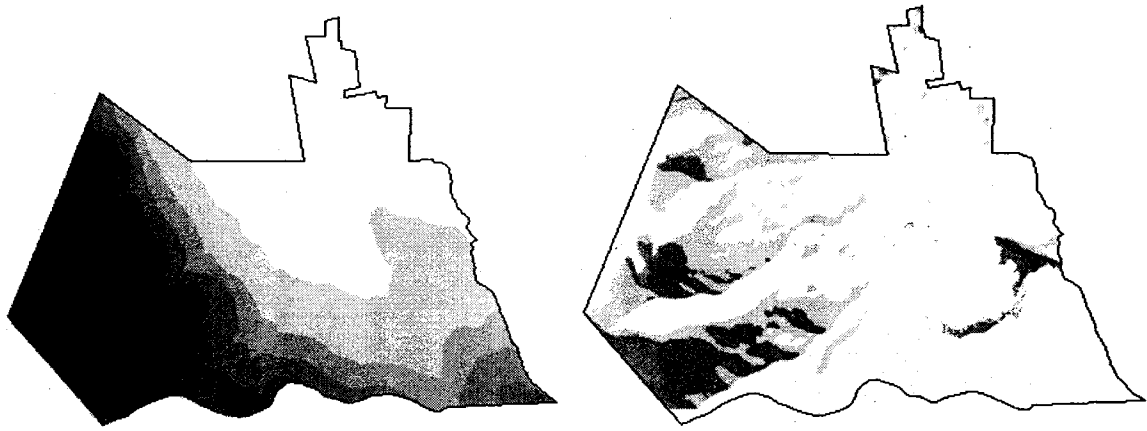
Figure 3.2   Bartlett Experimental Forest. Selected Aspects and Elevations
Elevation grades from 300 (gray) – 850 m (black) in 50 meter classes
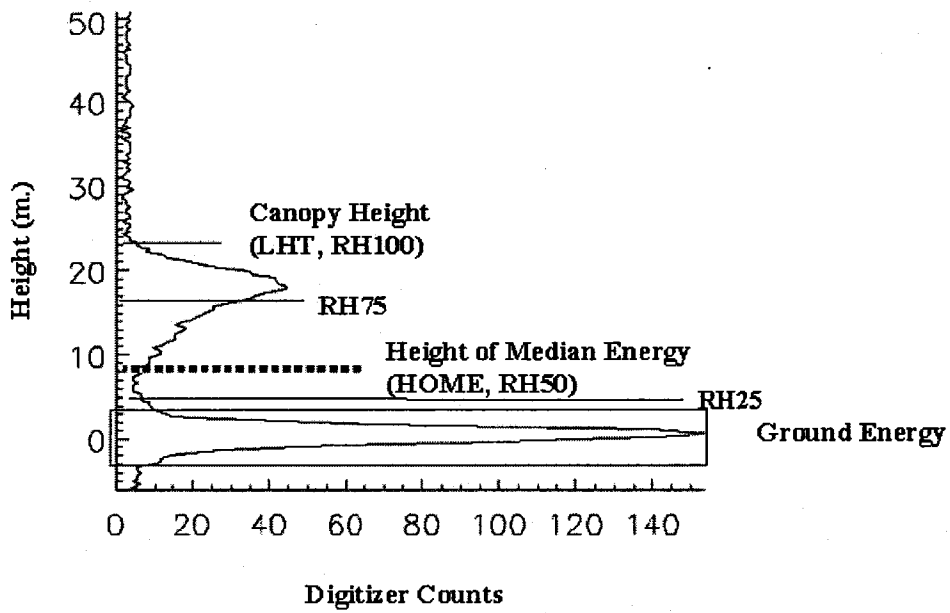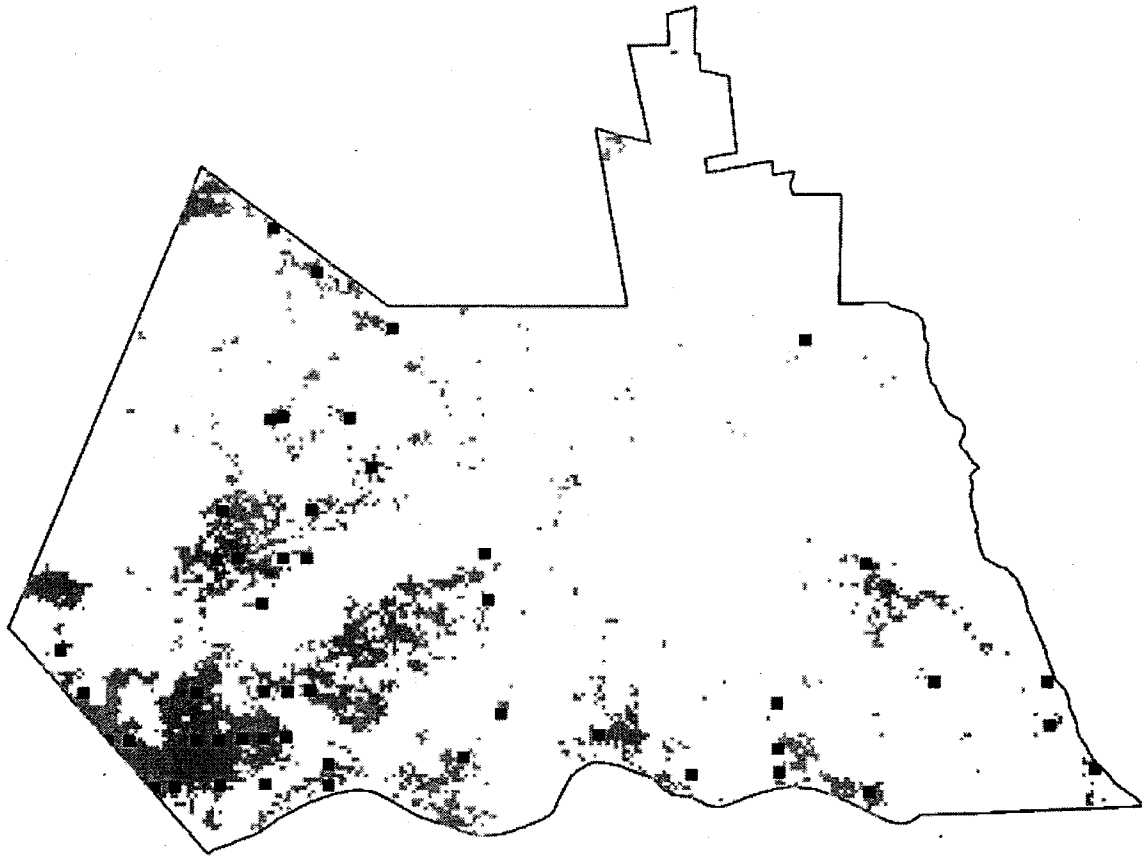East = yellow; Southeast = green; South = blue

137

Figure 3.3 Metrics derived from lidar waveforms. Adapted from Drake et al. 2002.

Figure 3.4   Sugar Maple (*Acer saccharum*) basal area > 30% (slate blue shading) derived
from 1997 AVIRIS imagery and fraction of sugar maple biomass > 0.3 (dark blue squares)
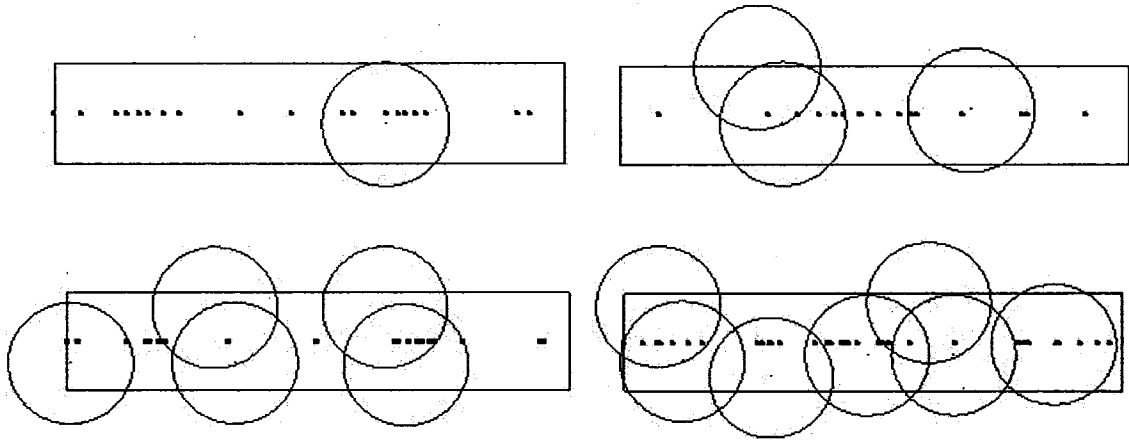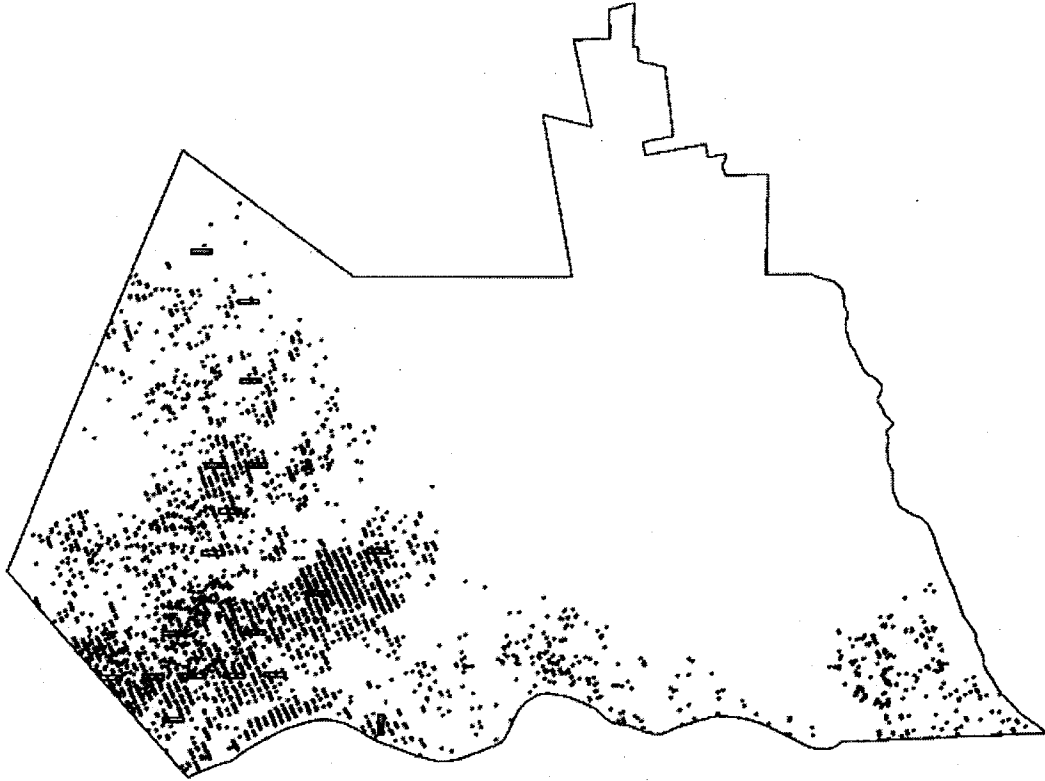derived from 2001-2003 USFS NERS inventory.

139

Figure 3.5 Selected examples of CWD transects (the intercepts of individual logs/branches with transects are shown as black points) and 1999 LVIS footprints (25 meter diameter blue circles) within 100 m by 20 m polygons originated from USFS NERS plot primary corners.

140

Figure 3.6   Locations of 18 CWD transects (black polygons). Transects were selected by restricting analyses to only those sites where the aggregated 1999 LVIS ground energy metrics were relatively high (mean ground energy > 2250), LVIS mean elevation was greater than 325 m, and LVIS minimum canopy height was above 19 m (62 ft.) for the forest as a whole. These restrictions select for those areas of Bartlett that contain predominately mature northern hardwood forest with open or damaged canopy, thus allowing LVIS photons to reach the ground at higher levels. The transects selected are all located within the area of Bartlett that suffered the greatest damage from the January 1998 ice storm.
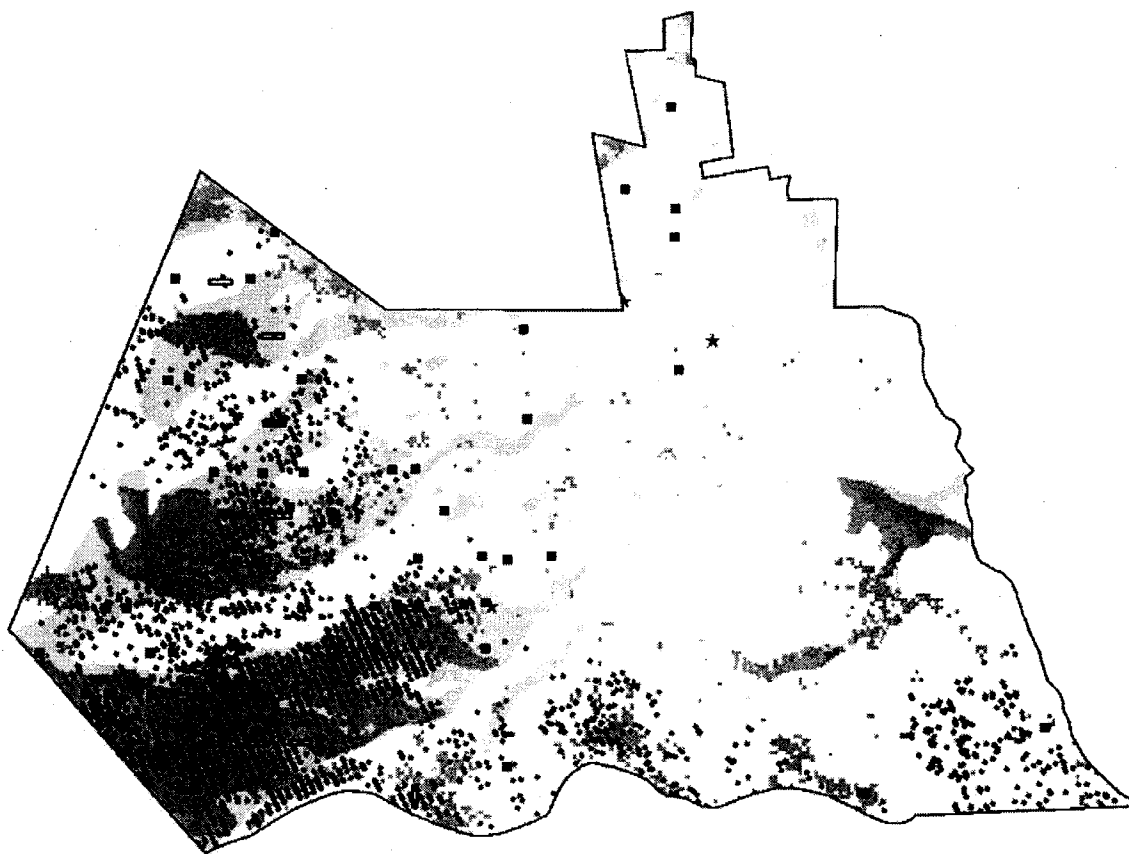
Figure 3.7 Sugar maple abundance (basal area > 30%; slate blue shading) derived from 1997 AVIRIS imagery and 1999 LVIS ground energy returns (GRND_E > 2250 in mature forest (LHT > 19 m) above elevations of 325 m; red footprints) overlaid on southern through eastern aspects (south = light blue; southeast = green; east = yellow). USFS NERS records of inventory plots with basal area damage > 20 % from the 1938 hurricane are designated by black squares. Selected CWD transects designated by black rectangles. Sugar maple coarse woody debris from decay classes I and II shown as solid black stars (N= 8 logs of 467; 2 %).
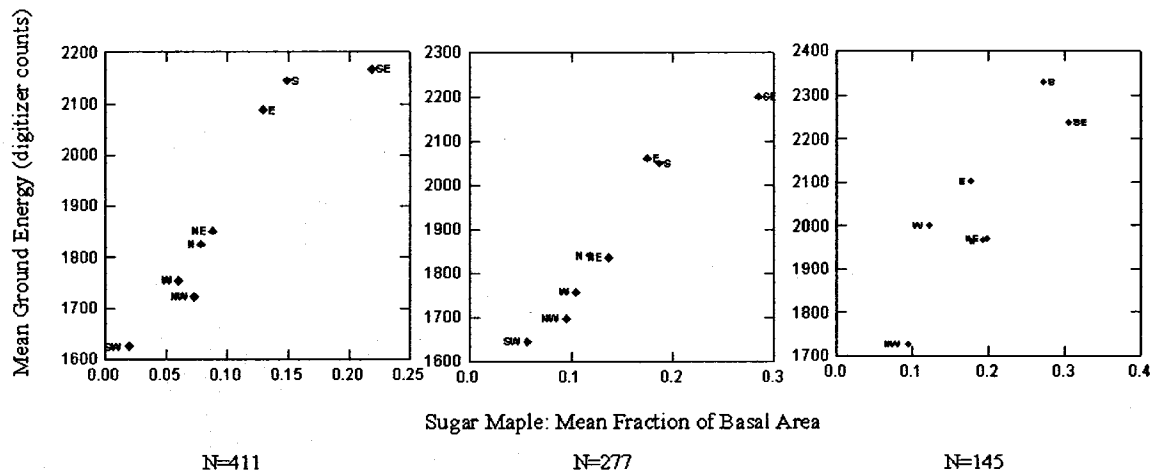
Figure 3.8 USFS NERS inventory plot data for the Bartlett Experimental Forest were used to examine relationships between sugar maple abundance, aspect and 1999 LVIS measures of ground return energy. Analysis examined all sampled plots (N=411), the subset of plots where sugar maple was present (N=277), and the subset of plots where sugar maple was present at elevations above 325 m and mean tree height exceeded 19 m (N=145). Plots were aggregated by aspect with mean values of sugar maple abundance and mean ground energy generated for each group.

143
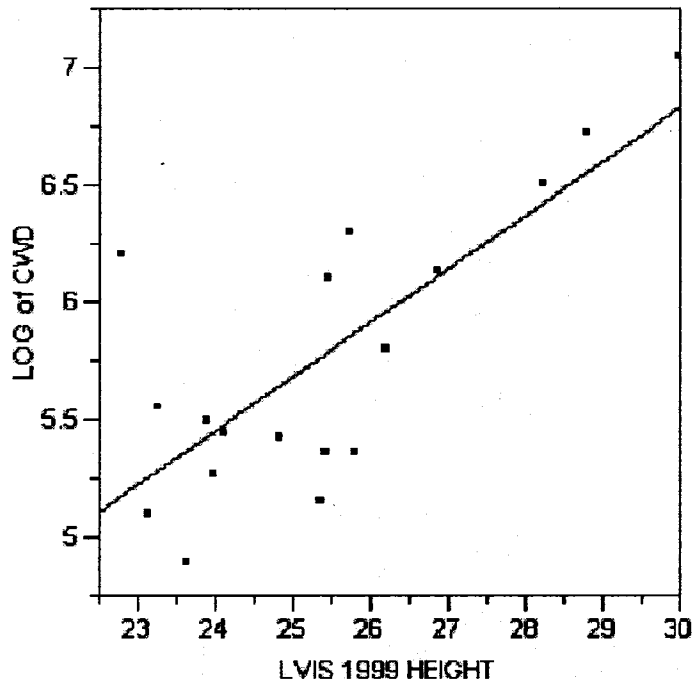
Figure 3.9 Scatter plot of the natural log of the sum of CWD log volumes (adjusted to reflect a per acre figure for logs that have fallen within the last six years) per CWD transect with the mean canopy height of aggregated 1999 LVIS metrics. Simple linear regression generated the following results: $r^2 = 0.58$, PRESS RMSE 0.44, N = 18, p = 0.003. CWD transects were restricted by choosing only sites where the LVIS ground energy metrics were relatively high (mean ground energy > 2250), mean elevation exceeded 325 m, and LVIS minimum canopy height was greater than 19 m. for the forest as a whole.

144

CHAPTER 4

CONCLUSIONS

The capability of waveform lidar, used singly and through integration with high-resolution spectral data, to describe and predict various aspects of the heterogeneous structure of a northern temperate forest has been explored in this dissertation. A remarkable confluence of multiple remote sensing and field data sets specific to the Bartlett Experimental Forest has allowed examination of such relationships at varying scales and with varying aggregations of data.

The heterogeneity inherent in the northern temperate mixed conifer-deciduous forests exemplified by Bartlett has been long recognized. Over a dozen tree species are known to comprise the forest at Bartlett, with three quarters of those species able to reach levels of relative abundance exceeding 50% at varying places within the forest. The historical approach to forest management for this region, emphasizing small-scale partial cuttings

combined with the impacts seen from ice and windstorms of intermediate severity, adds to this complexity. The dense nature of mature forest cover is also a challenge to remote sensing efforts here.

Bartlett was originally chosen as a research site for waveform lidar as part of a larger NASA effort to assess LVIS in a wide variety of biomes; adding it to one of only a few sites worldwide where calibration and validation studies carefully geo-locate individual footprint-level field plots with coincident individual LVIS footprints. Waveform lidar did successfully correlate with maximum canopy height and other common forest metrics at the smallest scale of the LVIS footprint at Bartlett. These results augment a growing literature that demonstrates that lidar can recover certain measurements of forest structure with a high degree of accuracy relative to field measurements.

Nonetheless, the mixed hardwood-conifer conditions inherent to this forest confounded relationships examined at the slightly larger (and less precisely geo-located) scale provided by the pre-existing plot grid of the USFS NERS permanent inventory for Bartlett. Stratification based on land-use or species composition and/or integration of multiple sensor data (AVIRIS and LVIS), however, did provide the means to establish reasonable regression relationships at this scale.

The integration of waveform lidar with hyperspectral data did clearly enhance the ability to remotely describe a number of common measures of forest structure. Improvements of 8-9 % across all forest conditions were seen in the coefficients of determination for

146

measures of AGBM, BA, and QMSD through the use of the integrated data. Estimates of error dropped by 5-8% for the same measures. It is plausible that the predictive nature of these relationships could be improved further with the use of waveform lidar amplitude metrics such as ground energy and canopy energy (and the resultant relative measure of canopy closure derived from them) that were not employed in this study. There may be some cross-product relationships between lidar cover and height metrics that deserve further research. It could also be valuable to explore integrated LVIS-AVIRIS relationships with an expanded and more precisely geo-registered series of footprint-level plots.

Restrictions on plot selection set by land-use were explored as a means to improve both the descriptive and predictive power of the regression analyses. Geo-location error, in combination with the abrupt changes in height found in tracts subject to recent partial cuttings, in particular, weakened regression relationships between the LVIS sensor and ground data. These results indicate that the stratification of data based on broad patterns of management history (recently managed versus unmanaged conditions) can be used as a tool to sharpen the predictive relationships explored through regression analyses. This gain, obtained by isolating tracts (and plots) of forest with no recent management actions within the analyses, carried over to relationships established using integrated data from waveform lidar and hyperspectral sensors. Notably, AGBM coefficients of determination improved by 25% or more, while corresponding error levels decreased by over 25%, using integrated data sets stratified to reflect an absence of recent forest management

147

when compared to results obtained using data from a single sensor (AVIRIS or LVIS) applied across all forest conditions.

Species composition was another factor of importance at Bartlett. The predominance of certain structurally distinctive conifers, such as red spruce or white pine and/or (at BEF) the closely associated absence of the dense cover and more homogeneous canopy structure of the northern hardwood species of beech or yellow birch resulted in stronger relationships between measures of AGBM and the LVIS height metrics. The recognized ability of AVIRIS to predict levels of species-specific abundance was evident even in the mixed conditions of this forest for four of the dominant trees species. Of these northern hardwoods species (beech, red maple, sugar maple and hemlock), only red maple benefited notably from the integration of LVIS metrics into the analyses. The strength of AVIRIS data was apparent in this regard, explaining nearly all of the variance for the other three species and most of the variance in the red maple relationship. AVIRIS data allowed species-specific patterns of abundance to be predicted that could be ultimately matched with other measures of forest structure better predicted through LVIS metrics (e.g. height, QMSD) or through the use of integrated LVIS and AVIRIS data (e.g. AGBM, BA).

It is this use of hyperspectral and waveform lidar data, in tandem, to create maps predicting species abundance patterns (derived primarily from AVIRIS data) augmented with coincident patterns of stem size or height (derived primarily from LVIS data) for several of the dominant tree species of this region that may be one of the most useful

148

outcomes of this research. Remotely derived maps for large tracts of land reflecting species-specific abundance and size data have a wide range of potential application in forestry and conservation planning. Landscape patterns could be explored to identify remnant areas of structural complexity and their attendant biodiversity in these northern forests. The ability to model such spatial patterns on a landscape scale could also be a more sensitive means of monitoring changes seen in the dynamics of individual species populations brought on by global warming and other environmental change over time. While these relationships were only established for a small number of species in this study, additional field data, especially for conifer species such as red spruce and white pine, may allow other predictive relationships to be uncovered.

It has been a long-standing objective of remote sensing working within forest ecosystems to provide results that are the near equivalent of ground-based forest inventory efforts. The results here, in actuality, provide a level of detail on the spatial dynamics and variability seen in forest structure not readily accessed through typical approaches to forest sampling. Lessons learned about the accuracy gained in prediction (fit and error) when land-use and/or species composition patterns were used to stratify the initial data set are important here, bringing estimates of error closer to those generally expected from field sampling efforts. These techniques, did, in various manners specific to this forest setting, compensate for situations where less precise horizontal geo-location data were available. This is evident in the comparison (below) of the strongest descriptive relationships found in the analyses of AGBM (or a species-specific fraction of AGBM) at Bartlett.

149

AGBM using only LVIS data (footprint level):

$r^2 = 0.61$; PRESS RMSE = 58.03 Mg ha^{-1}

AGBM using integrated AVIRIS and LVIS data - unmanaged forest (plot level):

$r^2 = 0.55$; PRESS RMSE = 41.03 Mg ha^{-1}

Species abundance (fraction of AGBM) using only AVIRIS data (plot level):

American Beech: $r^2 = 0.65$; PRESS RMSE = 0.16

Eastern Hemlock: $r^2 = 0.57$; PRESS RMSE = 0.12

Species abundance (fraction of AGBM) using integrated AVIRIS and LVIS data (plot level):

Red Maple: $r^2 = 0.61$; PRESS RMSE = 0.13

This dissertation also explored the use of a broader set of 1999 LVIS metrics, inclusive of canopy energy and ground energy variables, to look at questions of spatial patterning due to natural disturbance. Examination of higher amplitude values of 1999 LVIS ground return metrics, obtained within two years of the January 1998 ice storm, suggested that this variable appears to provide a spatial record of higher levels of canopy damage within older, unmanaged forest tracts. Analyses using USFS NERS plot compositional abundance data, 1997 AVIRIS data, 1999 LVIS metrics, unpublished Forest Service records of the 1938 hurricane damage, and a 2004 coarse woody debris data (CWD) set

150

provide evidence that southeastern aspects at Bartlett, in particular, exhibit site susceptibility to repeated disturbance caused by storms of intermediate severity over time. This susceptibility corresponds to portions of the landscape that currently retain notably higher levels of sugar maple abundance. Viewed through extended passages of time, this susceptibility may, perhaps, factor as one of the forces maintaining this compositional pattern.

LVIS height metrics were used here to explore a statistical relationship with extensive coarse woody debris data in areas hardest hit by the 1998 ice storm. To our knowledge, this is a new application of LVIS data, directly drawing on its strength to measure height accurately, and indirectly exploring a recognized relationship between tree volume (and it's relatively strong correlation with canopy height) and the corresponding volume of CWD. The fact that a statistical relationship between levels of CWD and LVIS height metrics could be established in those areas of Bartlett that were most recently subject to levels of moderate to severe disturbance offers the possibility to forest managers that predictions of amounts of CWD created in the aftermath of large storm events might be modeled based on knowledge of overall height spatial patterns provided by imaging sensor data such as lidar.

The generality of relationships on all of these measures of forest structure established at Bartlett should be explored at Hubbard Brook Experimental Forest in West Thornton, N.H. and vice versa. It is a rare opportunity to have extensive ground and multiple remote sensor data sets at such comparable sites within roughly 50 km of one another. The

adaptation and application of a generalized biomass equation proposed by Lefsky et al. (2002) to two different levels of data in this study allowed some assessment of its' potential in these forests. At the footprint scale, even with the substitution of another metric and exclusion of cover metrics, the results were only slightly weaker than those seen in the best-fit model of coincident ground AGBM measures and LVIS metrics. Establishing and refining such predictive and generalized multi-sensor relationships within the Northern Forest stretching from New York through Maine and into forests of maritime Canada should remain a priority.

Literature Cited

Lefsky, M.A., Cohen, W.B., Harding, D.J., Parker, G.G., Acker, S.A., & Gower, S.T. (2002). Lidar remote sensing of above-ground biomass in three biomes. *Global Ecology & Biogeography*, 11, 393-399.